CHARACTERIZATION OF MODIFIED NEUTRON FIELDS WITH AMERICIUM-BERYLLIUM AND CALIFORNIUM-252 SOURCES

A Thesis
Presented to
The Academic Faculty

by

Peter Riley Exline

In Partial Fulfillment
of the Requirements for the Degree
Master of Science in Nuclear Engineering

Georgia Institute of Technology

August 2011

CHARACTERIZATION OF MODIFIED NEUTRON FIELDS WITH AMERICIUM-BERYLLIUM AND CALIFORNIUM-252 SOURCES

Approved by:

Dr. Nolan Hertel
Woodruff School of Mechanical Engineering
Georgia Institute of Technology

Dr. Chris Wang
Woodruff School of Mechanical Engineering
Georgia Institute of Technology

Dr. Michael Shannon
Defense Threat Reduction Agency
United States Military Academy

Date Approved: April 22nd, 2011

To Team Hertel and Team Exline

ACKNOWLEDGEMENTS

First I would like to thank my compatriots in "Team Hertel", including Spencer Mickum, Tim Cahill, and MAJ Amy Eastburg. Special thanks goes to Randi Palmer and Emily Freibert, whose help structuring MCNP codes and organizing my thesis saved countless hours of work.

The experienced hand of Dwayne Blaylock proved invaluable in configuring and troubleshooting my detector setup. The tireless efforts of machinist extraordinaire Anna McLendon saw 400 pound lead hemispheres lift up in the air and into position. Nazia Zakir's efforts in revising the access policy cleared my way in. Christina Tabor and Gary Spichiger not only handled many source movements, but often went well beyond their job requirements and normal work hours to see that the RCZ ran safely.

Dr. Chris Wang was the professor who taught my first radiation detection class and generated my interest in the field. MAJ Mike Shannon helped me understand the bigger picture of applying my nuclear engineering work to the US Army's needs. I'd like to thank them both for serving on my thesis committee.

Dr. Nolan Hertel has served as my mentor. There is none better. Whether I needed resources, personal MCNP classes, a volunteer to handle the AmBe source, or midnight proofreading from France, he worked without ceasing to make me successful.

My wife, Jessica Exline, bore the greatest burdens of all. Without the least complaint, she juggled all our responsibilities, including moving us to another state, while I completed this work. I cannot thank her enough.

Finally, I'd like to thank the Lord for all these people and His greatest gift to us.

TABLE OF CONTENTS

LIST OF TABLES

LIST OF FIGURES

NOMENCLATURE

^{252}Cf	Californium isotope 252
AmBe	Americium-Beryllium
BSS	Bonner Sphere System
BUNKI	US Naval Research Laboratory Code for unfolding spectra
BUNKIUT	Unfolding code based on BUNKI
BUMS	Bonner sphere Unfolding Made Simple
D_2O	Deuterium (^2H) dioxide (heavy water)
ESJ	Eisenhauer, Schwartz and Johnson model
MCA	Multichannel Analyzer
MCNP	Monte Carlo N-Particle code
ROI	Region of Interest
SNM	Special Nuclear Materials

SUMMARY

There are a variety of uses for reference neutron fields including detector response and dosimeter studies. The Georgia Institute of Technology has a ^{252}Cf spontaneous fission source and an AmBe (α, n) source available for use in its research programs. In addition, it has iron, lead, beryllium, tantalum, heavy water, and polyethylene spheres to modify the neutron energy distributions from these neutron sources. This research characterized the neutron leakage spectra from the source inside spherical shells using a Bonner sphere spectrometer. All the neutron fields measured were also computed with a Monte Carlo code to determine the neutron fluence rate and ambient dose equivalent rate. The comparison of experimental data and calculations are used to provide further insight into the neutron spectra as modified by the spheres. The characterization of these modified sources will provide data to assist in using the resulting neutron fields in other research activities.

To measure each neutron field combination, one of the two sources was placed in the center of an attenuating sphere. The neutron field was first measured at a variety of source-to-detector distances with a Bonner Sphere System. The spectrometer measurements, specifically the count rates of the different Bonner spheres, as a function of distance from the source is fitted to obtain corrections for room-scatter and air-scatter of neutrons using the Eisenhauer, Schwartz, and Johnson method. Using these corrections, the count rates free of room return is obtained at 1 m from the source and unfolded using the BUMS software to obtain the reported fluence and dose equivalent rates.

These results are compared to those generated by the Monte Carlo Neutral Particle (MCNP) code. Models were made in MCNP for each of the source and moderating sphere combinations. The neutron fluence and dose rates were tallied during the MCNP simulation. The unfolded experimental data and the MCNP calculations showed good agreement for most of source-attenuating sphere combinations, thereby reinforcing the experimental results.

CHAPTER 1: INTRODUCTION

The characterization of neutron fields continues to be needed for nuclear facilities for a variety of applications. More recently, the possibilities of rogue nations or non-state actors acquiring nuclear weapons technology and material for use in nuclear terrorism have placed emphasis on the ability to detect special nuclear material (SNM). SNM include uranium-233 and -235 and plutonium isotopes [1]. These fissile materials are weapons capable when sufficiently enriched and obtaining them is the most difficult task facing potential nuclear terrorists [2]. These SNM are radioactive, releasing radiation that can be detected, allowing for material monitoring and interdiction. Part of this radiation comes from gamma rays, which are detectable, but are also easy to shield with high-Z elements including lead [3]. Some isotopes emit neutrons, which are not readily shielded by the same materials, and also are not emitted by many of the non-SNM radioactive materials that would be false positives for a detection operation. Additionally, SNM can be actively interrogated to release neutrons via reactions. Neutron detectors can thus serve as ideal SNM detection candidates.

1.1 Neutron Detection

The detection of neutrons relies on reactions that release charged particles like alpha particles or recoil particles from scattering [4]. The charged particle reactions principally used for thermal neutron detection include the $^{10}B(n, \alpha)$, $^{6}Li(n, \alpha)$, and $^{3}He(n, \alpha)$ reactions. The most effective systems for detecting thermal neutrons use the helium-3

reaction. Unfortunately, the supply of helium-3 is currently very scarce [5]. Alternative systems in development include lithium and boron coated scintillator detectors.

Testing new detector materials and designs requires known neutron fields. Americium-beryllium (n, α) and californium-252 (spontaneous fission) are two commonly used laboratory sources of neutrons. Both sources have been extensively characterized [6, 7]. It should be noted that AmBe source fields are dependent on the geometry and composition of the sources. In order to generate additional neutron fields, particularly to simulate softer fields that are found in most workplaces, the sources can be placed inside of shielding/attenuating materials to change the magnitude and energy dependence of their fluence spectra. Common shielding materials including tantalum, beryllium, polyethylene and lead previously have been studied using sources and the resultant spectra measured and computed [6].

The neutron leakage spectra generated with such sources inside spherical shells of materials depends on the source energy distribution, the shielding/attenuating sphere, room and air scatter, and geometric configuration. This thesis research seeks to characterize the neutron fields resulting from bare AmBe and ^{252}Cf sources and the fields produced when they are placed inside spherical shells of shielding/attenuating materials available at the Georgia Institute of Technology, in particular lead, steel, beryllium, tantalum, polyethylene, and heavy water spheres.

1.2 Neutron Leakage Spectra Characterization Process Overview

Characterizing the neutron fields requires measurement of the neutron spectra and can be supplemented by simulating the spectra with neutron transport codes. The

experimental and calculated results are then compared for consistency and the fields characterized for further research applications.

To experimentally measure the neutron field for each source-attenuator combination, measurements were made with a BSS at a variety of distances (Chapter 2.1). For each shielding/attenuating material, one of the two sources (Chapter 2.2) was placed in the center of one of the attenuating spheres (Chapter 2.3). Count rates are recorded for each of the BSS detector systems at several distances from the source center. Corrections for room scatter and air scatter of neutrons are then made using the ESJ model (Chapter 2.4). The Axton method is used to correct count rates for the geometry of the system. After these corrections, the count rate data can be unfolded to reconstruct a neutron spectrum using the BUMS software (Chapter 2.5). The resulting fluence and dose equivalent rates are then reported.

These results are compared to those generated by the MCNP simulations (Chapter 3.1). Models were made in MCNP for each of the source and attenuating sphere combinations (Chapter 3.2). The models were executed and neutron fluence and dose measurements were tallied and normalized to the neutron source strengths and compared to the BUMS output (Chapter 3.3).

The unfolded experimental data and the MCNP calculations are then analyzed and checked for consistency, which would lend confidence to the results (Chapter 4.1). The results were then used to create new starting spectra for BUMS that reflect the new neutron fields that can be generated at Georgia Tech (Chapter 4.2 and Appendix A). The MCNP models were also refined and documented to allow future researchers to modify

and use them in further work with these characterized neutron fields (Appendix B). The process is summarized in Figure 1.2.1 below.

.

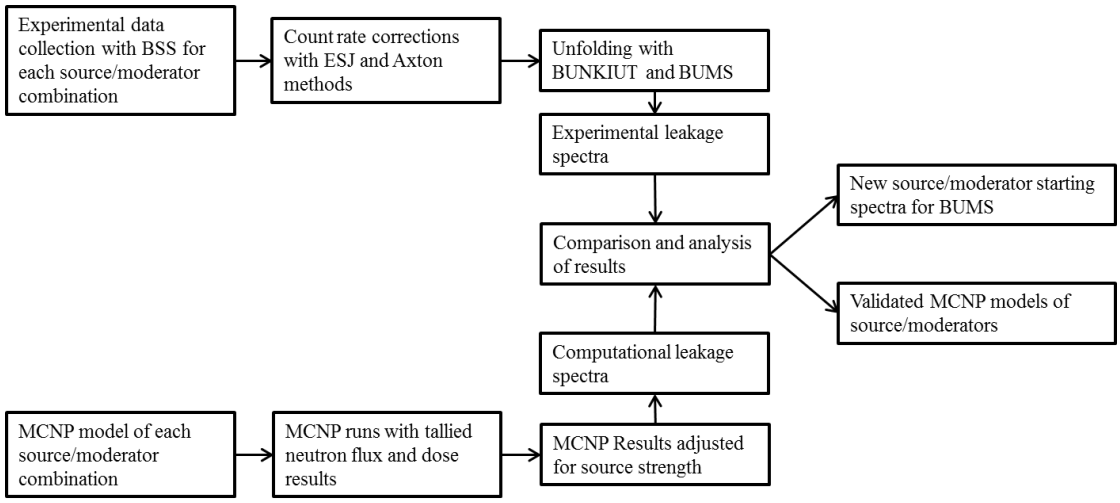

Figure 1.2.1. Neutron Leakage Spectra Characterization Process Overview

CHAPTER 2: EXPERIMENTAL METHODOLOGY AND MATERIALS

In this chapter, the measurement portion of this research is developed, including equipment setup, materials studied, experimental procedures, and analysis procedures for taking collected raw data and generating flux, dose, and neutron energy spectra.

2.1 BSS Detector System

2.1.1 BSS Operating Fundamentals

The BSS was first designed in 1960 by Bramblett, Ewing and Bonner at Rice University [7]. The system is named for one of the principal creators, T. W. Bonner. The principle of operation is to place a thermal neutron detector at the center of a moderating sphere that could be easily changed to a variety of sizes to obtain different energy sensitivities. By varying the amount of moderation an incoming neutron field experiences before interacting with the detector, the detector could be made sensitive to different energy ranges, including those too high for it to efficiently detect otherwise [8]. For this experiment, a BSS set manufactured by Ludlum, model 42-5 [9], is used. It includes a 4mm x 4mm Ø LiI(Eu) scintillator detector and 2”, 3”, 5”, 8”, 10”, and 12” diameter polyethylene moderating spheres. The relative count rate per unit fluence versus neutron energy level is shown in Figure 2.1.1.1.

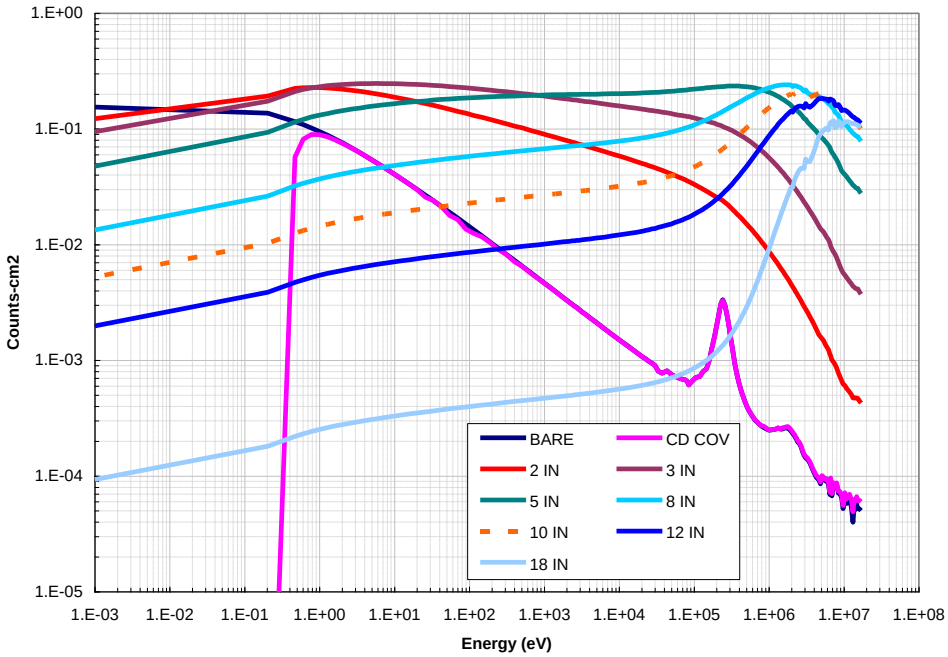

Figure 2.1.1.1 Count Rates per Unit Fluence of Different Bonner Spheres [10]

In Figure 2.1.1.1, it is shown that several of the moderated detectors peak at higher energies and others at lower energies. A weakness of the BSS is that none of the moderator responses have strong structure in the intermediate energy range, which limits energy resolution in this area [11]. The details of going from raw count rates to neutron fluence spectra, also known as unfolding, will be covered later in this chapter.

2.1.2 Experimental BSS Equipment Setup

In addition to the Ludlum model 42-5 BSS equipment, other electronics and software were needed to capture neutron count rates for the experiment. To minimize dose to the operators, the detector was placed on the far side of a shielding wall in the Radiation Control Zone IC area of the Neely Nuclear Research Center at the Georgia

Institute of Technology. Wires were run through conduits to the preamplifier and detector, while the remainder of the equipment remained on the other side of the shielding wall. The shielding wall consisted of concrete blocks and a sheet of 1" borated polyethylene. The power and signal flow is summarized in Figure 2.1.2.1, and the detector room setup is shown in Figure 2.1.2.2. The list of equipment is in Table 2.1.2.1. (Note that the exact location of the source sometimes varied due to limitations on the overhead crane's travel range when lifting the heavier attenuating/shielding spheres into position. These differences are accounted for in the measurement process. Regardless of crane limitations, no source or detector location was within 1 meter of scattering surface other than their own supports.)

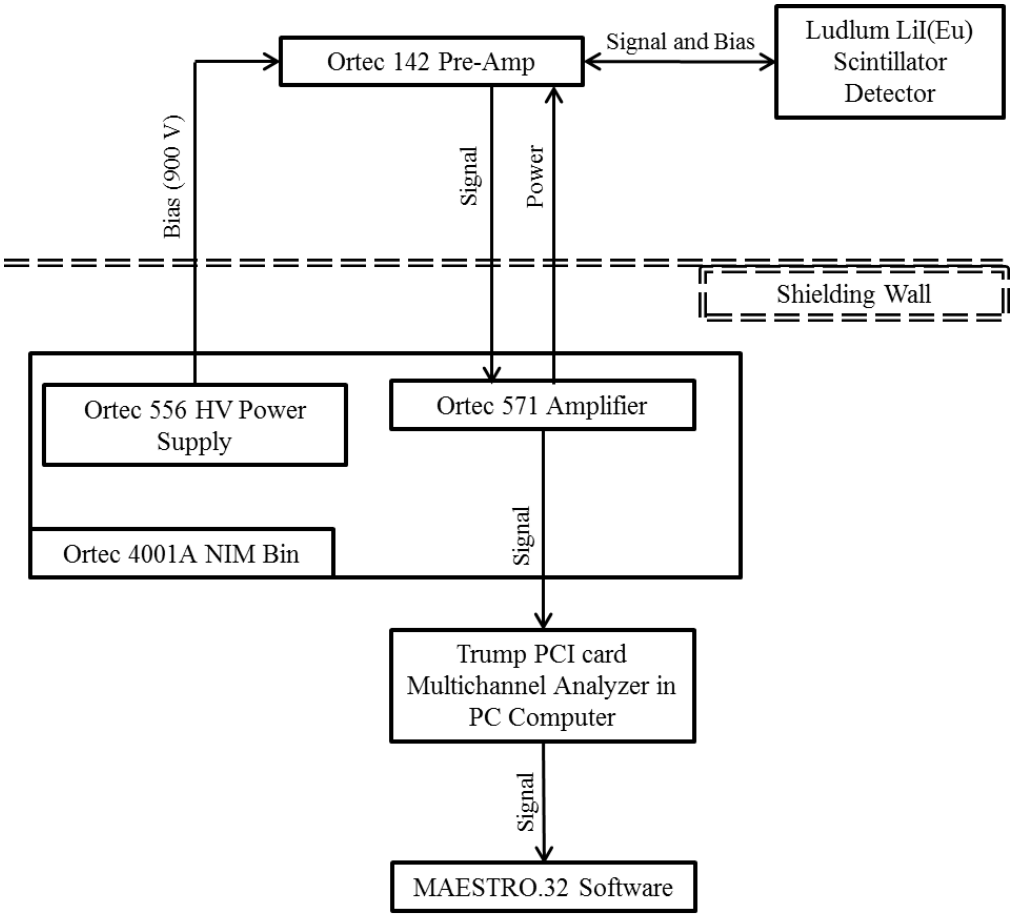

Figure 2.1.2.1 Signal and Power Flow of BSS

Table 2.1.2.1. List of Equipment

Type	Manufacturer	Model	Serial Number
Detector	Ludlum	42-5 A	PR036710
Pre-Amplifier	Ortec	142	n/a
HV Power Supply	Ortec	556	0103716
Amplifier	Ortec	571	n/a
NIM bin	Ortec	4001A/4002A	4133, rev. 31
MCA card	TRUMP	PTRU-003	785
PC	Dell	Vostro 200	FKQZRH1
Software	Ortec	Maestro.32	n/a

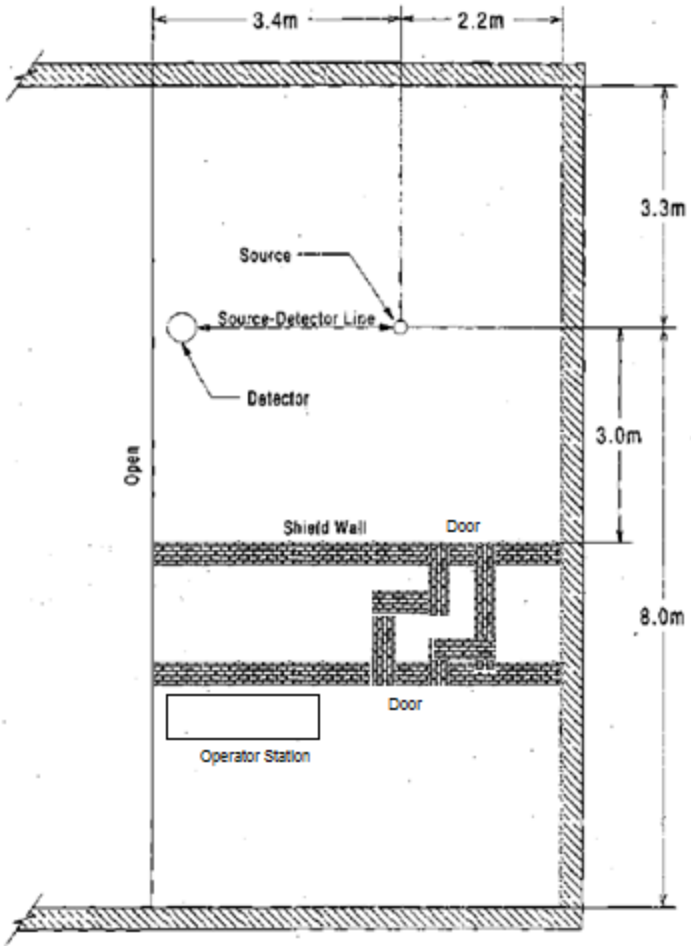

Figure 2.1.2.2 Overview of Detection Room [12]

2.1.3 Data Collection Procedure

For each source and attenuator combination, data were collected for each of the Bonner spheres at seven different source-detector distances. Establishing seven data points for each setup allows for later room scattering and air scattering corrections to be made. The distances were selected with the goal of finding a corrected count rate for a one meter distance, so distances closer and farther this distance were picked. The lower distance limit was set by the dead time experienced by the detector with the Bonner sphere having the highest count rate for that source/moderator combination and in no

case was closer to the source than 40 cm measured from the center of both the detector and source. Dead time was not allowed to exceed 4%.

For each measurement, integral counts for the neutron-induced peak were recorded. Setting a ROI about the neutron-induced peak allowed the MAESTRO software to perform a gamma ray background subtraction. This MCA software was also configured to stop collection when 10,000 net counts were made in the ROI encompassing the peak. The live time needed to reach this threshold was then recorded and divided into the final number of counts to determine the count rate.

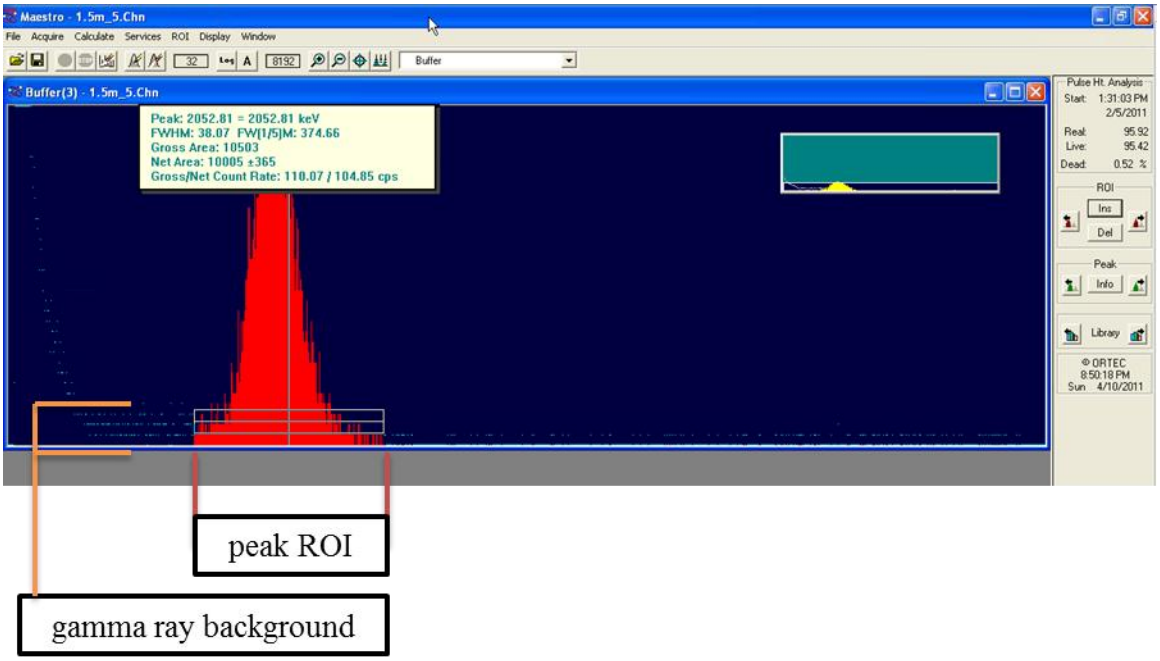

Figure 2.1.3.1 Sample Spectrum Analysis from MAESTRO MCA software. The ROI about the alpha peak is shown in red. Note that the software gives the net counts for the ROI and reports an associated error.

Figure 2.1.3.1 above shows the spectrum result in MAESTRO for the bare AmBe source measured with a 5" Bonner sphere at a source-detector distance of 1.5m. The box

at the top of the ROI shows the gross and net integrated counts, and an estimation of error. This estimation of error is based on MAESTRO's interpretation of the background counts. MAESTRO determines this by taking the average of the first three channels of the ROI and the last three channels of the ROI, and applying the trapezoidal rule in between them. This figure is then subtracted from the gross counts to get the net counts, and an associated error.

This leads to some nuances in properly selecting the ROI for each spectrum. When the overall background is low, MAESTRO's error estimation becomes very sensitive to the exact channels selected for the edges of the ROI. A change of 10 channels (out of 8192 being recorded) can result in the error estimate varying more than 50% and vary the net counts up to 10%. This is due to even a small background undulation in the first or last three channels having a disproportionate effect on the calculation. To create consistent results, it is necessary to select an ROI slightly larger than the strict peak area, and to ensure that both boundaries lay in consistent background areas (not near small spikes in background). The larger ROI does not significantly increase the counts measured, but greatly increases consistency in measurement.

Just as background small spikes can increase error, selecting unusually low background areas for bounds resulted in significant underreporting of error. For consistency, errors less than 180 counts (1.8%) or greater than 360 counts (3.6%) triggered a reevaluation of the ROI for small spikes or dead spaces in the background. In every case, the background error could be increased above 180, and in almost every case, reduced below 360. The only exceptions were when the backgrounds counts were

legitimately high compared to normal, which occurred most often when the detector was used without a moderating sphere (a "bare" detector measurement).

After an appropriate ROI had been determined, the following data were recorded: source/attenuator combination, date, time of measurement start, source-detector distance, Bonner sphere used, lowest ROI channel, highest ROI channel, gross counts, net counts, MAESTRO-reported error, detector live time, and total time. The captured pulse-height file was also saved to the PC to allow later review and ROI adjustment if needed.

This procedure was repeated for all six Bonner spheres and the bare detector for each source-detector distance. Data sets for seven different source-detector distances were recorded for each source-moderator combination. These 49 count rate data points became the starting point for the unfolding process covered in Chapter 2.4.

2.2 Sources

The experiments were conducted with two sources, ^{252}Cf and AmBe.

2.2.1 ^{252}Cf Source

The ^{252}Cf source emits neutrons by spontaneous fission. It has an effective half-life of 2.645 years, with a spontaneous fission half-life of 85.5 years. The encapsulation is illustrated in Figure 2.2.1.1. The encapsulated source has an outer radius of 0.47 cm and a length of 3.76 cm, not including the small stem attached for safer handling. The ISO standard neutron fluence spectrum from this source is available in Appendix D. On 12/31/2010, the source mass was 13.078 µg, giving a source strength of 3.03×10^7 neutrons/second based on an emission rate of 2.314×10^6 per second per microgram of

Cf-252 [13]. Source strength adjustment for radioactive decay and source anisotropy are discussed later in this chapter. The source is modeled in MCNP using a Maxwellian distribution with temperature of 1.42 MeV.

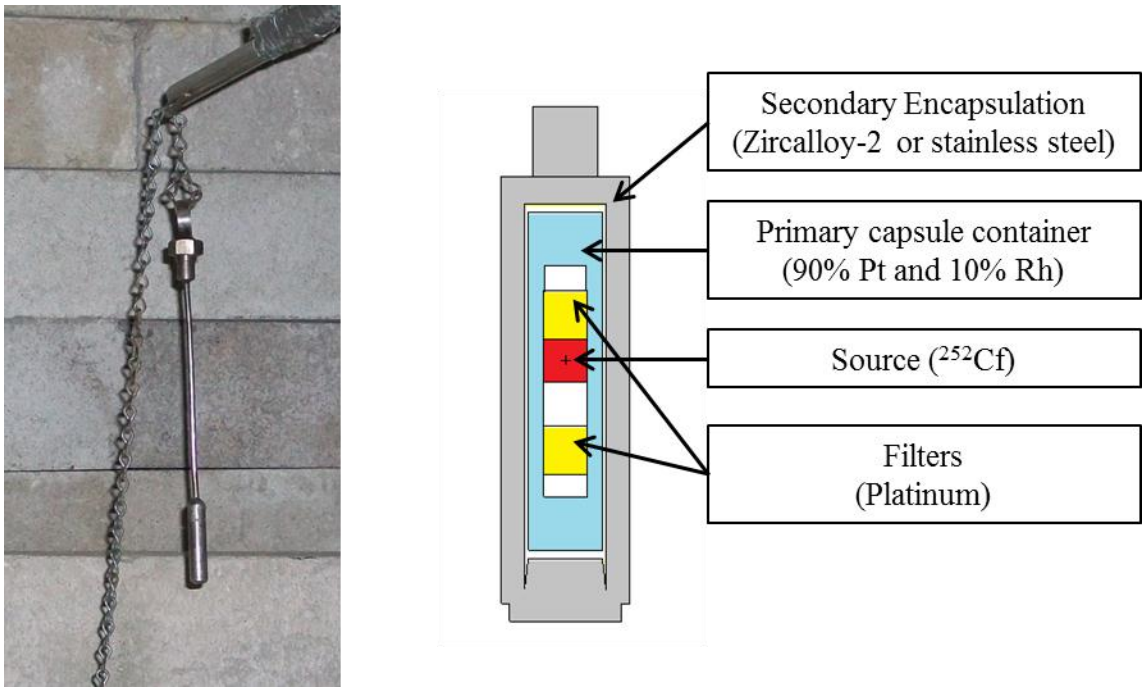

Figure 2.2.1.1 Encapsulation of ^{252}Cf Source

Two difficulties were encountered in using this source. First, its cylindrical geometry had to be adapted for centering in some of the attenuating spheres that had spherical source cavities. The source was positioned in the spherical cavities by inserting it into a styrofoam ball (diameter = 6.1 cm) with a hole cut into it to fit the ^{252}Cf source. Styrofoam was assumed to be of sufficiently low density as to not be included in the neutron transport calculations [14]. This premise was tested with MCNP by placing the ^{252}Cf source in a Styrofoam sphere and comparing the results to the bare source. The

validation of this premise can be seen in Appendix D. The second issue was that the stem, originally designed to unscrew from the source, could not be unscrewed for measurements. This caused the experimental setups to need adjustment to accommodate the metal stem, thereby reducing the spherical symmetry. The source/sphere systems were modeled including that asymmetry and it is discussed in the sections on the attenuator/shielding sections. Most notably this occasionally forced the ^{252}Cf source into a horizontal orientation rather than the preferred vertical orientation pictured in Figure 2.2.1.1. The resulting anisotropy effect was accounted for by the modeling of the actual measurement geometry.

2.2.2 AmBe Source

The AmBe source emits neutrons via the $^{9}Be(\alpha, n)^{12}C$ reaction using the 5.486 MeV alpha particles emitted by ^{241}Am. ^{241}Am has a half-life of 432.2 years, so no decay correction is needed for the measurement period. The AmBe source is a spherical source that was first used at NASA to do shielding studies [6]. The source construction is illustrated in Figure 2.2.2.1. (A non-radioactive replica of the source is pictured on the left, to minimize dose during photography.)

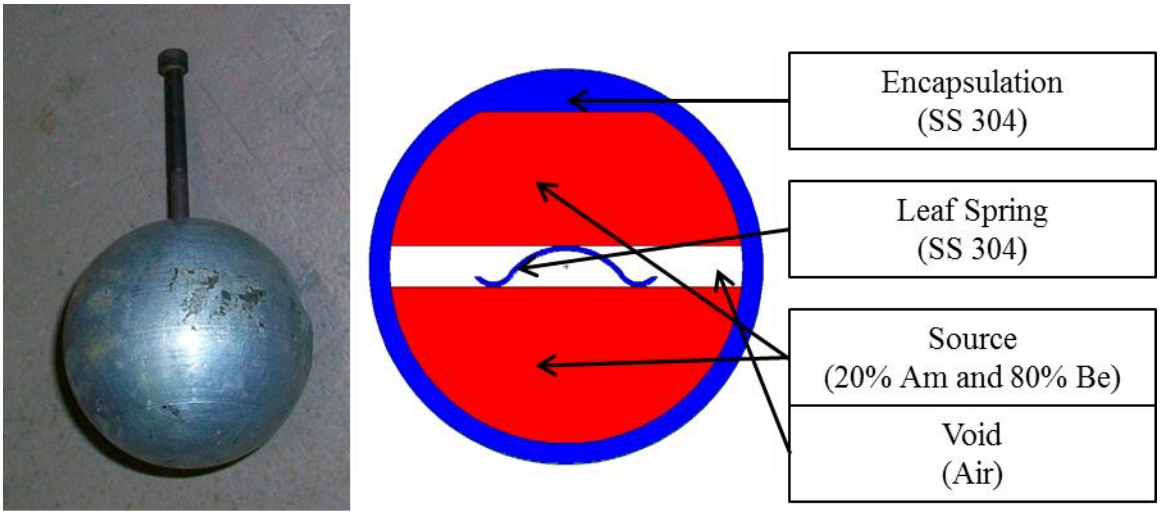

Figure 2.2.2.1 Encapsulation of AmBe Source.

The encapsulated source has an outer radius of 3.05 cm not including the small screw attached for safer handling at the top of the source. The ISO reference neutron spectrum for AmBe is in Appendix D. The source strength was first constructed in January, 1966 and when decayed to the experimental period, the source strength is 1.2 x 10^8 neutrons/second [15]. The source is modeled in MCNP using the energy distributions provided by the NASA manual [15].

The AmBe source fit several of the moderator geometries perfectly as they were originally designed for use with it [6] and its screw is detachable, greatly reducing some of the difficulties faced when placing the ^{252}Cf source with its stem attached. However, the AmBe source presents a higher dose rate when handling, requiring careful planning to reduce exposure during source movements [16].

2.3 Moderators

Using the two sources as bare sources and the attenuating/shielding spheres, a total of 12 unique neutron fields (including each source without moderation) can be generated. The spheres used to alter the Cf-252 and AmBe source spectra are beryllium, lead, iron, tantalum, polyethylene, and heavy water. (Due to geometric constraints, i.e. the absence of a spherical cavity in the center, only the ^{252}Cf source could be placed in the last two aforementioned moderators.)

2.3.1 Beryllium Sphere

The beryllium sphere was selected because beryllium is a neutron multiplier, having a significant (n, 2n) reaction. The (n, 2n) reaction reaction threshold is 2.3 MeV [17]. Since a greater fraction of the AmBe neutrons are above this energy and the source strength is higher, more multiplication will occur for the AmBe source than the Cf-252 source. In either case, this will result in larger magnitude neutron fluence from the same sources, albeit at possibly lower energy levels due to scattering and absorption. A photograph of the Be sphere and its MCNP model with the different sources in it are pictured in Figure 2.3.1.1.

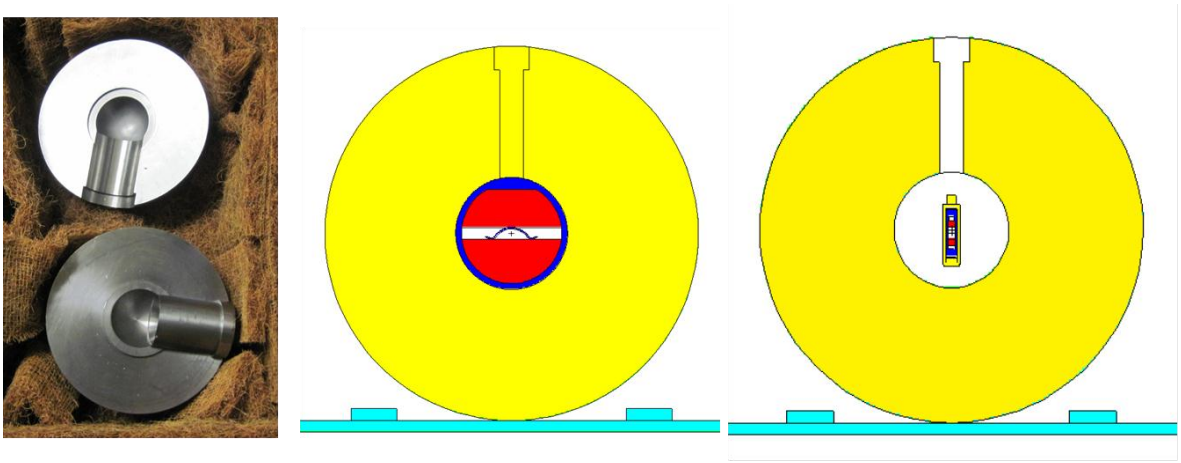

Figure 2.3.1.1. Beryllium Sphere and MCNP Models. The turquoise piece is the aluminum mounting stand and an aluminum ring to keep the sphere from rolling.

The beryllium sphere is machined into two hemispheres that lock together tightly. It also has a removable plug (pictured in Figure 2.3.1.1) that has a concentric smaller removable plug (not pictured, but depicted in the MCNP diagram.) Due to the inability to remove the stem of the ^{252}Cf source, this smaller plug had to be removed from the beryllium sphere for that measurement set, and was appropriately modeled in MCNP.

The beryllium sphere is not excessively heavy, but did require handling with care due to the toxicity of the metal. The sphere was placed on an aluminum table for measurements, also shown at the bottom of the MCNP model.

2.3.2 Lead Sphere

The lead sphere available at Georgia Tech is 15.25 inches (38.735 cm) in diameter. It is of interest when designing detectors attempting to track SNM, as lead is a likely gamma ray shielding choice for smugglers. Its large atomic number results in little

slowing down of neutrons per scatter. It has an (n, 2n) threshold of about 11 MeV. The sphere and its MCNP model are pictured in Figure 2.3.2.1 below.

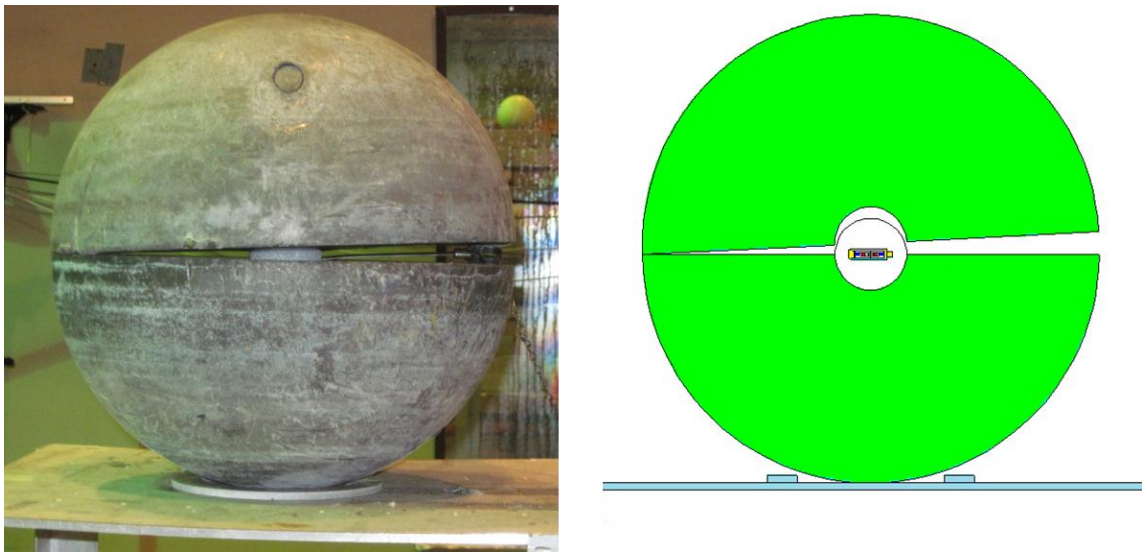

Figure 2.3.2.1 Lead Sphere and MCNP Model.

The lead sphere was manufactured as two hemispheres that lay on each other without interlocking. There is a cavity in the center sized correctly for the AmBe source or the styrofoam-mounted ^{252}Cf source. Pictured and modeled above is the situation caused by the ^{252}Cf source's stem. The detector was placed in the opposite direction from the opening caused by the stem to minimize impact of the air gap, but the gap was modeled in MCNP. (The AmBe source caused no issues in closing the sphere correctly.)

The lead sphere weighs over 800 pounds, and proved challenging to lift into place on the aluminum table. The top of the sphere had a convenient removable plug that could be replaced by a steel bar to lift with, but the bottom half had no such place to lift from.

A machinist had to create a lifting assembling for use with the crane to move this into position. The assembly was removable once the lead sphere was in position.

2.3.3 Iron Sphere

The iron sphere, strictly speaking, was made of steel, and had low concentrations of carbon, manganese, phosphor and sulfur [18]. It did consist of over 99% iron and thus retained its moniker. (The actual composition was reflected in MCNP and is shown in Table 2.3.3.1.) The overall radius of the sphere is 38.1 cm, although the sphere is made of truncated conical sections which approximate a sphere. The sphere and its MCNP model are pictured in Figure 2.3.3.1.

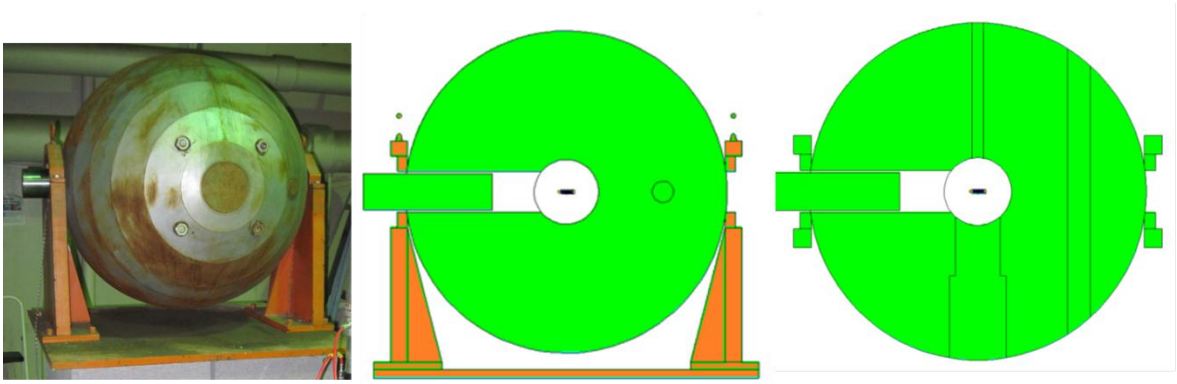

Figure 2.3.3.1 Iron Sphere and MCNP Model (top-down view on right)

Table 2.3.3.1. Composition of Iron Sphere

Composition of Iron Sphere	
Element	Weight %
Iron	99.283
Carbon	0.21
Manganese	0.47
Phosphor	0.013
Sulfur	0.024

The iron sphere was machined as one solid piece constructed out of multiple sandwiched layers. There are four different ports for inserting sources or detectors; all but the one pictured were completely plugged with iron. The central cavity was designed for larger sources than those used, actually to accommodate an accelerator drift tube and target. A styrofoam support structure was used for both sources. Pictured in Figure 2.3.3.1 is the displacement of the final plug caused by the ^{252}Cf's stem. This stem also forced the horizontal source orientation in this sphere. Both are modeled in MCNP. To minimize dose while handling the AmBe in this configuration, the screw and cord were left on, creating a slight displacement in the left plug, which was also modeled.

The iron sphere weighs over 3000 pounds and required a concrete block stand to be constructed. It did come with its own steel support structure (painted orange in Figure 2.3.3.1.)

2.3.4 Tantalum Sphere

The tantalum sphere was selected because, when initially modeled in MCNP, it appeared to shift the neutron fluence spectrum to lower energies while reducing overall

fluence by only 25%. This should be a good test of the analysis in the 0.1 – 1.0 MeV range. The sphere and its MCNP model are pictured in Figure 2.3.4.1.

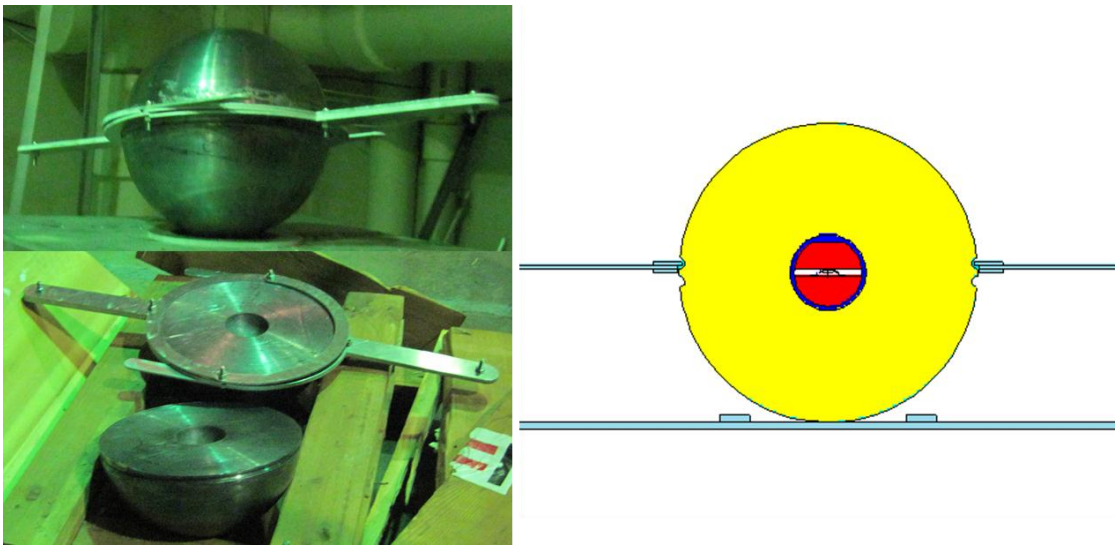

Figure 2.3.4.1 Tantalum Sphere and MCNP Model and the lifting device which was left on during the measurements.

The tantalum sphere has a density of 16.69 g/cm^3 so this 12 cm radius sphere proved difficult to lift. Like the lead sphere, it consisted of two non-interlocking hemispheres with a cavity that fit the AmBe source and styrofoam-mounted ^{252}Cf source. The hemispheres each had small grooves near their equator that could be used to grip for lifting. The bottom sphere was able to be lifted onto the aluminum table with the crane using a wide nylon strap. The top sphere, lacking the lifting point provided on the lead sphere, required an elaborate aluminum attachment to be machined and attached. In order to reduce received dose for the experimenters, it was decided to leave this aluminum attachment in place for the duration of the measurements and model it in MCNP.

The ^{252}Cf's stem only caused very minor hemisphere displacement in this setup, as the end of the stem (which is thicker than the rest of the stem) resided outside the back of the sphere.

2.3.5 Polyethylene Sphere

The polyethylene sphere was selected because its neutron scattering properties are well-known and could be used to compare experimental results to established data. The sphere and its MCNP model are pictured in Figure 2.3.5.1. The sphere is 15.24 cm in radius and did not prove especially difficult to mount on its aluminum stand or to model. Since it is constructed out of one solid piece of material with a hole drilled for only a small source, the AmBe source could not be used with this moderator. The stand was not included in the computation.

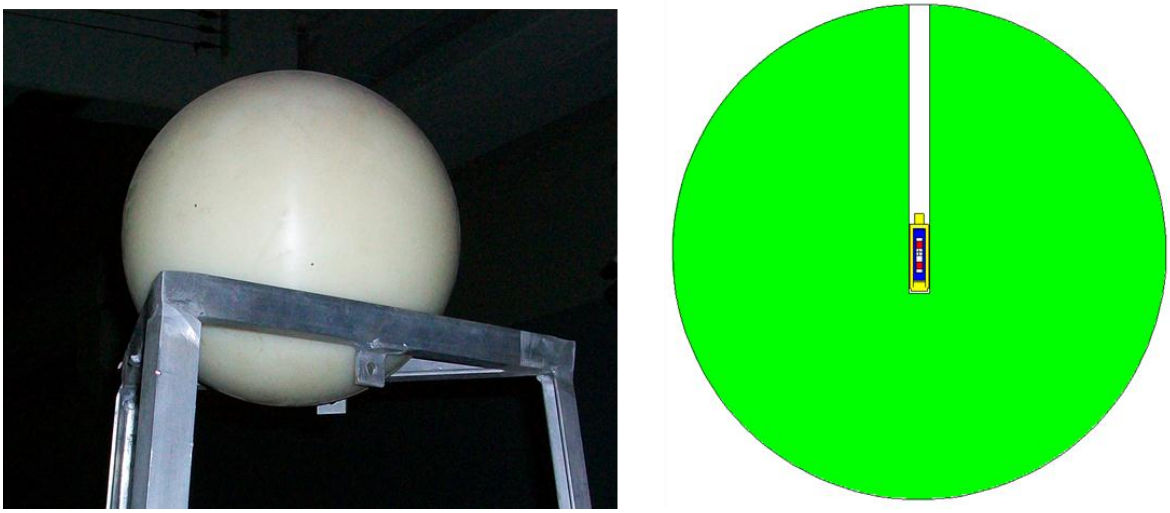

Figure 2.3.5.1 Polyethylene Sphere and MCNP Model

2.3.6 Heavy Water Sphere

The heavy water sphere was selected because it is a standard for calibrating dosimeters and neutron survey instruments [19, 20]. Since the spectrum from this sphere has a substantial number of neutrons below 1 MeV, it is used to calibrate neutron instruments for use in nuclear reactor facilities. The sphere and its MCNP model are pictured in Figure 2.3.6.1.

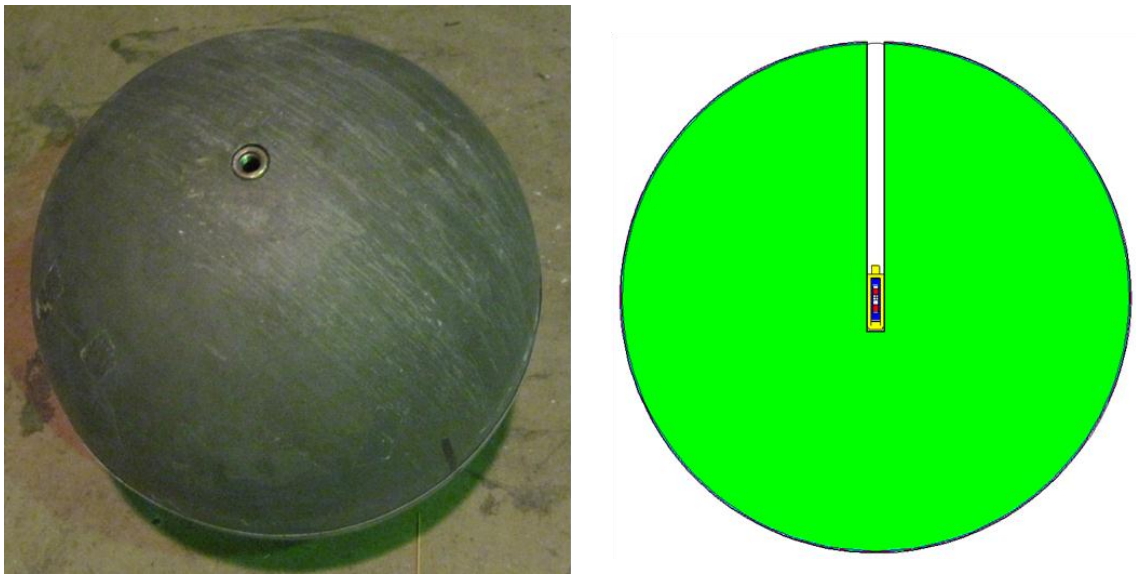

Figure 2.3.6.1 Heavy Water Sphere and MCNP Model

The heavy water portion of the sphere is 15 cm in radius and is contained in a thin stainless steel shell 0.08 cm thick. The moderator also comes with a thin, removable cadmium cover 0.05cm thick, which was left in place. This removed neutrons with energies below the "cadmium cutoff" of 0.414 eV. Like the polyethylene sphere, its

cavity was not large enough to use with the AmBe source, but otherwise it proved to have no difficulties in mounting on its aluminum stand or in modeling.

2.4 ESJ Method with Axton Correction

Unfolding the raw count rate data into a neutron fluence spectrum requires corrections for room scattering, air scattering, and the geometries between the source and detector. A proven technique involves performing a modification for geometry of the system, then applying a least-squares fit to solve for the scattering corrections. This technique is known as the ESJ fitting method with the Axton correction. The discussion of this technique below is derived directly from the works of J. B. Hunt [21] and J. E. Sweezy, et al. [22]. Note that since the MCNP model includes air scatter, the ESJ method was followed but with setting air scatter coefficients to zero.

In an ideal measurement room of infinite dimensions, a perfect vacuum, and using a source and detector combination that required no supporting structures, there would be no room-scatter or air-scatter. The dead-time corrected count rate of the detector, C, would be inversely proportional to the square of the source-detector distance, D for a point source. The product of these two, CD^2, is known as the characteristic constant, and follows the inverse-square law.

In realistic measurement rooms of smaller dimensions, room and air scatter must be accounted for, and significant modification of the original relationship is required. Accounting for the source's anisotropy, room-scatter, and air-scatter yields:

$$C(D) = \frac{KF_I F_1(D) F_2(D)}{(D+R)^2}$$

where D is the source-detector distance, F_I is the source anisotropy correction factor, $F_1(D)$ is the correction for the non-uniform illumination of the detector, $F_2(D)$ is the air and room scattering correction factor, R is the radius of the spherical detector (including any Bonner sphere on it), and K is the scatter-free detector response at a unit distance from the source in a vacuum.

The source anisotropy factor is specific to each source design, and is a function of the angle between the source orientation and the line-of-sight to the detector. It can be ascertained experimentally or modeled. In this research, values of anisotropy from manufacturer's data and previous research were obtained [23], but since the geometry and orientation of the source could be modeled in MNCP, this correction was not needed.

The need for the $F_1(D)$ geometric correction factor was shown by E. J. Axton [24]. The correction is due to the divergent, non-parallel beams coming from a source impacting a much larger detector sphere at a close source-detector distance D. J. B. Hunt derived an exact expression for this factor from Axton's theory [20]:

$$F_1(D) = 1 + \delta\left\{\frac{2D_o^2}{R^2}\left[1 - (1 - \frac{R^2}{D_o^2})^{0.5}\right] - 1\right\}$$

D_o is the effective center distance between the source and detector center, and is generally close to $D + R$. δ is an empirical factor accounting for the relative effectiveness of the extra neutrons present in a divergent beam above what would be expected from a

parallel beam, and a value of 2/3 is generally accepted. This Axton correction is used correcting count rates in this research, and was largest when the 12" Bonner sphere was nearest the source.

There are several techniques for evaluating the $F_2(D)$ scattering correction factor. The ESJ model assumes that the air scattering component is very small, and evaluates the $F_2(D)$ as:

$$F_2(D) = (1 + SD_o^2)(1 + AD_o)$$

S is the room-scattered component, and *A* is the air-scattered component (set to zero for this research as the air scatter is modeled in MCNP and does not need correcting for comparison). Substituting into the original $C(D)$ equation yields:

$$C(D) = \frac{KF_IF_1(D)(1 + SD_o^2)(1 + AD_o)}{(D + R)^2}$$

$$C(D)D_o^2 = KF_IF_1(D)(1 + SD_o^2)(1 + AD_o)$$

$$\frac{C(D)D_o^2}{F_IF_1(D)(1 + AD_o)} = K(1 + SD_o^2)$$

Defining $C_1(D)$ as the anisotropic, geometric, and air-scattered corrected count rate on the left hand side of the equation yields:

$$C_1(D)D_o^2 = K_1(1 + SD_o^2)$$

This form of the equation can be solved using a linear least-squares fitting technique to find values for K_1 and S. Since some of these factors vary with the size of the Bonner sphere (which affects the detector radius R), the fit is done independently for each Bonner sphere size within a source/moderator combination. There are data points reflecting seven different D's for each Bonner sphere in the measurement set.

A corrected count rate is thus obtained for each Bonner sphere at a unit distance (1 meter) for each source/moderator combination. This count rate data is now ready to be unfolded into a neutron spectrum.

2.5 Unfolding with BUNKIUT and BUMS

Unfolding the raw count rate data into a neutron fluence spectrum requires knowledge of the response of each Bonner sphere to a given neutron spectrum. The discussion of this unfolding process closely follows that given by E. A. Burgett [25]. The count rate of each sphere is related to the response function and neutron spectrum through the following first order Fredholm integral equation:

$$C_i = \int_0^\infty R_i(E)\varphi(E)dE \qquad i = 1,2,3 \rightarrow N$$

where C_i is the count rate of the ith Bonner sphere, $R_i(E)$ is the response function for the ith detector at energy E, and $\varphi(E)$ is the energy-dependent neutron flux.

To solve this equation, it is reduced into discrete groups created by energy bins. This allows the equation to be written in matrix form:

$$C_i = \sum_{g=1}^{G} R_{i,g}\varphi_g \qquad i = 1,2,3 \rightarrow N$$

where g represents each energy group, G represents the highest energy group, $R_{i,g}$ is the response function of the ith detector in the gth energy group, and φ_g is the group flux between E_g and E_{g-1}.

To create a descriptive spectrum, it is desired to have a large number of energy groups G, often in excess of the number of detectors (Bonner spheres) I. This results in a matrix equation that is underdetermined, lending itself to an iterative solution. To get physically meaningful results, a good selection for the initial starting spectrum is important for the iterative process.

The BUMS system designed by J. E. Sweezy et al. integrates multiple computer iterative unfolding codes, including SPUNIT, BON, MAXED and SAND-II [26]. It accepts inputted count rates from a BSS, and allows the user to set various parameters, including selecting the starting spectrum, unfolding method, and unfolding matrix. The user interface is shown in Figure 2.5.1 below.

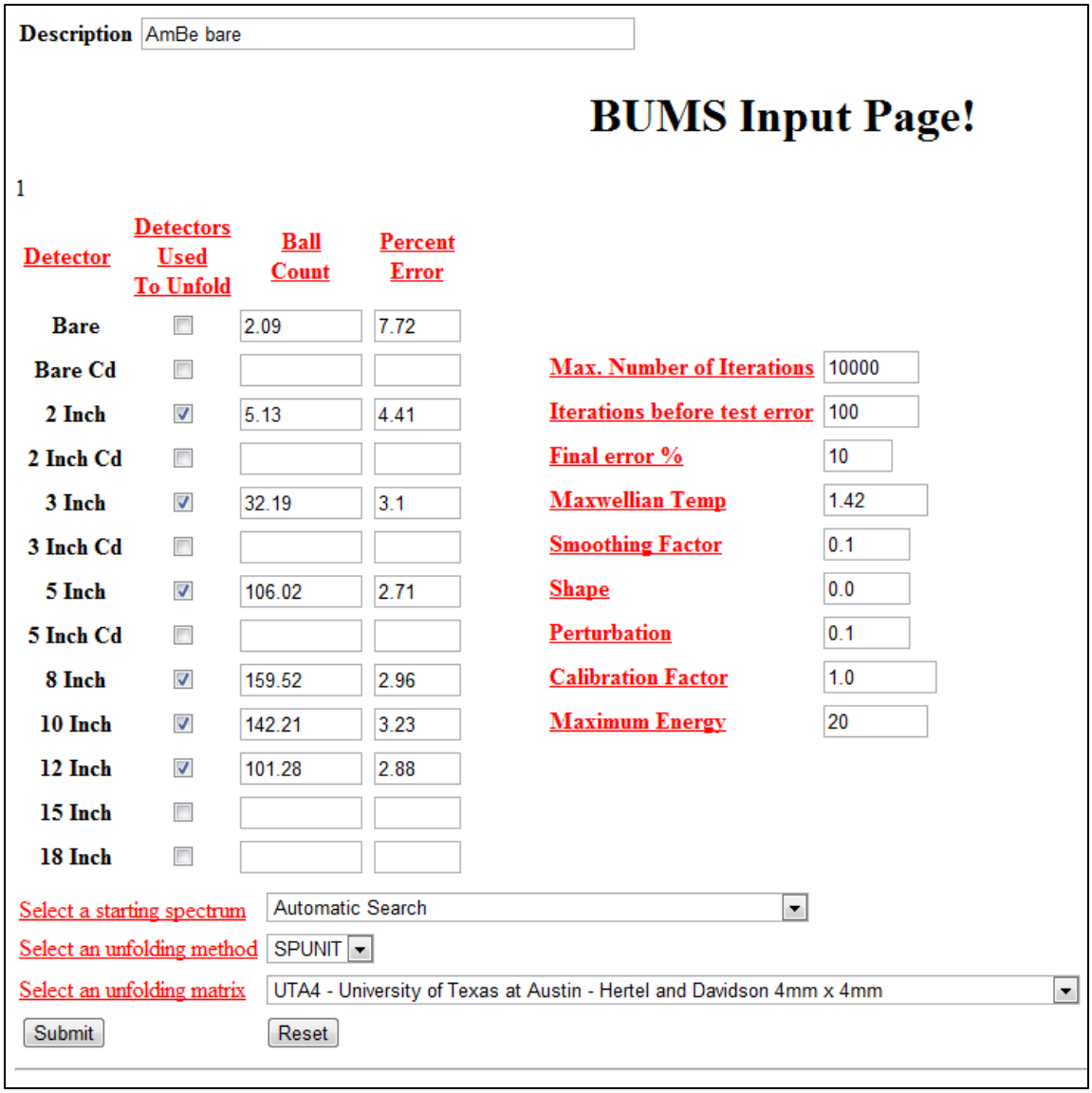

Figure 2.5.1. BUMS User Interface

The BUMS system features an automatic search option for the starting spectrum, which runs the input count rates against all the available starting spectra and determines which fit gives the least amount of error. This option was used for source/moderator combinations that had known spectrum in BUMS, and resulted in the correct selection of the starting spectrum each time. This included both bare sources and the ^{252}Cf in the D_2O

moderator. For the combinations that lacked a known baseline spectrum in BUMS, the MAXIET algorithm was used in lieu of a set starting spectrum. This algorithm creates a starting spectrum based on the input count rates, and assumes a general shape with a high-energy Maxwellian peak, a $(1/E)^x$ intermediate energy component, and a thermal peak. The algorithm iterates to fit these parameters to arrive at a starting spectrum which seeds the iterative process that yields an unfolded spectrum for the input count rates [26].

The BUMS system outputs a large amount of information based on the fluence, including the fluence per unit lethargy as a function of energy and the average error in the ball counts (a function of the difference between the measured and calculated ball counts). It also provides the total fluence and a variety of dose equivalent quantities including the ICRP-74 ambient dose equivalent H*(10) values. The table and these two values are used in the comparison to both known spectrums and values, and the MCNP calculations, to evaluate the validity of the experimental process and to generate new starting spectra for BUMS. A sample of the BUMS output with comments showing which data are used for this analysis is available in Appendix E.

CHAPTER 3: COMPUTATIONAL MODELS

Computational modeling and simulation can be used to generate complementary information about experimental procedures and results while simultaneously allowing for perturbation of testing parameters to see changes in results without conducting additional time-consuming or expensive experiments. Consistency between known values, experimental data, and computational model output is necessary for the latter to be a reliable tool in the research process. A goal of this research is to produce both valid neutron energy spectra and baseline computational input codes for the source/moderator combinations being characterized. These spectra and codes can provide starting data for further research using these moderated neutron fields.

3.1 MCNP Code

The MCNP code was developed by Los Alamos National Laboratory uses the Monte Carlo method to simulate the propagation of particles, including neutrons and photons [27]. It is able to integrate the latest cross-sectional data for simulation and can generate output based on user-defined tallies. The source and moderator geometries and composition, along with the desired tally scheme, are created in an MCNP input file. The input files designed for the new source/moderator combinations being characterized will, when validated, be outputs of this research and useful to future work with these neutron fields.

This research used MCNP 5 version 1.51. All input files were created using a text editor, but could be visualized and checked for geometric consistency using the included

VISED X_22S visual editor [28]. This release of MCNP 5 also included compiled Windows binaries including an executable capable of multithreading (mcnp5_threads.exe). This greatly reduced computational time when using high-end desktop machines with six core processors.

3.2 MCNP Input Files

The MCNP input files created used some universal parameters that are summarized in Table 3.1.1 below. The complete input files are available in Appendix B.

Table 3.1.1. MCNP Universal Input Parameters

Parameter	Value	Comment
Number of particles	1×10^{7}	Point of diminished return on error reduction for these models
Tally sphere radius	100 cm	Enclosed all models and allowed for direct comparison of fluence spectra with BUMS output
Energy Cutoff for neutrons	1×10^{-10} eV	Reduced computational load for particles below thermal energy threshold and beyond energy resolution of experimental setup
Energy Cutoff for photons	1×10^{-2} eV	Reduced computational load for photons that had little effect on calculated dose rates
Composition of Air	7014 -.7558 8016 -.2314 18000 -.0128	Simulated air consisted of 75.58% N, 23.14% O, and 1.28% Ar by weight

The tallies used for this research include an F2 neutron surface crossing tally collected on a 100 cm sphere, and subdivided into 10 regions each subtending an equal solid angle. Also tallied was the ICRP 74 dose equivalence for neutrons on the same

tally surface. Finally, for source/moderator combinations with significant geometric asymmetries, a point detector was used at 100 cm in the direction where the actual detector was placed during the experimental setup. Samples of these output tallies are available in Appendix F.

When available the S(α, β) data was used to better simulate thermal neutron behavior. Appendix G of Volume I of the MCNP5 manual [27] lists those elements for which such data exist. These materials included deuterium when combined into heavy water, metallic beryllium, aluminum, and hydrogen in polyethylene. The exact data used is noted in the input files in Appendix B.

Air (and hence air scatter) is modeled in the final MCNP input files. The tally was set on a spherical surface 100 cm, and the air extended to 300 cm before the simulation was cut off to account for backscatter.

3.3 MCNP Output and Normalization to Experimental Results

The MCNP fluence tallies used are already normalized per one source neutron so these tallies must be multiplied by the source strength used in the experiments. The source strength used here must be divided by the number of neutrons escaping the source per source particle generated by MCNP, which is a significant factor for the AmBe source and it's inherit neutron multiplication. This factor was reported in the MCNP model as 1.034.

Likewise, the total fluence and ICRP 74 ambient dose equivalent had to be multiplied by the source. Finally, the group fluences must be normalized per unit lethargy:

$$\frac{\varphi_g}{lethargy} = \frac{\varphi_g}{\ln \frac{E_g}{E_{g-1}}}$$

.

CHAPTER 4: RESULTS

This chapter compares the results from the experimental data processed as outlined in Chapter 2 with the computational model outputs detailed in Chapter 3. The total fluences, total ICRP 74 ambient dose equivalents, and neutron fluence spectra will be compared and discussed.

4.1 Total Fluence

The total fluence is expressed in terms of neutrons/cm^2/second. It is specific to the sources and moderators in use at the Georgia Institute of Technology and will be affected over time by radioactive decay. A comparison of the BUMS output and the MCNP output is in Table 4.1.1 below.

Table 4.1.1. Total Fluence Rate Comparison

Fluence Rate (n/cm^2/second)			
	MCNP	BUMS	Ratio
Cf-252 Bare	254.66	263.6	1.04
Cf-252 Be	276.20	289.5	1.05
Cf-252 Pb	314.92	259.2	0.82
Cf-252 Fe	232.45	256	1.10
Cf-252 Ta	201.15	196.1	0.97
Cf-252 Poly	64.59	68.37	1.06
Cf-252 D2O	225.00	223.3	0.99
AmBe Bare	951.25	1074	1.13
AmBe Be	1238.85	1272	1.03
AmBe Pb	1037.59	1054	1.02
AmBe Fe	919.11	930.1	1.01
AmBe Ta	821.10	784.9	0.96

The fluence rate reported by BUMS shows an overall good correlation with that calculated from the MCNP codes. The expected increase in flux due to neutron multiplication in beryllium is observed. For most source/moderator combinations, BUMS is close to or slightly over reports the flux compared to the MCNP code. The exceptions are the ^{252}Cf source in lead and polyethylene. The discrepancy in lead could be due to the unusual geometry forced by the attached stem, as pictured in Figure 2.3.2.1, and failure of the model to fully capture the geometry. The ideal representation of the stem-modified geometry in MCNP has the upper half the source positioned where it has an almost clean line-of-sight to the detector, passing only through a very small amount of lead at the contact point of the two hemispheres. In reality, the alignment could not be that perfect, and even a small displacement in the alignment causes a lot more lead to be in the line-of-sight. In addition, the equator of the two lead spheres may have tilted forward due to the shift in the center of gravity, again placing more lead in the line-of-sight. This results in an overreporting of flux from the MCNP code. To test this theory, the MCNP code was reran with the point detector displaced various vertical distances from the perfect centerline. A total displacement of 5cm (2.9 degrees off-equator) matched the experimental results closely. In the future, the stem must be removed from the ^{252}Cf for a useful field.

There was also underreporting of the flux from the AmBe unmoderated source. This experiment was completely redone with similar results. A systemic error is suspected and possible causes are discussed in Chapter 4.3.5.

4.2 ICRP 74 Ambient Dose Equivalent H*(10)

The ICRP 74 ambient dose equivalent H*(10) is the dose equivalent in the ICRU sphere at a depth of 10 mm and is the operational quantity that area monitors are to reproduce [29]. It is measured in units of mSv/second. A comparison of the BUMS output and the MCNP output is in Table 4.2.1 below.

Table 4.2.1. ICRP 74 Ambient Dose Equivalent H*(10)

ICRP 74 Ambient dose H*(10) (mSv/second)			
	MCNP	BUMS	Ratio
Cf-252 Bare	9.68E-06	9.7E-06	1.00
Cf-252 Be	6.56E-06	6.77E-06	1.03
Cf-252 Pb	1.13E-05	8.8E-06	0.78
Cf-252 Fe	5.06E-06	5.09E-06	1.01
Cf-252 Ta	5.72E-06	5.36E-06	0.94
Cf-252 Poly	1.11E-06	1.25E-06	1.12
Cf-252 D2O	2.5E-06	2.45E-06	0.98
AmBe Bare	3.63E-05	3.67E-05	1.01
AmBe Be	3.1E-05	3.09E-05	1.00
AmBe Pb	3.55E-05	3.29E-05	0.93
AmBe Fe	2E-05	1.85E-05	0.92
AmBe Ta	2.38E-05	2.12E-05	0.89

The ratio of the BUMS to MCNP measured dose averages around 0.96, but fluctuates between overreporting and underreporting depending on the source/moderator combination. (This average excludes the geometrical issues of the ^{252}Cf in lead setup discussed in the previous section. The alignment change fixed the dose equivalent results as well.) For many of the combinations, the two results align within a few percentage points, a good correlation for a system with limited energy resolution. The BUMS output consistently underreports on the AmBe source combinations, with the iron, lead and

tantalum amounts around 10% lower. This could be due to the maxima and minima shown in the spectrum for iron in Figure 4.3.3.2 and to the scattering in the tantalum. Both of these are discussed in Chapter 4.3.

BUMS closely brackets the MCNP output with the ^{252}Cf source combinations, though it overreports the dose from the polyethylene moderator by 12%. The possible explanations for these discrepancies are currently speculative, and focus on the BSS systems lack of energy resolution in some of the areas where the ICRP 74 dose coefficients are high. Small errors in these energy areas, which are outside of the BSS optimal energy reporting due to the detector response functions shown in Figure 2.1.1.1, could lead to large discrepancies in experimentally obtained dose readings. This combination of relatively important dose-contributing energy groups with those same energy groups lacking resolution in the BSS is most acutely seen in the 10 keV – 0.1 MeV energy range. The ICRP 74 dose conversion coefficients for H*(10) are Table A.42 in the ICRP 74 tables annex [29]. It is likely that this weakness in the BSS system and methodology contributes to the error.

In the following section, the spectra are compared, and figures will show how the neutron fluence spectra for some of these combinations are in the BSS system's less accurate reporting ranges.

4.3 Neutron Fluence Spectra

The total neutron fluence rate spectra are shown in this section. They are displayed in plots of neutrons/cm^2/second/lethargy. Energy level bounds on the figures are selected to maximize the meaningful detail displayed. The charts are paired by

moderator when appropriate. (To visually compare each newly moderated spectrum to its bare source spectrum, see the charts in Appendix G.) Also included is the BUMS output generated when the MCNP generated spectrum is used as the starting spectrum for the BUMS iterative process.

4.3.1 Beryllium Sphere

The beryllium sphere is pictured in Figure 2.3.1.1. The resulting flux spectra are compared in Figures 4.3.1.1 and 4.3.1.2 below.

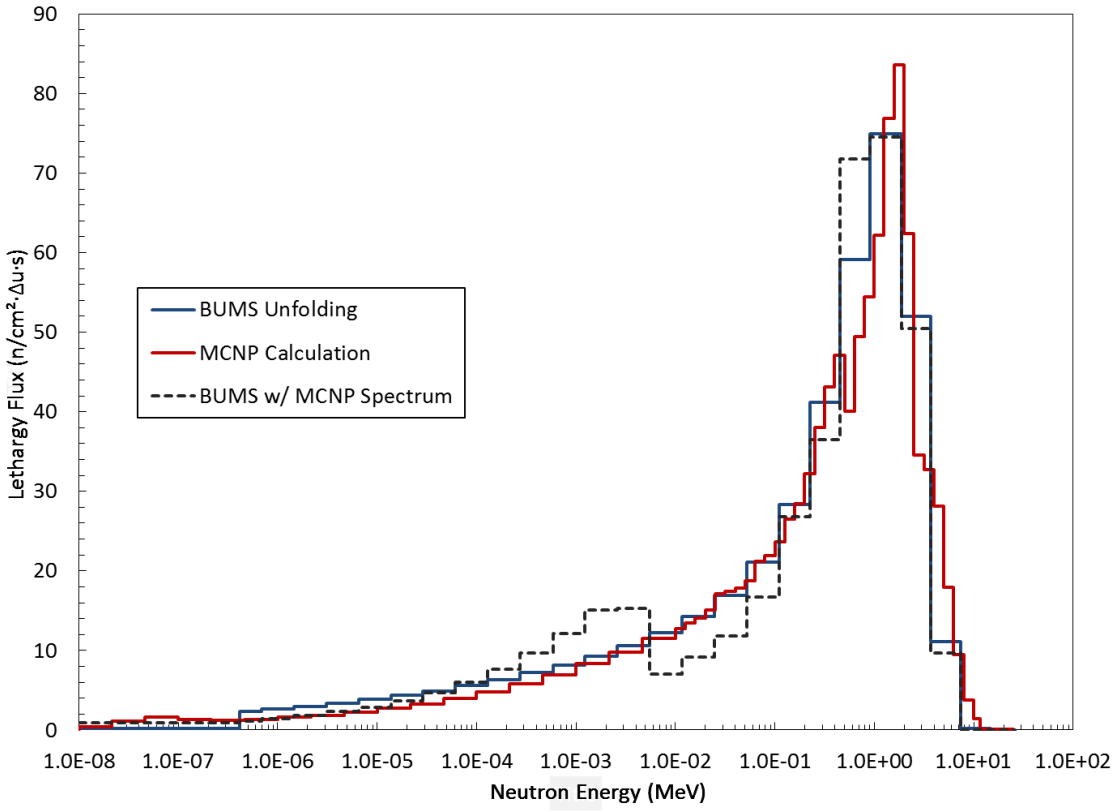

Figure 4.3.1.1. ^{252}Cf / Beryllium Sphere Spectra

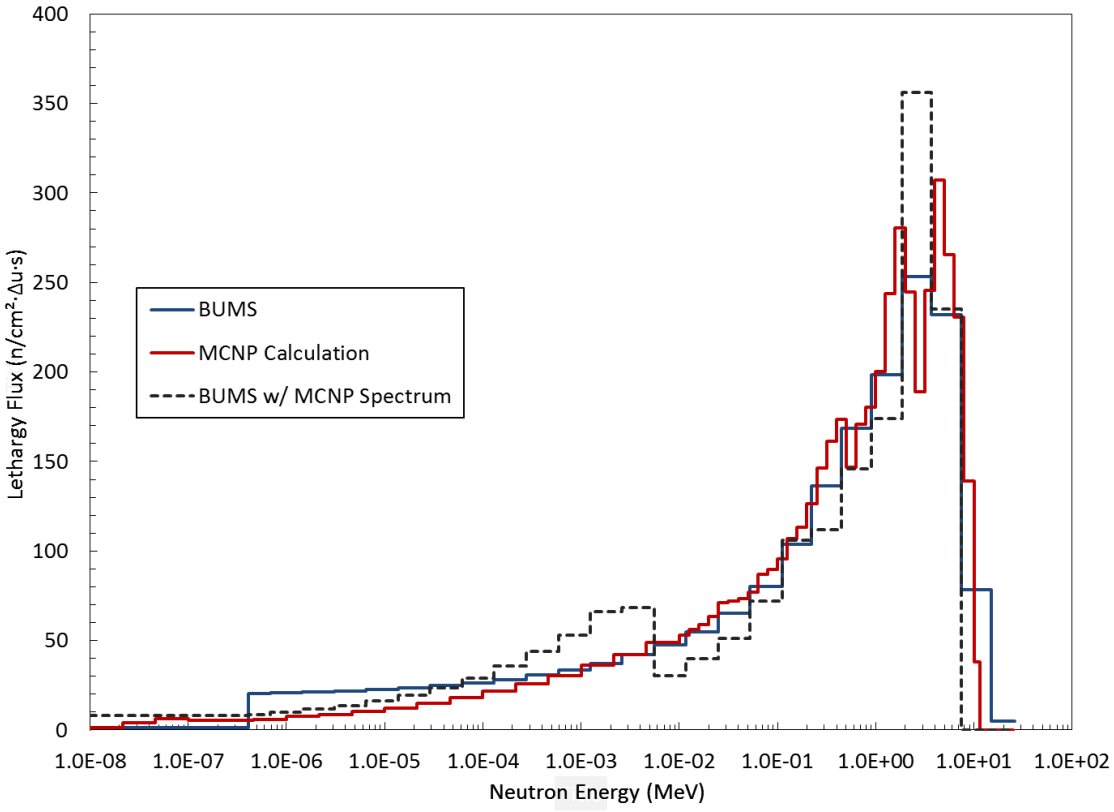

Figure 4.3.1.2. AmBe / Beryllium Sphere Spectra

Both of these spectra show good agreement between the unfolded spectra using BUMS, with a starting spectrum generated by the MAXIET algorithm, and the MCNP calculations. Note that the smaller group structure of the MCNP calculations makes comparison on an energy-by-energy basis difficult since the BBS is a low resolution system. The BUMS energy groups can be arbitrarily tightened, but without more data points, there would be no real increase in energy resolution.

4.3.2 Lead Sphere

The lead sphere is pictured in Figure 2.3.2.1. The resulting spectra are compared in Figures 4.3.2.1 and 4.3.2.2 below.

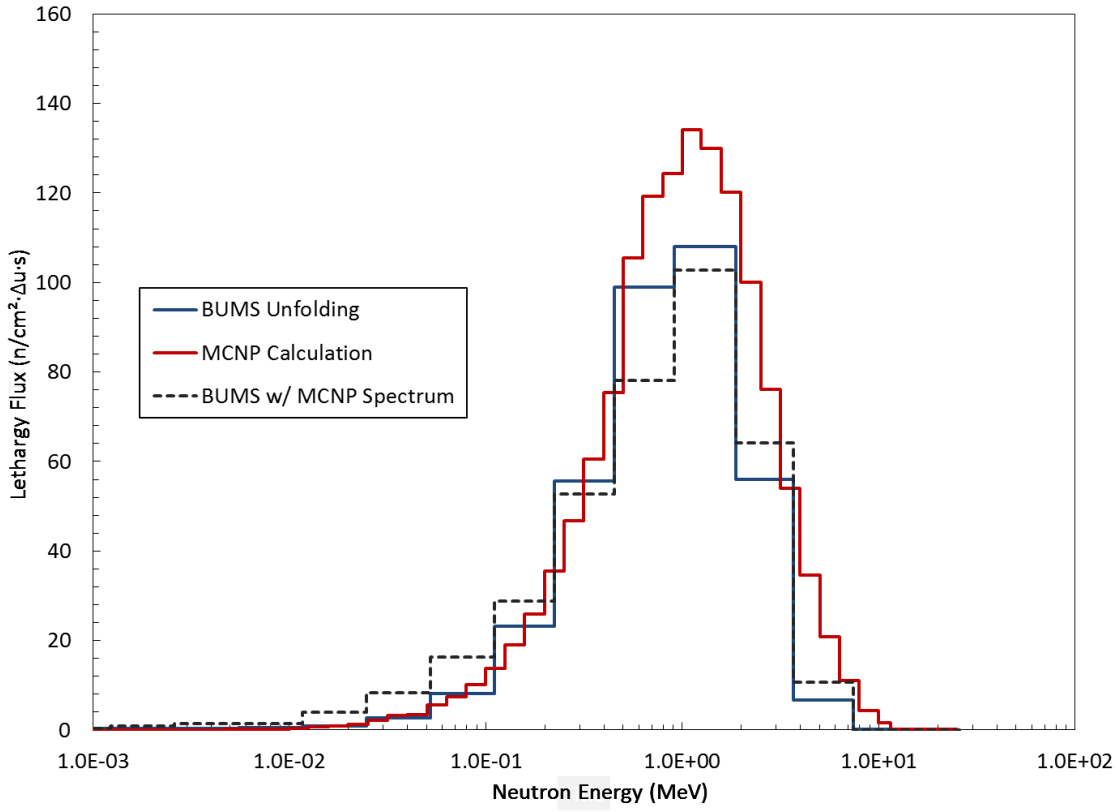

Figure 4.3.2.1. ^{252}Cf / Lead Sphere Spectra

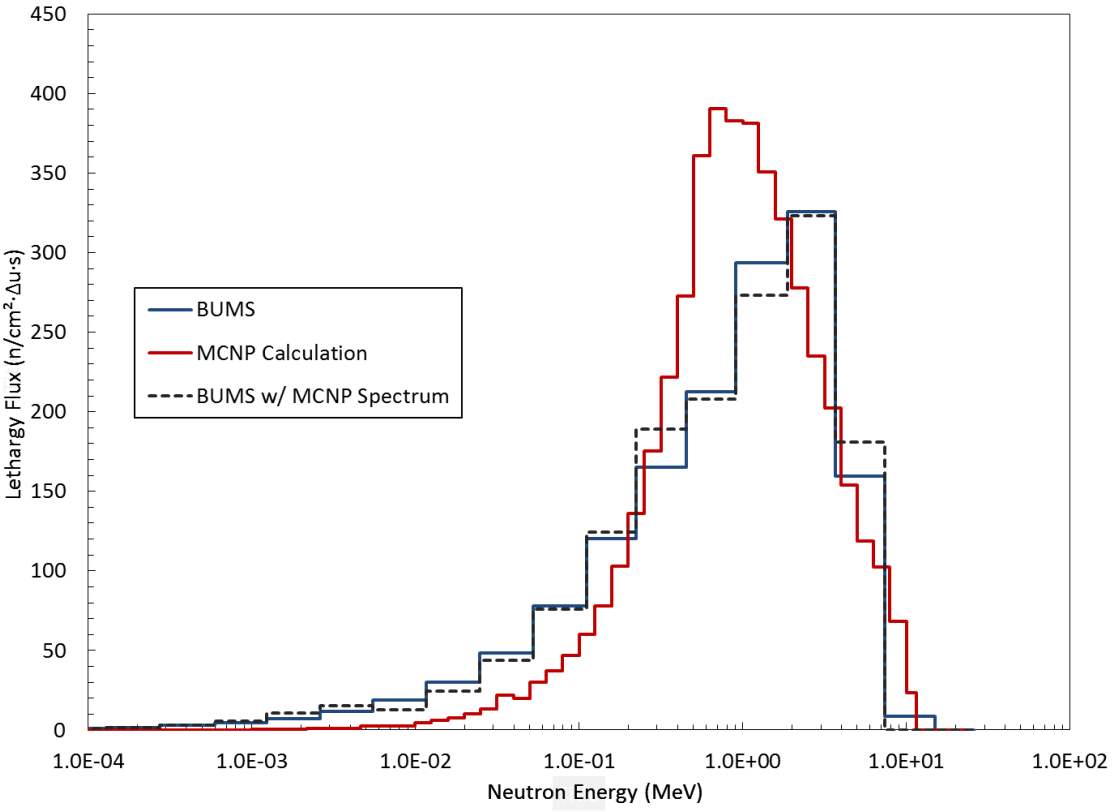

Figure 4.3.2.2. AmBe / Lead Sphere Spectra

The BUMS underreporting of total flux encountered for the ^{252}Cf source in lead can be attributed to the rapid drop off of measured flux above 2 MeV for the BUMS spectrum. The cause of this drop-off is not certain, but could be related to the peculiar geometry shown in Figure 2.1.1.1. This was discussed in more depth in Chapter 4.2. It could also be a function of the lesser energy resolution of the BUMS system, as the MCNP code shows a similar fluence drop-off, but has it happen more gradually with increasing energy.

4.3.3 Iron Sphere

The iron sphere is pictured in Figure 2.3.3.1. The resulting spectra are compared in Figures 4.3.3.1 and 4.3.3.2 below.

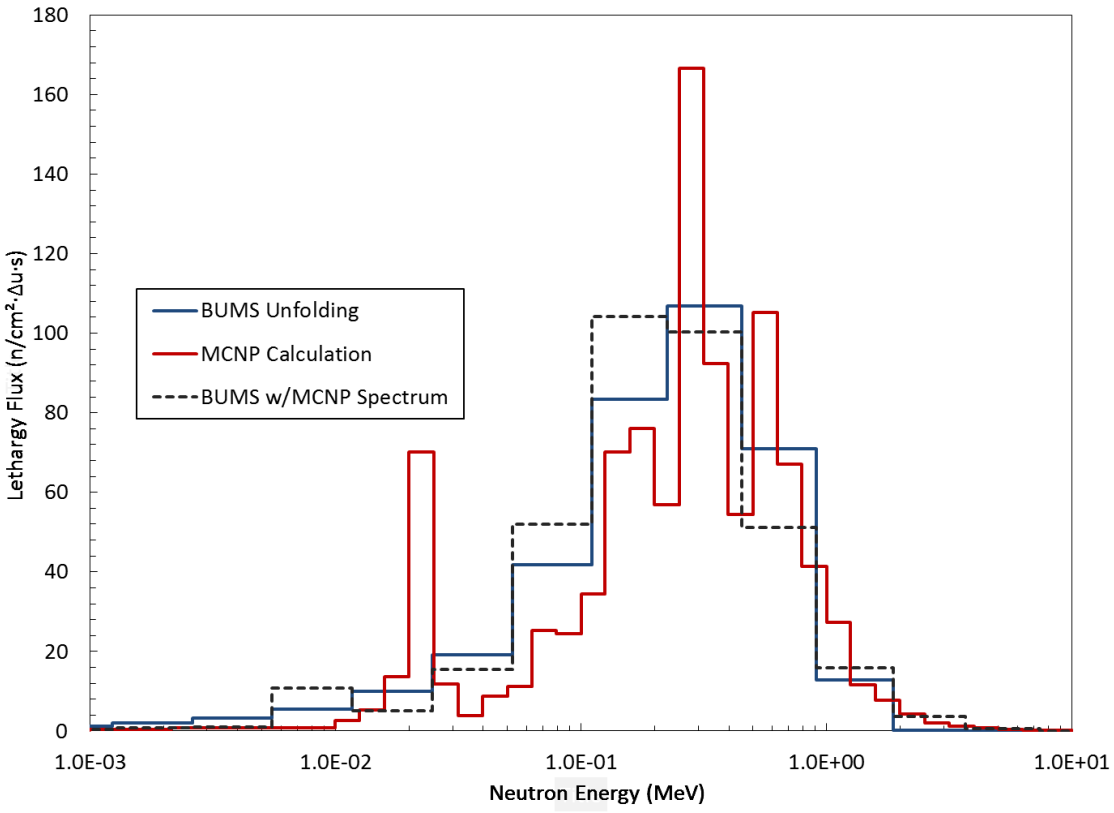

Figure 4.3.3.1. ^{252}Cf / Iron Sphere Spectra

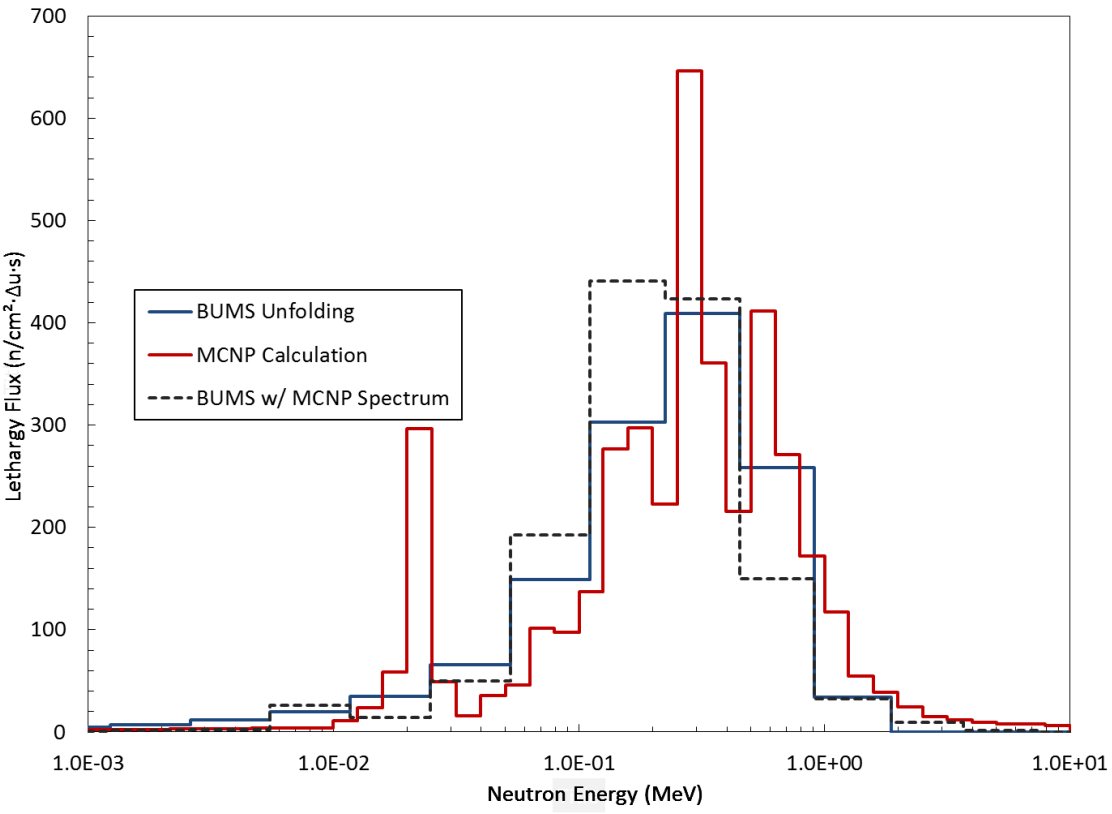

Figure 4.3.3.2. AmBe / Iron Sphere Spectra

The iron spectra strongly show the difference in energy resolution between the two methods. The iron moderator significantly shifts the energy levels of the emitted neutron fluence down towards the sub-MeV range, where the BSS has relatively less energy resolution. The sharp peaks caused by maxima and minima in the iron cross section cannot be replicated by the BSS and could have led to underreporting of dose from the AmBe source. However, the MCNP fluence integrated over the BSS group structure would appear to be close to the BSS group fluencies. While the BSS is not capable of capturing a spectrum with finely detailed energy resolution, it is capable of correctly estimating fluence and dose with a very simple detector setup.

4.3.4 Tantalum Sphere

The tantalum sphere is pictured in Figure 2.3.4.1. The resulting spectra are compared in Figures 4.3.4.1 and 4.3.4.2 below.

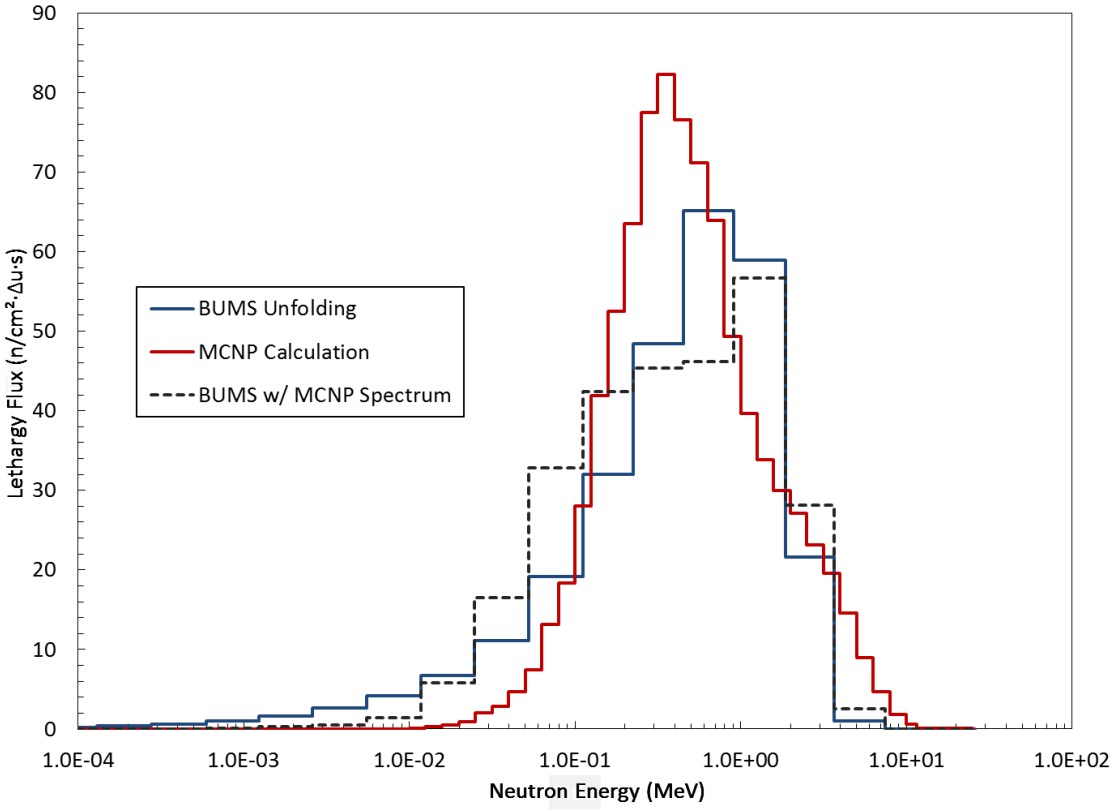

Figure 4.3.4.1. ^{252}Cf / Tantalum Sphere Spectra

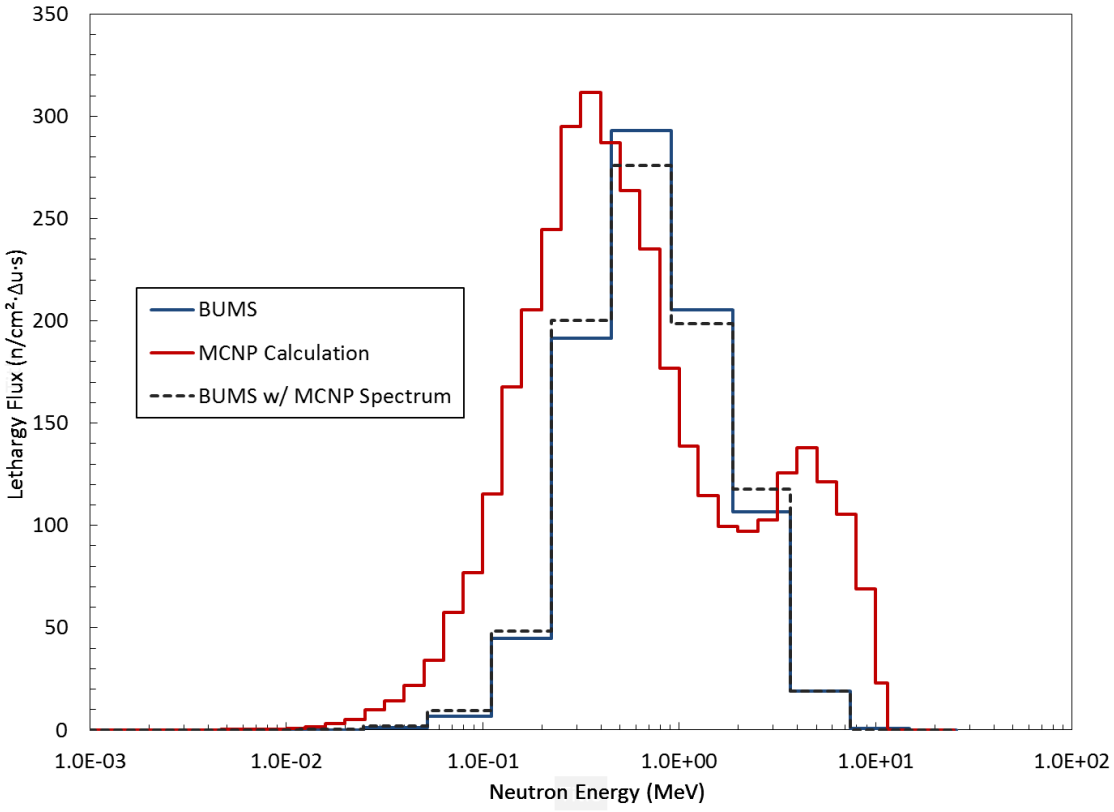

Figure 4.3.4.2. AmBe / Tantalum Sphere Spectra

The tantalum spheres shifted the spectra to lower energy levels as expected, and created neutron fields with smoother changes in fluence than the jagged peaks encounter with the iron moderator. While the overall fluence and dose values tracked reasonably well, these figures show that the BUMS reported peaks did not shift as much as the MCNP peaks. This could again be due to the limits on energy resolution, especially below 1 MeV, for the BSS system. Since some of this energy range is important for the dose conversion chart, it led to an underreporting of dose, especially from the AmBe source.

4.3.5 Bare Source

The bare sources are diagrammed in Figure 2.2.1.1 and 2.2.2.1. The resulting spectra are compared in Figures 4.3.5.1 and 4.3.5.2 below.

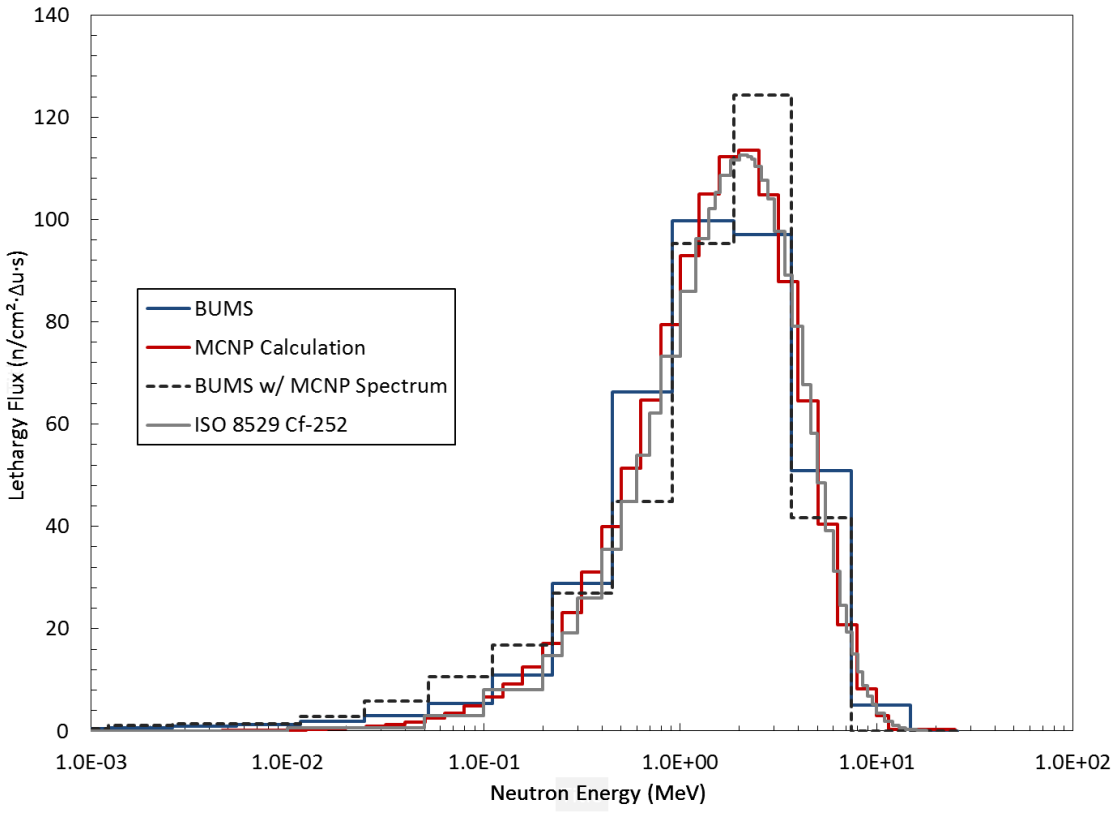

Figure 4.3.5.1. ^{252}Cf Bare Spectra

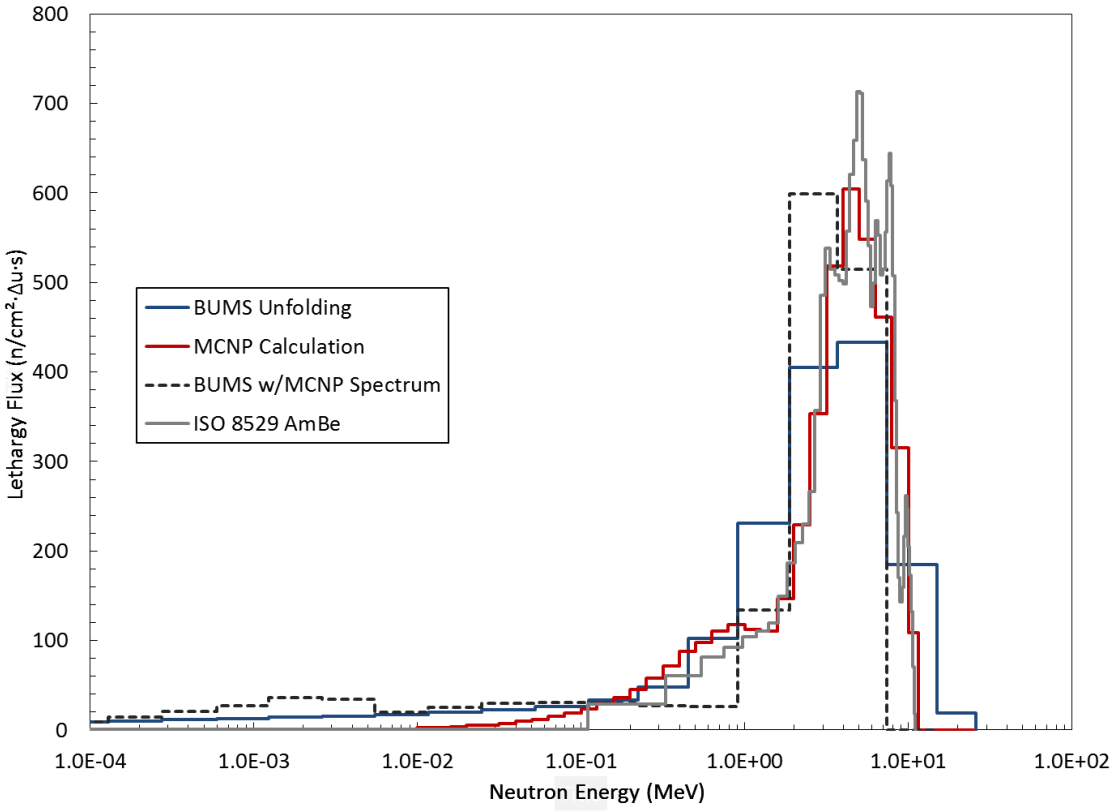

Figure 4.3.5.2. AmBe Bare Spectra

The bare source measurements had the highest gamma ray backgrounds observed and counted in the spectra displayed in Maestro. This was manifested in the background counts subtracted by the software. The ^{252}Cf source results matched up well with the MCNP code and served to help validate the experimental method. The differences between the spectra are explained by the lower energy resolution of the BSS.

The AmBe bare source spectrum has a significantly lower peak from unfolding than from calculation. Comparison to an established neutron field from the ISO 8529 publication supports the MCNP model's results [23], also shown in Figure 4.3.5.2.

One possible explanation is a systemic error in measurement of the bare source. When this discrepancy was noted, a completely new set of experimental data was taken

for the bare AmBe source. The setup, while completely reestablished after collecting other sets of data, did use the same equipment as the original test. Examining the data to see what may be unique about this situation compared to the other data collected shows that the overall fluence levels for the bare AmBe source are far higher than any other source with the exception of a small peak in the AmBe / iron sphere combination. It is possible that this high fluence is somehow underreported by the detector or unfolding process. (Dead times were within acceptable limits and similar dead times were observed in other measurements without this issue.) Also noteworthy on the BUMS spectrum is that there is a lot more low energy flux than predicted by the MCNP and ISO models. Since the moderating spheres generally do away with this low energy flux, it could explain why the excess flux is present in the bare source measurements but not the moderated measurements.

4.3.6 ^{252}Cf in Polyethylene

The polyethylene moderator could only be used with the ^{252}Cf source. The combination is pictured in Figure 2.3.5.1. The resulting spectra are compared in Figure 4.3.6.1 below.

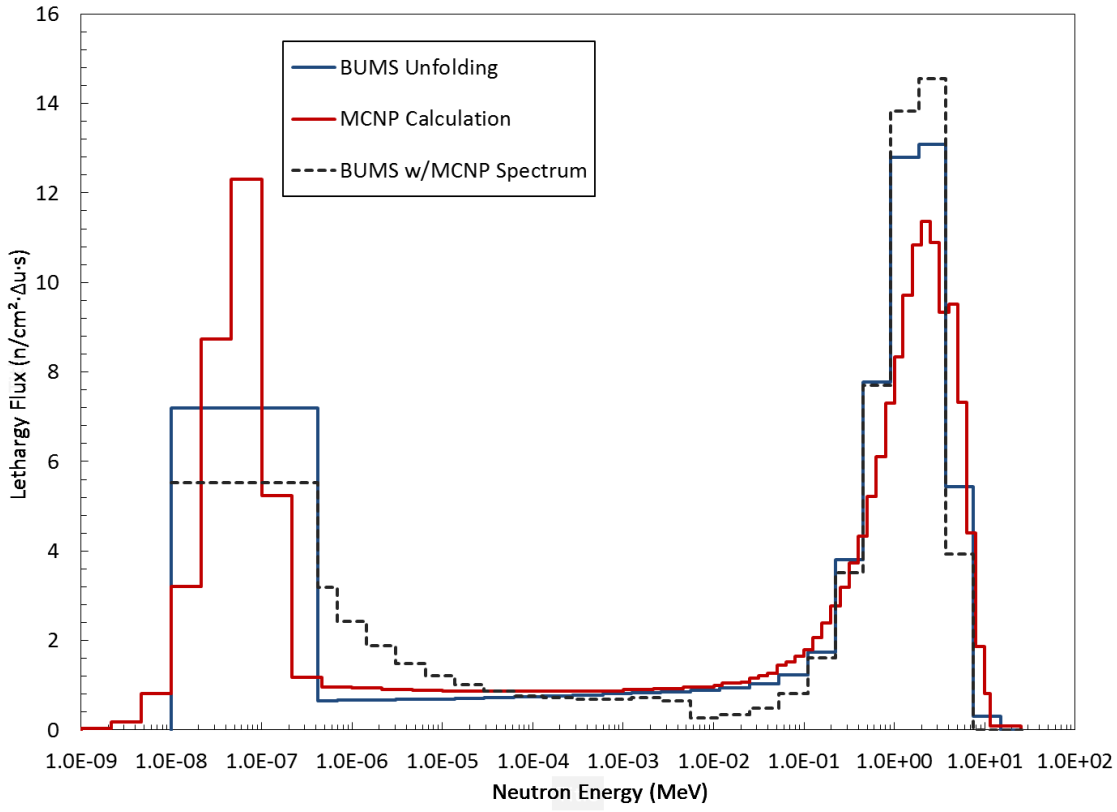

Figure 4.3.6.1. ^{252}Cf / Polyethylene Spectra

The downscattering from polyethylene creates interesting spectra with fluence peaks both in the MeV and thermal energy ranges, and a small but consistent field for eight orders of magnitude in-between, although some of this may be the famed Bonner dip. Although the limited energy resolution of the BSS does overreport in the 0.5 – 3 MeV range, it does capture the essence of the higher energy peak. Given the constraints on the system measuring low energy fluences with much energy resolution, the BSS did a remarkable job capturing the in-between fluence and the presence of the lower energy peak.

4.3.7 ^{252}Cf in Heavy Water

The heavy water moderator could only be used with the ^{252}Cf source. The combination is pictured in Figure 2.3.6.1. The resulting spectra are compared with ISO reference spectra in Figure 4.3.7.1 [30].

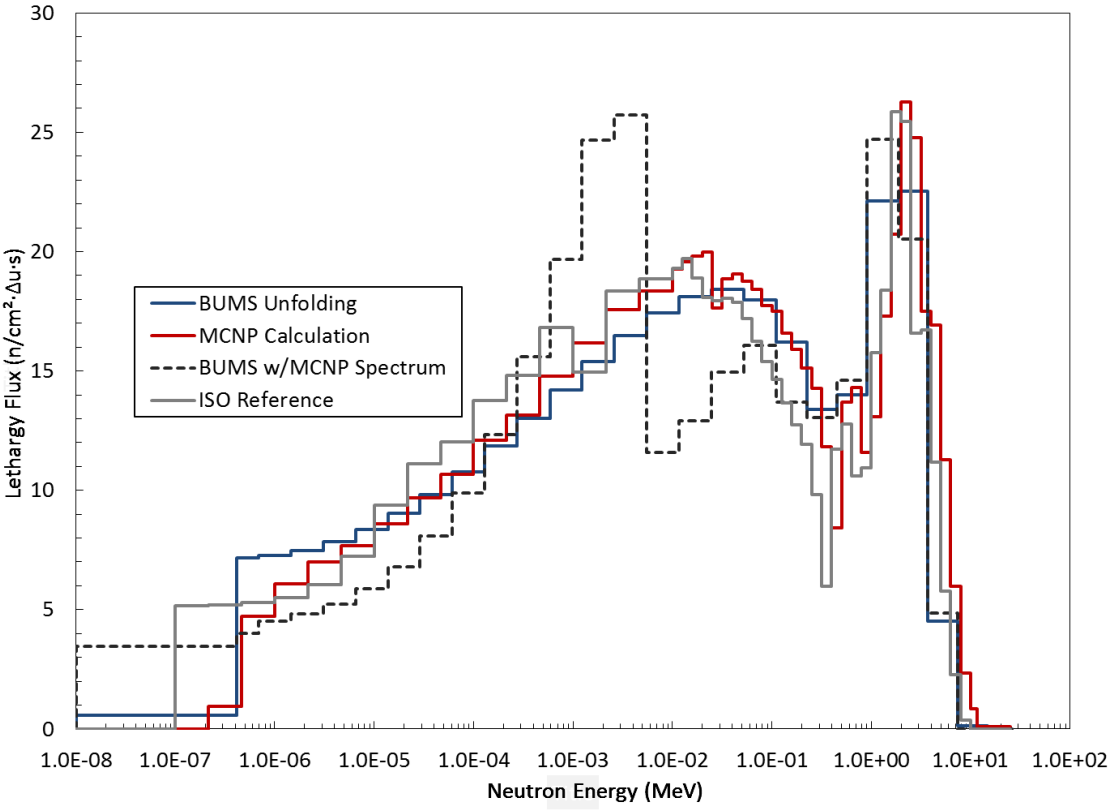

Figure 4.3.7.1. ^{252}Cf / Heavy Water Spectra

These spectra show the value of having a known starting spectrum for accurate iterative solving through BUMS. The empirical data is well-fitted to the MCNP model (which was produced independent of the starting spectrum data in BUMS). The BUMS peak

overreports somewhat, and does so at a slightly lower energy level than the peak established by MCNP and existing literature [30].

This drop-off, while not excessively important on otherwise good fit, bears resemblance to the drop-off noted in with the AmBe source earlier in this chapter. Both of these MCNP spectra used known starting spectra, and both spectra featured established spectra that rapidly dropped off near the 7-10 MeV energy range. Another limitation is that the BUMS system does not capture the low-energy cadmium cutoff around 0.5 eV. The room return also may not be fully corrected for. The background radiation on this measurement is too high for the bare detector measurement to capture this.

CHAPTER 5: CONCLUSION

The BSS works well within its inherent energy resolution limitations. High correlation between unfolding experimental data, MCNP models, and established standard reference spectra supported the results. Areas where discrepancies arose have either been addressed or will be addressed in future work.

Due the success of the experimental validation, the majority of the generated starting spectra for BUMS and other unfolding schemes can be published and used for further research. Likewise, the detailed MCNP models created can also be passed on to future users of these characterized neutron fields, and are given in the appendices.

Discrepancies between the experimental results and established values, most notably on the bare AmBe measurements, must be explained and reconciled before that data can be used.

The BSS, when used with appropriate scattering and geometric corrections and a flexible unfolding algorithm, is an inexpensive, simple to operate, effective neutron detector. Combined with MCNP modeling, accurate fluence totals, dose, and fluence energy spectra can be collected and analyzed in a variety of applications.

CHAPTER 6: FUTURE WORK

The first priority for future work must be to identify the source of discrepancy between the bare AmBe measurements and the established fluence total and spectrum. Explaining the drop-off above 10 MeV for unfolded data in terms of detector or procedural limitations would clear up the only significant issue with the results.

Using a larger number of Bonner spheres would allow for greater energy resolution, especially if these spheres can be designed to have response peaks in energy ranges that current Bonner spheres do not. This is not a new idea and such a moderator may not be found.

Taking data from a larger number of source-detector distances will allow better fits on the scattering parameters in the ESJ method. It would also allow testing of the corrected count rates through selectively disregarding individual distance sets to see how sensitive the corrected data is to each point measured at.

The usefulness of some of the ^{252}Cf geometries is constrained by the stem, especially when using the lead sphere. The stem must be removed in the future for more useful results.

The most important future work will be research that uses these published spectra and MCNP input codes as the foundation for work with these characterized neutron fields.

APPENDIX A: STARTING SPECTRA FOR ITERATIVE UNFOLDING

Appendix Notes:

1. Listings are in a raw format that can be directly copy and pasted into a text file that can be parsed by BUMS.
2. The first column is the top of the energy bin in MeV.
3. The second column is the fluence in neutrons/cm^2/second/lethargy.
4. Only spectra not already present in BUMS are listed.

A.1 ^{252}Cf in Be Starting Spectrum

```
Cf in 10.16cm r Be sphere
1.00E-09       9.37E-04
2.15E-09       4.36E-03
4.64E-09       2.01E-02
1.00E-08       8.63E-02
2.15E-08       3.19E-01
4.64E-08       8.37E-01
1.00E-07       1.26E+00
2.15E-07       1.03E+00
4.64E-07       9.22E-01
1.00E-06       1.04E+00
2.15E-06       1.23E+00
4.64E-06       1.44E+00
1.00E-05       1.74E+00
2.15E-05       2.08E+00
4.64E-05       2.53E+00
1.00E-04       3.05E+00
2.15E-04       3.65E+00
4.64E-04       4.44E+00
1.00E-03       5.30E+00
2.15E-03       6.37E+00
4.64E-03       7.54E+00
1.00E-02       8.87E+00
1.25E-02       2.85E+00
1.58E-02       3.14E+00
1.99E-02       3.24E+00
2.51E-02       3.51E+00
3.16E-02       3.95E+00
3.98E-02       4.01E+00
5.01E-02       4.10E+00
6.30E-02       4.30E+00
7.94E-02       4.90E+00
1.00E-01       5.06E+00
1.25E-01       5.29E+00
1.58E-01       6.22E+00
1.99E-01       6.56E+00
2.51E-01       7.47E+00
3.16E-01       8.75E+00
3.98E-01       9.94E+00
5.01E-01       1.08E+01
6.30E-01       9.19E+00
7.94E-01       1.14E+01
1.00E+00       1.26E+01
1.25E+00       1.39E+01
1.58E+00       1.80E+01
1.99E+00       1.93E+01
2.51E+00       1.45E+01
3.16E+00       7.95E+00
3.98E+00       7.56E+00
5.01E+00       6.46E+00
6.30E+00       4.11E+00
7.94E+00       2.20E+00
1.00E+01       8.69E-01
1.15E+01       1.95E-01
2.50E+01       1.14E-01
```

A.2 ^{252}Cf in Pb Starting Spectrum

```
Cf in 19 cm r Pb sphere
1.00E-09       0.00E+00
2.15E-09       0.00E+00
4.64E-09       0.00E+00
1.00E-08       0.00E+00
2.15E-08       0.00E+00
4.64E-08       0.00E+00
1.00E-07       0.00E+00
2.15E-07       0.00E+00
4.64E-07       0.00E+00
1.00E-06       0.00E+00
2.15E-06       0.00E+00
4.64E-06       0.00E+00
1.00E-05       0.00E+00
2.15E-05       1.53E-05
4.64E-05       9.44E-06
1.00E-04       3.20E-05
2.15E-04       4.24E-04
4.64E-04       1.83E-03
1.00E-03       3.85E-03
2.15E-03       1.70E-02
4.64E-03       5.22E-02
1.00E-02       1.58E-01
1.25E-02       1.01E-01
1.58E-02       1.58E-01
1.99E-02       2.14E-01
2.51E-02       3.18E-01
3.16E-02       4.89E-01
3.98E-02       7.68E-01
5.01E-02       8.10E-01
6.30E-02       1.30E+00
7.94E-02       1.76E+00
1.00E-01       2.39E+00
1.25E-01       3.12E+00
1.58E-01       4.51E+00
1.99E-01       6.07E+00
2.51E-01       8.38E+00
3.16E-01       1.09E+01
3.98E-01       1.42E+01
5.01E-01       1.76E+01
6.30E-01       2.45E+01
7.94E-01       2.80E+01
1.00E+00       2.91E+01
1.25E+00       3.03E+01
1.58E+00       3.09E+01
1.99E+00       2.81E+01
2.51E+00       2.35E+01
3.16E+00       1.78E+01
3.98E+00       1.26E+01
5.01E+00       8.07E+00
6.30E+00       4.84E+00
7.94E+00       2.58E+00
1.00E+01       1.01E+00
1.15E+01       2.20E-01
2.50E+01       1.25E-01
```

A.3 ^{252}Cf in Fe Starting Spectrum

```
Cf in 30"d Fe sphere
1.00E-09       0.00E+00
2.15E-09       0.00E+00
4.64E-09       0.00E+00
1.00E-08       0.00E+00
2.15E-08       0.00E+00
4.64E-08       1.35E-05
1.00E-07       1.88E-04
2.15E-07       4.52E-04
4.64E-07       2.73E-03
1.00E-06       9.77E-03
2.15E-06       2.45E-02
4.64E-06       4.09E-02
1.00E-05       5.61E-02
2.15E-05       7.54E-02
4.64E-05       9.84E-02
1.00E-04       1.14E-01
2.15E-04       1.43E-01
4.64E-04       1.36E-01
1.00E-03       2.11E-01
2.15E-03       3.54E-01
4.64E-03       6.19E-01
1.00E-02       6.31E-01
1.25E-02       5.68E-01
1.58E-02       1.26E+00
1.99E-02       3.16E+00
2.51E-02       1.63E+01
3.16E-02       2.71E+00
3.98E-02       8.83E-01
5.01E-02       2.01E+00
6.30E-02       2.59E+00
7.94E-02       5.83E+00
1.00E-01       5.62E+00
1.25E-01       7.70E+00
1.58E-01       1.64E+01
1.99E-01       1.75E+01
2.51E-01       1.32E+01
3.16E-01       3.84E+01
3.98E-01       2.13E+01
5.01E-01       1.25E+01
6.30E-01       2.41E+01
7.94E-01       1.55E+01
1.00E+00       9.52E+00
1.25E+00       6.09E+00
1.58E+00       2.72E+00
1.99E+00       1.79E+00
2.51E+00       9.77E-01
3.16E+00       4.78E-01
3.98E+00       2.98E-01
5.01E+00       1.69E-01
6.30E+00       1.14E-01
7.94E+00       6.25E-02
1.00E+01       3.22E-02
1.15E+01       9.97E-03
2.50E+01       5.76E-03
```

A.4 ^{252}Cf in Ta Starting Spectrum

```
Cf in 12.065 cm r Ta sphere
1.00E-09       0.00E+00
2.15E-09       0.00E+00
4.64E-09       0.00E+00
1.00E-08       0.00E+00
2.15E-08       0.00E+00
4.64E-08       0.00E+00
1.00E-07       0.00E+00
2.15E-07       0.00E+00
4.64E-07       0.00E+00
1.00E-06       0.00E+00
2.15E-06       0.00E+00
4.64E-06       0.00E+00
1.00E-05       0.00E+00
2.15E-05       0.00E+00
4.64E-05       0.00E+00
1.00E-04       1.11E-05
2.15E-04       1.97E-05
4.64E-04       2.62E-06
1.00E-03       8.36E-05
2.15E-03       2.69E-04
4.64E-03       3.39E-03
1.00E-02       2.87E-02
1.25E-02       3.05E-02
1.58E-02       6.77E-02
1.99E-02       1.26E-01
2.51E-02       2.24E-01
3.16E-02       4.64E-01
3.98E-02       6.78E-01
5.01E-02       1.08E+00
6.30E-02       1.74E+00
7.94E-02       3.10E+00
1.00E-01       4.30E+00
1.25E-01       6.33E+00
1.58E-01       9.95E+00
1.99E-01       1.23E+01
2.51E-01       1.50E+01
3.16E-01       1.81E+01
3.98E-01       1.92E+01
5.01E-01       1.79E+01
6.30E-01       1.65E+01
7.94E-01       1.50E+01
1.00E+00       1.15E+01
1.25E+00       8.96E+00
1.58E+00       8.04E+00
1.99E+00       7.01E+00
2.51E+00       6.38E+00
3.16E+00       5.40E+00
3.98E+00       4.57E+00
5.01E+00       3.39E+00
6.30E+00       2.09E+00
7.94E+00       1.11E+00
1.00E+01       4.29E-01
1.15E+01       9.31E-02
2.50E+01       5.98E-02
```

A.5 ^{252}Cf in Polyethylene Starting Spectrum

Cf in 12" d Poly sphere	
1.00E-09	8.61E-03
2.15E-09	3.25E-02
4.64E-09	1.38E-01
1.00E-08	6.29E-01
2.15E-08	2.46E+00
4.64E-08	6.72E+00
1.00E-07	9.45E+00
2.15E-07	4.02E+00
4.64E-07	9.08E-01
1.00E-06	7.38E-01
2.15E-06	7.18E-01
4.64E-06	6.99E-01
1.00E-05	6.76E-01
2.15E-05	6.72E-01
4.64E-05	6.70E-01
1.00E-04	6.72E-01
2.15E-04	6.60E-01
4.64E-04	6.63E-01
1.00E-03	6.73E-01
2.15E-03	6.89E-01
4.64E-03	7.09E-01
1.00E-02	7.38E-01
1.25E-02	2.22E-01
1.58E-02	2.46E-01
1.99E-02	2.43E-01
2.51E-02	2.48E-01
3.16E-02	2.65E-01
3.98E-02	2.81E-01
5.01E-02	2.94E-01
6.30E-02	3.31E-01
7.94E-02	3.51E-01
1.00E-01	3.82E-01
1.25E-01	4.02E-01
1.58E-01	4.84E-01
1.99E-01	5.51E-01
2.51E-01	6.43E-01
3.16E-01	7.34E-01
3.98E-01	8.61E-01
5.01E-01	9.96E-01
6.30E-01	1.20E+00
7.94E-01	1.41E+00
1.00E+00	1.68E+00
1.25E+00	1.86E+00
1.58E+00	2.28E+00
1.99E+00	2.50E+00
2.51E+00	2.64E+00
3.16E+00	2.51E+00
3.98E+00	2.15E+00
5.01E+00	2.19E+00
6.30E+00	1.68E+00
7.94E+00	1.02E+00
1.00E+01	4.30E-01
1.15E+01	1.13E-01
2.50E+01	7.14E-02

A.6 AmBe in Be Starting Spectrum

```
AmBe in 10.16 cm r Be sphere
1.00E-09       3.76E-03
2.15E-09       1.39E-02
4.64E-09       7.09E-02
1.00E-08       2.99E-01
2.15E-08       1.09E+00
4.64E-08       2.92E+00
1.00E-07       4.64E+00
2.15E-07       4.08E+00
4.64E-07       3.90E+00
1.00E-06       4.47E+00
2.15E-06       5.68E+00
4.64E-06       6.46E+00
1.00E-05       7.70E+00
2.15E-05       9.16E+00
4.64E-05       1.12E+01
1.00E-04       1.34E+01
2.15E-04       1.60E+01
4.64E-04       1.91E+01
1.00E-03       2.25E+01
2.15E-03       2.67E+01
4.64E-03       3.11E+01
1.00E-02       3.62E+01
1.25E-02       1.14E+01
1.58E-02       1.27E+01
1.99E-02       1.31E+01
2.51E-02       1.41E+01
3.16E-02       1.58E+01
3.98E-02       1.60E+01
5.01E-02       1.63E+01
6.30E-02       1.70E+01
7.94E-02       1.93E+01
1.00E-01       1.99E+01
1.25E-01       2.06E+01
1.58E-01       2.41E+01
1.99E-01       2.52E+01
2.51E-01       2.83E+01
3.16E-01       3.24E+01
3.98E-01       3.58E+01
5.01E-01       3.85E+01
6.30E-01       3.24E+01
7.94E-01       3.80E+01
1.00E+00       4.01E+01
1.25E+00       4.30E+01
1.58E+00       5.50E+01
1.99E+00       6.23E+01
2.51E+00       5.47E+01
3.16E+00       4.19E+01
3.98E+00       5.46E+01
5.01E+00       6.81E+01
6.30E+00       5.86E+01
7.94E+00       5.14E+01
1.00E+01       3.09E+01
1.15E+01       5.09E+00
2.50E+01       4.51E-03
```

A.7 AmBe in Pb Starting Spectrum

AmBe in 19cm r	Pb sphere
1.00E-09	0.00E+00
2.15E-09	0.00E+00
4.64E-09	0.00E+00
1.00E-08	0.00E+00
2.15E-08	0.00E+00
4.64E-08	0.00E+00
1.00E-07	0.00E+00
2.15E-07	0.00E+00
4.64E-07	0.00E+00
1.00E-06	0.00E+00
2.15E-06	1.02E-05
4.64E-06	3.71E-04
1.00E-05	1.35E-03
2.15E-05	2.93E-03
4.64E-05	4.60E-03
1.00E-04	1.39E-02
2.15E-04	3.83E-02
4.64E-04	6.73E-02
1.00E-03	1.61E-01
2.15E-03	3.82E-01
4.64E-03	8.53E-01
1.00E-02	1.98E+00
1.25E-02	9.94E-01
1.58E-02	1.37E+00
1.99E-02	1.73E+00
2.51E-02	2.33E+00
3.16E-02	2.99E+00
3.98E-02	4.82E+00
5.01E-02	4.36E+00
6.30E-02	6.68E+00
7.94E-02	8.29E+00
1.00E-01	1.04E+01
1.25E-01	1.30E+01
1.58E-01	1.76E+01
1.99E-01	2.28E+01
2.51E-01	3.05E+01
3.16E-01	3.89E+01
3.98E-01	4.93E+01
5.01E-01	6.05E+01
6.30E-01	7.96E+01
7.94E-01	8.70E+01
1.00E+00	8.51E+01
1.25E+00	8.19E+01
1.58E+00	7.91E+01
1.99E+00	7.13E+01
2.51E+00	6.21E+01
3.16E+00	5.21E+01
3.98E+00	4.50E+01
5.01E+00	3.41E+01
6.30E+00	2.61E+01
7.94E+00	2.28E+01
1.00E+01	1.52E+01
1.15E+01	3.14E+00
2.50E+01	3.77E-03

A.8 AmBe in Fe Starting Spectrum

AmBe in 30" d Fe sphere	
1.00E-09	0.00E+00
2.15E-09	0.00E+00
4.64E-09	0.00E+00
1.00E-08	0.00E+00
2.15E-08	0.00E+00
4.64E-08	1.82E-05
1.00E-07	3.57E-04
2.15E-07	2.54E-03
4.64E-07	1.41E-02
1.00E-06	4.69E-02
2.15E-06	1.05E-01
4.64E-06	1.89E-01
1.00E-05	2.79E-01
2.15E-05	3.73E-01
4.64E-05	4.53E-01
1.00E-04	5.06E-01
2.15E-04	5.76E-01
4.64E-04	6.03E-01
1.00E-03	9.58E-01
2.15E-03	1.49E+00
4.64E-03	2.57E+00
1.00E-02	2.63E+00
1.25E-02	2.44E+00
1.58E-02	5.37E+00
1.99E-02	1.31E+01
2.51E-02	6.62E+01
3.16E-02	1.09E+01
3.98E-02	3.50E+00
5.01E-02	7.93E+00
6.30E-02	1.01E+01
7.94E-02	2.26E+01
1.00E-01	2.17E+01
1.25E-01	2.94E+01
1.58E-01	6.24E+01
1.99E-01	6.61E+01
2.51E-01	4.97E+01
3.16E-01	1.43E+02
3.98E-01	8.01E+01
5.01E-01	4.78E+01
6.30E-01	9.08E+01
7.94E-01	6.04E+01
1.00E+00	3.82E+01
1.25E+00	2.52E+01
1.58E+00	1.23E+01
1.99E+00	8.64E+00
2.51E+00	5.56E+00
3.16E+00	3.33E+00
3.98E+00	2.56E+00
5.01E+00	2.02E+00
6.30E+00	1.67E+00
7.94E+00	1.80E+00
1.00E+01	1.43E+00
1.15E+01	3.34E-01
2.50E+01	5.60E-05

A.9 AmBe in Ta Starting Spectrum

```
AmBe in 12.065 cm r Ta sphere
1.00E-09        0.00E+00
2.15E-09        0.00E+00
4.64E-09        0.00E+00
1.00E-08        0.00E+00
2.15E-08        0.00E+00
4.64E-08        0.00E+00
1.00E-07        0.00E+00
2.15E-07        0.00E+00
4.64E-07        0.00E+00
1.00E-06        8.11E-06
2.15E-06        0.00E+00
4.64E-06        0.00E+00
1.00E-05        2.44E-05
2.15E-05        2.85E-04
4.64E-05        2.75E-04
1.00E-04        9.79E-04
2.15E-04        1.54E-03
4.64E-04        4.62E-04
1.00E-03        4.20E-05
2.15E-03        8.31E-04
4.64E-03        1.94E-02
1.00E-02        1.58E-01
1.25E-02        1.74E-01
1.58E-02        3.61E-01
1.99E-02        6.61E-01
2.51E-02        1.18E+00
3.16E-02        2.18E+00
3.98E-02        3.18E+00
5.01E-02        4.86E+00
6.30E-02        7.51E+00
7.94E-02        1.28E+01
1.00E-01        1.71E+01
1.25E-01        2.48E+01
1.58E-01        3.78E+01
1.99E-01        4.57E+01
2.51E-01        5.47E+01
3.16E-01        6.54E+01
3.98E-01        6.92E+01
5.01E-01        6.36E+01
6.30E-01        5.82E+01
7.94E-01        5.24E+01
1.00E+00        3.93E+01
1.25E+00        2.99E+01
1.58E+00        2.59E+01
1.99E+00        2.21E+01
2.51E+00        2.17E+01
3.16E+00        2.28E+01
3.98E+00        2.79E+01
5.01E+00        3.06E+01
6.30E+00        2.68E+01
7.94E+00        2.35E+01
1.00E+01        1.53E+01
1.15E+01        3.10E+00
2.50E+01        4.16E-03
```

APPENDIX B: MCNP INPUT FILES

Appendix notes:

1. MCNP files are displayed in a raw format that can be copy/pasted into a text editor and saved as an MCNP input file.
2. Some previous modeling work for the sources was done by N. E. Hertel. Much of the ^{252}Cf bare source model is based on his previous unpublished work.
3. The remainder of the model files is the product of the author and may be reused as long as credit is given.

B.1 ^{252}Cf Bare MCNP Input

```
Cf Bare
c by Pete Exline
c Cell Cards
c cells for bare source with no PNL rabbit
c
c ***PRIMARY ENCAPSULATION***
c
c CF oxide source volume (no material assumed for the moment**
c
1 0      -12 18 -17 imp:n=1 imp:p=1
c
c Lower porous platinum filter (1/2 full density assumed)
c
2 1 -10.68 -12 17 -16 imp:n=1 imp:p=1
c
c Lower void
c
3 0      -13 16 -15 imp:n=1 imp:p=1
c
c Middle void
c
4 0      -12 19 -18 imp:n=1 imp:p=1
c
c upper porous platinum filter (1/2 full density assumed)
c
5 1 -10.68 -12 -19 20 imp:n=1 imp:p=1
c
c Upper void
c
6 0      -12 -20 21 imp:n=1 imp:p=1
c
c Primary capsule container (90% Pt and 10% Rh)
c
7 2 -19.9541 #(-15 -13 16:-16 -12 21) 22 -11 -14 imp:n=1 imp:p=1
c
c Gap between the primnary and secondary capsules
c
8 0       #(22 -11 -14) (23 -6 -7):(-6 10 -23 35) imp:n=1 imp:p=1
c
c **SECONDARY CAPSULE OF ZIRCALLOY-2***
c
9 3 -6.415 #(-7 -6 35) (-4 8 -3):-8 9 -5:-10 -23 35 imp:n=1 imp:p=1
c
c The threads of the secondary capsule
c
10 3 -6.415 -2 -1 3 imp:n=1 imp:p=1
c
c Air outside the source -- used as a tally surface
c
11 304  -1.24e-3    (-322 1 -2 3):(-322 4 -3 8):(-322 5 -8 9):&
(-322 2):(-322 -9) imp:n=1 imp:p=1
c
c Air beyond the tally surface to edge of universe
c
12 304 -1.24e-3      322 -24 imp:n=1 imp:p=1
```

```
c
13 0 24 imp:n=0 imp:p=0  $terminate particles beyond universe
c XXXXXXX** air to combine for Be Sphere **
c 401 304 -1.24e-3  (-301 1 -2 3):(-301 4 -3 8):(-301 5 -8 9):(-301 2):(-301 -9) &
c imp:n=1 imp:p=1

c Surface Cards
c Cylinder and planes to define the theaded portion of the
c     secondary capsule
c
1 CZ 0.2413
2 PZ 1.8542
3 PZ 1.3462
c
c Cylinders to define the secondary encapsulation
c
4 CZ 0.4699
5 CZ 0.4115
6 CZ 0.2972
c
c planes and cone to define the seconday encapsulation
c
7 PZ 1.143
8 PZ -1.778
9 PZ -1.905
10 KZ 1.720611544 0.007654266 -1
c
c Cylinders to define the primary encapsulation
c
11 CZ 0.2769
12 CZ 0.1636
13 CZ 0.1524
c
c Planes to define the primary encapsulation
c
14 PZ 1.0859
15 PZ 0.6922
16 PZ 0.5144
17 PZ 0.1588
18 PZ -0.1588
19 PZ -0.4763
20 PZ -0.8319
21 PZ -0.9970
22 PZ -1.3907
23 PZ -1.4478
35 PZ -1.6764
322 SO 100      $100cm Sphere around source
24 SO 500 $edge of universe
c
c  The next set of planes will be used to segment surface 22 to do the angular
c  dependent tally.  They do not have to be used in the cell descriptions.
c
324 PZ 98.7688340595138
325 PZ 95.1056516295154
326 PZ 89.1006524188368
327 PZ 80.9016994374947
328 PZ 70.7106781186548
329 PZ 58.7785252292473
330 PZ 45.3990499739547
331 PZ 30.9016994374947
332 PZ 15.6434465040231
333 PZ 0
334 PZ -15.6434465040231
335 PZ -30.9016994374947
336 PZ -45.3990499739547
337 PZ -58.7785252292473
338 PZ -70.7106781186547
339 PZ -80.9016994374947
340 PZ -89.1006524188368
```

```
341 PZ -95.1056516295154
342 PZ -98.7688340595138
c **

c Material Cards
c
c Materials: M1 is the porous filter, M2 is the 90% Pt, 10% Rh
c    and M4 is the Zircalloy-2
c
M1 78000 1.0
M2 78000 -0.9 45103 -0.1
M3 50000 -0.015 26000 -0.0012 24000 -0.001 28000 -0.0005 &
40090 -.5053934 40091 -.1102141 40092 -.1684645 40094 -.1707237 &
40096 -.0275044
c **
m304 7014 -.7558 8016 -.2314 18000 -.0128 $air
c **
c
c the source is input in cell one region using a Maxwellian with
c   temperature of 1.42 MeV
c
c old syntax -- SRC4 3J 1 1 0.0 0.1636 0.1588 0. 0. 1.
SDEF ERG=D1 CEL=1 PAR =1 POS=0 0 0 AXS=0 0 1 EXT=D3 RAD=D2
SI3 -0.159 0.159
SI2 0 0.164
SP2 -21 1
SP1 -2 1.42
c
c Tallies
F2:N  322
FC2  Neutron Flux
FS2 -334 -332 T $plus/minus 15.6cm cutoffs
c Current Tally of whole sphere
F1:N  322
FC1 number of neutrons per spherical surface segments at 100 cm
c Segmented Tally across z plans of the sphere
FS1  -342 -341 -340 -339 -338 -337 -336 -335 -334 -333 -332 -331 &
-330 -329 -328 -327 -326 -325 -324
c
F12:N 322
FC12  Icrp 74 ambient dose equivalent on spherical surface at 100 cm
c Segmented Tally across z plans of the sphere
FS12  -342 -341 -340 -339 -338 -337 -336 -335 -334 -333 -332 -331 &
-330 -329 -328 -327 -326 -325 -324
c
c  gamma fluence tally at 100 cm
F22:P  322
FC22  Gamma Ray Fluence induced by neutrons at 100 cm
FS22 -334 -332 T $plus/minus 15.6cm cutoffs
c
F32:P   322
FC32  Gamma Ray Dose rate at 100 cm
FS32 -334 -332 T $plus/minus 15.6cm cutoffs
c
F5:N -100.0001 0 0 .1
FC5 Point Neutron Detector at 100cm
c
F25:N -100.0001 0 0 .1
FC25 ICRP 74 ambient dose equivalent on Point Neutron Detector at 100cm
c Energy groups used to bin fluence
e1   1.00E-09   2.15E-09   4.64E-09   1.00E-08   2.15E-08   4.64E-08
     1.00E-07   2.15E-07   4.64E-07   1.00E-06   2.15E-06   4.64E-06
     1.00E-05   2.15E-05   4.64E-05   1.00E-04   2.15E-04   4.64E-04
     1.00E-03   2.15E-03   4.64E-03   1.00E-02   1.25E-02   1.58E-02
     1.99E-02   2.51E-02   3.16E-02   3.98E-02   5.01E-02   6.30E-02
     7.94E-02   1.00E-01   1.25E-01   1.58E-01   1.99E-01   2.51E-01
     3.16E-01   3.98E-01   5.01E-01   6.30E-01   7.94E-01   1.00E+00
     1.25E+00   1.58E+00   1.99E+00   2.51E+00   3.16E+00   3.98E+00
     5.01E+00   6.30E+00   7.94E+00   1.00E+01   1.15E+01   25.
```

```
c
e2   1.00E-09   2.15E-09   4.64E-09   1.00E-08   2.15E-08   4.64E-08
     1.00E-07   2.15E-07   4.64E-07   1.00E-06   2.15E-06   4.64E-06
     1.00E-05   2.15E-05   4.64E-05   1.00E-04   2.15E-04   4.64E-04
     1.00E-03   2.15E-03   4.64E-03   1.00E-02   1.25E-02   1.58E-02
     1.99E-02   2.51E-02   3.16E-02   3.98E-02   5.01E-02   6.30E-02
     7.94E-02   1.00E-01   1.25E-01   1.58E-01   1.99E-01   2.51E-01
     3.16E-01   3.98E-01   5.01E-01   6.30E-01   7.94E-01   1.00E+00
     1.25E+00   1.58E+00   1.99E+00   2.51E+00   3.16E+00   3.98E+00
     5.01E+00   6.30E+00   7.94E+00   1.00E+01   1.15E+01   25.
c
e5   1.00E-09   2.15E-09   4.64E-09   1.00E-08   2.15E-08   4.64E-08
     1.00E-07   2.15E-07   4.64E-07   1.00E-06   2.15E-06   4.64E-06
     1.00E-05   2.15E-05   4.64E-05   1.00E-04   2.15E-04   4.64E-04
     1.00E-03   2.15E-03   4.64E-03   1.00E-02   1.25E-02   1.58E-02
     1.99E-02   2.51E-02   3.16E-02   3.98E-02   5.01E-02   6.30E-02
     7.94E-02   1.00E-01   1.25E-01   1.58E-01   1.99E-01   2.51E-01
     3.16E-01   3.98E-01   5.01E-01   6.30E-01   7.94E-01   1.00E+00
     1.25E+00   1.58E+00   1.99E+00   2.51E+00   3.16E+00   3.98E+00
     5.01E+00   6.30E+00   7.94E+00   1.00E+01   1.15E+01   25.
c
e12   1.00E-09   2.15E-09   4.64E-09   1.00E-08   2.15E-08   4.64E-08
     1.00E-07   2.15E-07   4.64E-07   1.00E-06   2.15E-06   4.64E-06
     1.00E-05   2.15E-05   4.64E-05   1.00E-04   2.15E-04   4.64E-04
     1.00E-03   2.15E-03   4.64E-03   1.00E-02   1.25E-02   1.58E-02
     1.99E-02   2.51E-02   3.16E-02   3.98E-02   5.01E-02   6.30E-02
     7.94E-02   1.00E-01   1.25E-01   1.58E-01   1.99E-01   2.51E-01
     3.16E-01   3.98E-01   5.01E-01   6.30E-01   7.94E-01   1.00E+00
     1.25E+00   1.58E+00   1.99E+00   2.51E+00   3.16E+00   3.98E+00
     5.01E+00   6.30E+00   7.94E+00   1.00E+01   1.15E+01   25.
c
e25   1.00E-09   2.15E-09   4.64E-09   1.00E-08   2.15E-08   4.64E-08
     1.00E-07   2.15E-07   4.64E-07   1.00E-06   2.15E-06   4.64E-06
     1.00E-05   2.15E-05   4.64E-05   1.00E-04   2.15E-04   4.64E-04
     1.00E-03   2.15E-03   4.64E-03   1.00E-02   1.25E-02   1.58E-02
     1.99E-02   2.51E-02   3.16E-02   3.98E-02   5.01E-02   6.30E-02
     7.94E-02   1.00E-01   1.25E-01   1.58E-01   1.99E-01   2.51E-01
     3.16E-01   3.98E-01   5.01E-01   6.30E-01   7.94E-01   1.00E+00
     1.25E+00   1.58E+00   1.99E+00   2.51E+00   3.16E+00   3.98E+00
     5.01E+00   6.30E+00   7.94E+00   1.00E+01   1.15E+01   25.
c
c  for gammas
e22  0.01   0.015   0.02   0.03   0.04   0.05   0.06   0.08   0.1
     0.15   0.2      0.3    0.4    0.5    0.6    0.8     1.   1.5
       2.    3.       4.     5.     6.     8.   10.0    12.    15.
c
c  ICRP 74 Dose Conversion coeffients
DE12  1.00E-09  1.00E-08  2.53E-08  1.00E-07  2.00E-07  5.00E-07
      1.00E-06  2.00E-06  5.00E-06  1.00E-05  2.00E-05  5.00E-05
      1.00E-04  2.00E-04  5.00E-04  1.00E-03  2.00E-03  5.00E-03
      1.00E-02  2.00E-02  3.00E-02  5.00E-02  7.00E-02  1.00E-01
      1.50E-01  2.00E-01  3.00E-01  5.00E-01  7.00E-01  9.00E-01
      1.00E+00  1.20E+00  2.00E+00  3.00E+00  4.00E+00  5.00E+00
      6.00E+00  7.00E+00  8.00E+00  9.00E+00  1.00E+01  1.20E+01
      1.40E+01  1.50E+01  1.60E+01  1.80E+01  2.00E+01  3.00E+01
      5.00E+01  7.50E+01  1.00E+02  1.25E+02  1.50E+02  1.75E+02
      2.01E+02
c
DF12  6.6  9   10.6  12.9  13.5  13.6  13.3  12.9   12   11.3  10.6
      9.9  9.4  8.9   8.3   7.9   7.7     8  10.5  16.6  23.7  41.1
       60   88  132   170   233   322   375   400   416   425   420
      412  408  405   400   405   409   420   440   480   520   540
      555  570  600   515   400   330   285   260   245   250   260
c
c  ICRP 74 Dose Conversion coeffients
DE25  1.00E-09  1.00E-08  2.53E-08  1.00E-07  2.00E-07  5.00E-07
      1.00E-06  2.00E-06  5.00E-06  1.00E-05  2.00E-05  5.00E-05
      1.00E-04  2.00E-04  5.00E-04  1.00E-03  2.00E-03  5.00E-03
      1.00E-02  2.00E-02  3.00E-02  5.00E-02  7.00E-02  1.00E-01
```

```
      1.50E-01  2.00E-01  3.00E-01  5.00E-01  7.00E-01  9.00E-01
      1.00E+00  1.20E+00  2.00E+00  3.00E+00  4.00E+00  5.00E+00
      6.00E+00  7.00E+00  8.00E+00  9.00E+00  1.00E+01  1.20E+01
      1.40E+01  1.50E+01  1.60E+01  1.80E+01  2.00E+01  3.00E+01
      5.00E+01  7.50E+01  1.00E+02  1.25E+02  1.50E+02  1.75E+02
      2.01E+02
c
DF25  6.6  9   10.6  12.9  13.5  13.6  13.3  12.9   12   11.3  10.6
      9.9  9.4  8.9   8.3   7.9   7.7     8  10.5  16.6  23.7  41.1
       60   88  132   170   233   322   375   400   416   425   420
      412  408  405   400   405   409   420   440   480   520   540
      555  570  600   515   400   330   285   260   245   250   260
c
c ICRP 74 DCCs for photons (pSv-cm2)
de32  0.01   0.015   0.02   0.03   0.04   0.05   0.06   0.08   0.1
     0.15   0.2      0.3    0.4    0.5    0.6    0.8     1.   1.5
       2.    3.       4.     5.     6.     8.   10.0
df32   0.061   0.83   1.05   0.81   0.64   0.55   0.51   0.53  0.61
       0.89    1.2    1.8    2.38   2.93   3.44   4.38    5.2   6.9
        8.6   11.1   13.4    15.5   17.6   21.6   25.6
c
mode n p
CUT:N  1J  1.e-10
CUT:P  1J   0.01
nps 1E7
```

B.2 ^{252}Cf in Beryllium MCNP Input

```
Cf in 20.32cm d Be sphere
c by Pete Exline
c Cell Cards
c cells for bare source with no PNL rabbit
c
c ***PRIMARY ENCAPSULATION***
c
c CF oxide source volume (no material assumed for the moment**
c
1 0      -12 18 -17 imp:n=1 imp:p=1
c
c Lower porous platinum filter (1/2 full density assumed)
c
2 1 -10.68 -12 17 -16 imp:n=1 imp:p=1
c
c Lower void
c
3 0      -13 16 -15 imp:n=1 imp:p=1
c
c Middle void
c
4 0      -12 19 -18 imp:n=1 imp:p=1
c
c upper porous platinum filter (1/2 full density assumed)
c
5 1 -10.68 -12 -19 20 imp:n=1 imp:p=1
c
c Upper void
c
6 0      -12 -20 21 imp:n=1 imp:p=1
c
c Primary capsule container (90% Pt and 10% Rh)
c
7 2 -19.9541 #(-15 -13 16:-16 -12 21) 22 -11 -14 imp:n=1 imp:p=1
c
c Gap between the primnary and secondary capsules
c
8 0       #(22 -11 -14) (23 -6 -7):(-6 10 -23 35) imp:n=1 imp:p=1
c
c **SECONDARY CAPSULE OF ZIRCALLOY-2***
c
9 3 -6.415 #(-7 -6 35) (-4 8 -3):-8 9 -5:-10 -23 35 imp:n=1 imp:p=1
c
c The threads of the secondary capsule
c
10 3 -6.415 -2 -1 3 imp:n=1 imp:p=1
c
c ** Be Sphere **
304 304 -1.24e-3 (-322 307 #(&
(-501 502 503 -504 505 -506):&
((-501 531 513 515 -503 -525):(-501 531 503 515 -523 -505))&
:((-501 531 524 -514 515 -505):(-501 531 504 -514 515 -525))&
:((-501 531 513 -516 -503 526):(-501 531 503 -516 -523 506))&
:((-501 531 524 -514 -516 506):(-501 531 504 -514 -516 526))&
:((-531 543 545 -503 -525):(-531 503 545 -523 -505))&
:((-531 524 -544 545 -505):(-531 504 -544 545 -525))&
:((-531 543 -546 -503 526):(-531 503 -546 -523 506))&
:((-531 524 -544 -546 506):(-531 504 -544 -546 526))&
:((501 -553 551 -552))))&
 imp:n=1 imp:p=1 $air from Be surface to tally sphere
305 304 -1.24e-3 322 -306   imp:n=1 imp:p=1 $air from sphere to edge of universe
c Be sphere (with last two terms removing plug)
306 303 -1.84  -307 301 (308:-312) (309:-311) imp:n=1 imp:p=1
307 0      306                   imp:n=0 imp:p=0 $Void space outside universe
c plug removed
308 304 -1.24e-3 -307 301 (-308 312 -307 301):(-309 311 -307 301) &
```

```
 imp:n=1 imp:p=1
c ** air to combine for Be Sphere **
401 304 -1.24e-3  (-301 1 -2 3):(-301 4 -3 8):(-301 5 -8 9):(-301 2):(-301 -9) &
imp:n=1 imp:p=1
c * Al table top*
501 305 -2.7 -501 502 503 -504 505 -506 imp:n=1 imp:p=1 $Al table top
511 305 -2.7 (-501 531 513 515 -503 -525):(-501 531 503 515 -523 -505) &
imp:n=1 imp:p=1 $bl leg
512 305 -2.7 (-501 531 524 -514 515 -505):(-501 531 504 -514 515 -525) &
imp:n=1 imp:p=1 $br leg
513 305 -2.7 (-501 531 513 -516 -503 526):(-501 531 503 -516 -523 506) &
imp:n=1 imp:p=1 $tl leg
514 305 -2.7 (-501 531 524 -514 -516 506):(-501 531 504 -514 -516 526) &
imp:n=1 imp:p=1 $tr leg
541 305 -2.7 (-531 -322 543 545 -503 -525):(-531 -322 503 545 -523 -505) &
imp:n=1 imp:p=1 $bl thick leg
542 305 -2.7 (-531 -322 524 -544 545 -505):(-531 -322 504 -544 545 -525) &
imp:n=1 imp:p=1 $br thick leg
543 305 -2.7 (-531 -322 543 -546 -503 526):(-531 -322 503 -546 -523 506) &
imp:n=1 imp:p=1 $tl thick leg
544 305 -2.7 (-531 -322 524 -544 -546 506):(-531 -322 504 -544 -546 526) &
imp:n=1 imp:p=1 $tr thick leg
551 305 -2.7 501 -553 551 -552 imp:n=1 imp:p=1 $Al stabilizer ring
c **

c Surface Cards
c Cylinder and planes to define the theaded portion of the
c     secondary capsule
c
1 CZ 0.2413
2 PZ 1.8542
3 PZ 1.3462
c
c Cylinders to define the secondary encapsulation
c
4 CZ 0.4699
5 CZ 0.4115
6 CZ 0.2972
c
c planes and cone to define the seconday encapsulation
c
7 PZ 1.143
8 PZ -1.778
9 PZ -1.905
10 KZ 1.720611544 0.007654266 -1
c
c Cylinders to define the primary encapsulation
c
11 CZ 0.2769
12 CZ 0.1636
13 CZ 0.1524
c
c Planes to define the primary encapsulation
c
14 PZ 1.0859
15 PZ 0.6922
16 PZ 0.5144
17 PZ 0.1588
18 PZ -0.1588
19 PZ -0.4763
20 PZ -0.8319
21 PZ -0.9970
22 PZ -1.3907
23 PZ -1.4478
35 PZ -1.6764
c **Be Sphere **
301  SO 3.048   $Outer surface of source sphere
306  SO 500     $Edge of the Universe
307  SO 10.16   $radius of Be spherical shell
```

```
308  CZ 0.635   $small radius of plug
309  CZ 0.9525  $larger radius of plug lip
310 PZ 3.175   $bottom of plug
311 PZ 8.89    $bottom of plug lip
312 PZ 0.001   $used to define upper half for plug geometries
322 SO 100     $100cm Sphere around source
c **
c *Al table top*
501  pz -10.16 $top of Al table top
502  pz -10.76 $bot of Al table top
503  px -25.325 $left of Al table top
504  px 25.325 $right of Al table top
505  py -25.325 $front of Al table top
506  py 25.325 $back of Al table top
513  px -25.475 $left of Al table leg
514  px 25.475 $right of Al table leg
515  py -25.475 $front of Al table leg
516  py 25.475 $back of Al table leg
523  px -20.575 $cutoff of Al table top
524  px 20.575 $cutoff of Al table top
525  py -20.575 $cutoff of Al table top
526  py 20.575 $cutoff of Al table top
531  pz -35.9675 $bot of thin legs/top of thick legs
543  px -26.075 $left of Al table thick leg
544  px 26.075 $right of Al table thick leg
545  py -26.075 $front of Al table thick leg
546  py 26.075 $back of Al table thick leg
551  cz 6.25 $inner radius of Al stabilizer
552  cz 8.75 $outer radius of Al stabilizer
553  pz -9.51 $top of Al stablizer
c **
c  The next set of planes will be used to segment surface 22 to do the angular
c  dependent tally.  They do not have to be used in the cell descriptions.
c
324 PZ 98.7688340595138
325 PZ 95.1056516295154
326 PZ 89.1006524188368
327 PZ 80.9016994374947
328 PZ 70.7106781186548
329 PZ 58.7785252292473
330 PZ 45.3990499739547
331 PZ 30.9016994374947
332 PZ 15.6434465040231
333 PZ 0
334 PZ -15.6434465040231
335 PZ -30.9016994374947
336 PZ -45.3990499739547
337 PZ -58.7785252292473
338 PZ -70.7106781186547
339 PZ -80.9016994374947
340 PZ -89.1006524188368
341 PZ -95.1056516295154
342 PZ -98.7688340595138
c **

c Material Cards
c
c Materials: M1 is the porous filter, M2 is the 90% Pt, 10% Rh
c    and M4 is the Zircalloy-2
c
M1 78000 1.0
M2 78000 -0.9 45103 -0.1
M3 50000 -0.015 26000 -0.0012 24000 -0.001 28000 -0.0005 &
40090 -.5053934 40091 -.1102141 40092 -.1684645 40094 -.1707237 &
40096 -.0275044
c ** Be Sphere **
m303 4009.62  1.0
c **
m304 7014 -.7558 8016 -.2314 18000 -.0128 $air
```

```
c **
m305 13027 1.0 $Al
c
c the source is input in cell one region using a Maxwellian with
c   temperature of 1.42 MeV
c
c old syntax -- SRC4 3J 1 1 0.0 0.1636 0.1588 0. 0. 1.
SDEF ERG=D1 CEL=1 PAR =1 POS=0 0 0 AXS=0 0 1 EXT=D3 RAD=D2
SI3 -0.159 0.159
SI2 0 0.164
SP2 -21 1
SP1 -2 1.42
c
c Tallies
F2:N  322
FC2  Neutron Flux
FS2 -334 -332 T $plus/minus 15.6cm cutoffs
c Current Tally of whole sphere
F1:N  322
FC1 number of neutrons per spherical surface segments at 100 cm
c Segmented Tally across z plans of the sphere
FS1  -342 -341 -340 -339 -338 -337 -336 -335 -334 -333 -332 -331 &
-330 -329 -328 -327 -326 -325 -324
c
F12:N 322
FC12  Icrp 74 ambient dose equivalent on spherical surface at 100 cm
c Segmented Tally across z plans of the sphere
FS12  -342 -341 -340 -339 -338 -337 -336 -335 -334 -333 -332 -331 &
-330 -329 -328 -327 -326 -325 -324
c
c  gamma fluence tally at 100 cm
F22:P  322
FC22  Gamma Ray Fluence induced by neutrons at 100 cm
FS22 -334 -332 T $plus/minus 15.6cm cutoffs
c
F32:P   322
FC32  Gamma Ray Dose rate at 100 cm
FS32 -334 -332 T $plus/minus 15.6cm cutoffs
c
F5:N -100.0001 0 0 .1
FC5 Point Neutron Detector at 100cm
c
F25:N -100.0001 0 0 .1
FC25 ICRP 74 ambient dose equivalent on Point Neutron Detector at 100cm
c Energy groups used to bin fluence
e1   1.00E-09   2.15E-09   4.64E-09   1.00E-08   2.15E-08   4.64E-08
     1.00E-07   2.15E-07   4.64E-07   1.00E-06   2.15E-06   4.64E-06
     1.00E-05   2.15E-05   4.64E-05   1.00E-04   2.15E-04   4.64E-04
     1.00E-03   2.15E-03   4.64E-03   1.00E-02   1.25E-02   1.58E-02
     1.99E-02   2.51E-02   3.16E-02   3.98E-02   5.01E-02   6.30E-02
     7.94E-02   1.00E-01   1.25E-01   1.58E-01   1.99E-01   2.51E-01
     3.16E-01   3.98E-01   5.01E-01   6.30E-01   7.94E-01   1.00E+00
     1.25E+00   1.58E+00   1.99E+00   2.51E+00   3.16E+00   3.98E+00
     5.01E+00   6.30E+00   7.94E+00   1.00E+01   1.15E+01   25.
c
e2   1.00E-09   2.15E-09   4.64E-09   1.00E-08   2.15E-08   4.64E-08
     1.00E-07   2.15E-07   4.64E-07   1.00E-06   2.15E-06   4.64E-06
     1.00E-05   2.15E-05   4.64E-05   1.00E-04   2.15E-04   4.64E-04
     1.00E-03   2.15E-03   4.64E-03   1.00E-02   1.25E-02   1.58E-02
     1.99E-02   2.51E-02   3.16E-02   3.98E-02   5.01E-02   6.30E-02
     7.94E-02   1.00E-01   1.25E-01   1.58E-01   1.99E-01   2.51E-01
     3.16E-01   3.98E-01   5.01E-01   6.30E-01   7.94E-01   1.00E+00
     1.25E+00   1.58E+00   1.99E+00   2.51E+00   3.16E+00   3.98E+00
     5.01E+00   6.30E+00   7.94E+00   1.00E+01   1.15E+01   25.
c
e5   1.00E-09   2.15E-09   4.64E-09   1.00E-08   2.15E-08   4.64E-08
     1.00E-07   2.15E-07   4.64E-07   1.00E-06   2.15E-06   4.64E-06
     1.00E-05   2.15E-05   4.64E-05   1.00E-04   2.15E-04   4.64E-04
     1.00E-03   2.15E-03   4.64E-03   1.00E-02   1.25E-02   1.58E-02
```

```
     1.99E-02   2.51E-02   3.16E-02   3.98E-02   5.01E-02   6.30E-02
     7.94E-02   1.00E-01   1.25E-01   1.58E-01   1.99E-01   2.51E-01
     3.16E-01   3.98E-01   5.01E-01   6.30E-01   7.94E-01   1.00E+00
     1.25E+00   1.58E+00   1.99E+00   2.51E+00   3.16E+00   3.98E+00
     5.01E+00   6.30E+00   7.94E+00   1.00E+01   1.15E+01   25.
c
e12   1.00E-09   2.15E-09   4.64E-09   1.00E-08   2.15E-08   4.64E-08
     1.00E-07   2.15E-07   4.64E-07   1.00E-06   2.15E-06   4.64E-06
     1.00E-05   2.15E-05   4.64E-05   1.00E-04   2.15E-04   4.64E-04
     1.00E-03   2.15E-03   4.64E-03   1.00E-02   1.25E-02   1.58E-02
     1.99E-02   2.51E-02   3.16E-02   3.98E-02   5.01E-02   6.30E-02
     7.94E-02   1.00E-01   1.25E-01   1.58E-01   1.99E-01   2.51E-01
     3.16E-01   3.98E-01   5.01E-01   6.30E-01   7.94E-01   1.00E+00
     1.25E+00   1.58E+00   1.99E+00   2.51E+00   3.16E+00   3.98E+00
     5.01E+00   6.30E+00   7.94E+00   1.00E+01   1.15E+01   25.
c
e25   1.00E-09   2.15E-09   4.64E-09   1.00E-08   2.15E-08   4.64E-08
     1.00E-07   2.15E-07   4.64E-07   1.00E-06   2.15E-06   4.64E-06
     1.00E-05   2.15E-05   4.64E-05   1.00E-04   2.15E-04   4.64E-04
     1.00E-03   2.15E-03   4.64E-03   1.00E-02   1.25E-02   1.58E-02
     1.99E-02   2.51E-02   3.16E-02   3.98E-02   5.01E-02   6.30E-02
     7.94E-02   1.00E-01   1.25E-01   1.58E-01   1.99E-01   2.51E-01
     3.16E-01   3.98E-01   5.01E-01   6.30E-01   7.94E-01   1.00E+00
     1.25E+00   1.58E+00   1.99E+00   2.51E+00   3.16E+00   3.98E+00
     5.01E+00   6.30E+00   7.94E+00   1.00E+01   1.15E+01   25.
c
c  for gammas
e22  0.01   0.015   0.02   0.03   0.04   0.05   0.06   0.08   0.1
     0.15   0.2      0.3    0.4    0.5    0.6    0.8     1.   1.5
       2.    3.       4.     5.     6.     8.   10.0    12.    15.
c
c  ICRP 74 Dose Conversion coeffients
DE12  1.00E-09  1.00E-08  2.53E-08  1.00E-07  2.00E-07  5.00E-07
      1.00E-06  2.00E-06  5.00E-06  1.00E-05  2.00E-05  5.00E-05
      1.00E-04  2.00E-04  5.00E-04  1.00E-03  2.00E-03  5.00E-03
      1.00E-02  2.00E-02  3.00E-02  5.00E-02  7.00E-02  1.00E-01
      1.50E-01  2.00E-01  3.00E-01  5.00E-01  7.00E-01  9.00E-01
      1.00E+00  1.20E+00  2.00E+00  3.00E+00  4.00E+00  5.00E+00
      6.00E+00  7.00E+00  8.00E+00  9.00E+00  1.00E+01  1.20E+01
      1.40E+01  1.50E+01  1.60E+01  1.80E+01  2.00E+01  3.00E+01
      5.00E+01  7.50E+01  1.00E+02  1.25E+02  1.50E+02  1.75E+02
      2.01E+02
c
DF12  6.6  9   10.6  12.9  13.5  13.6  13.3  12.9   12   11.3  10.6
      9.9  9.4  8.9   8.3   7.9   7.7     8  10.5  16.6  23.7  41.1
       60   88  132   170   233   322   375   400   416   425   420
      412  408  405   400   405   409   420   440   480   520   540
      555  570  600   515   400   330   285   260   245   250   260
c
c  ICRP 74 Dose Conversion coeffients
DE25  1.00E-09  1.00E-08  2.53E-08  1.00E-07  2.00E-07  5.00E-07
      1.00E-06  2.00E-06  5.00E-06  1.00E-05  2.00E-05  5.00E-05
      1.00E-04  2.00E-04  5.00E-04  1.00E-03  2.00E-03  5.00E-03
      1.00E-02  2.00E-02  3.00E-02  5.00E-02  7.00E-02  1.00E-01
      1.50E-01  2.00E-01  3.00E-01  5.00E-01  7.00E-01  9.00E-01
      1.00E+00  1.20E+00  2.00E+00  3.00E+00  4.00E+00  5.00E+00
      6.00E+00  7.00E+00  8.00E+00  9.00E+00  1.00E+01  1.20E+01
      1.40E+01  1.50E+01  1.60E+01  1.80E+01  2.00E+01  3.00E+01
      5.00E+01  7.50E+01  1.00E+02  1.25E+02  1.50E+02  1.75E+02
      2.01E+02
c
DF25  6.6  9   10.6  12.9  13.5  13.6  13.3  12.9   12   11.3  10.6
      9.9  9.4  8.9   8.3   7.9   7.7     8  10.5  16.6  23.7  41.1
       60   88  132   170   233   322   375   400   416   425   420
      412  408  405   400   405   409   420   440   480   520   540
      555  570  600   515   400   330   285   260   245   250   260
c
c ICRP 74 DCCs for photons (pSv-cm2)
de32  0.01   0.015   0.02   0.03   0.04   0.05   0.06   0.08   0.1
```

```
     0.15   0.2      0.3    0.4    0.5    0.6    0.8     1.   1.5
       2.    3.       4.     5.     6.     8.   10.0
df32   0.061   0.83   1.05   0.81   0.64   0.55   0.51   0.53  0.61
       0.89    1.2    1.8    2.38   2.93   3.44   4.38    5.2   6.9
        8.6   11.1   13.4    15.5   17.6   21.6   25.6
c
mode n p
CUT:N  1J  1.e-10
CUT:P  1J   0.01
nps 1E7
```

B.3 ^{252}Cf in Lead MCNP Input

```
Cf in 19.3675cm r Pb sphere
c by Pete Exline
c Cell Cards
c cells for bare source with no PNL rabbit
c
c ***PRIMARY ENCAPSULATION***
c
c CF oxide source volume (no material assumed for the moment**
c
1 0      -12 18 -17 imp:n=1 imp:p=1
c
c Lower porous platinum filter (1/2 full density assumed)
c
2 1 -10.68 -12 17 -16 imp:n=1 imp:p=1
c
c Lower void
c
3 0      -13 16 -15 imp:n=1 imp:p=1
c
c Middle void
c
4 0      -12 19 -18 imp:n=1 imp:p=1
c
c upper porous platinum filter (1/2 full density assumed)
c
5 1 -10.68 -12 -19 20 imp:n=1 imp:p=1
c
c Upper void
c
6 0      -12 -20 21 imp:n=1 imp:p=1
c
c Primary capsule container (90% Pt and 10% Rh)
c
7 2 -19.9541 #(-15 -13 16:-16 -12 21) 22 -11 -14 imp:n=1 imp:p=1
c
c Gap between the primnary and secondary capsules
c
8 0       #(22 -11 -14) (23 -6 -7):(-6 10 -23 35) imp:n=1 imp:p=1
c
c **SECONDARY CAPSULE OF ZIRCALLOY-2***
c
9 3 -6.415 #(-7 -6 35) (-4 8 -3):-8 9 -5:-10 -23 35 imp:n=1 imp:p=1
c
c The threads of the secondary capsule
c
10 3 -6.415 -2 -1 3 imp:n=1 imp:p=1
c
c ** Pb Sphere **
301 304 -1.24e-3 #(-301 302 -303) #(-304 305 307) &
          (-322 302 #(&
(-501 502 503 -504 505 -506):&
((-501 531 513 515 -503 -525):(-501 531 503 515 -523 -505))&
:((-501 531 524 -514 515 -505):(-501 531 504 -514 515 -525))&
:((-501 531 513 -516 -503 526):(-501 531 503 -516 -523 506))&
:((-501 531 524 -514 -516 506):(-501 531 504 -514 -516 526))&
:((-531 543 545 -503 -525):(-531 503 545 -523 -505))&
:((-531 524 -544 545 -505):(-531 504 -544 545 -525))&
:((-531 543 -546 -503 526):(-531 503 -546 -523 506))&
:((-531 524 -544 -546 506):(-531 504 -544 -546 526))&
:((501 -553 551 -552))))&
 imp:n=1 imp:p=1 $air from Pb surface to tally sph
302 304 -1.24e-3 322 -306         imp:n=1 imp:p=1 $air from sphere to edge of univ
303 301 -11.34  -301 302 -303     imp:n=1 imp:p=1 $Pb sphere bottom
304 0      306                    imp:n=0 imp:p=0 $Void space outside universe
305 301 -11.34 -304 305 307       imp:n=1 imp:p=1 $Pb sphere top
c **
```

```
c ** air to combine for Pb Sphere **
401 304 -1.24e-3  (-302 1 -2 3):(-302 4 -3 8):(-302 5 -8 9):(-302 2):(-302 -9) &
 imp:n=1 imp:p=1
c * Al table top*
501 305 -2.7 -501 502 503 -504 505 -506 imp:n=1 imp:p=1 $Al table top
511 305 -2.7 (-501 531 513 515 -503 -525):(-501 531 503 515 -523 -505) &
imp:n=1 imp:p=1 $bl leg
512 305 -2.7 (-501 531 524 -514 515 -505):(-501 531 504 -514 515 -525) &
imp:n=1 imp:p=1 $br leg
513 305 -2.7 (-501 531 513 -516 -503 526):(-501 531 503 -516 -523 506) &
imp:n=1 imp:p=1 $tl leg
514 305 -2.7 (-501 531 524 -514 -516 506):(-501 531 504 -514 -516 526) &
imp:n=1 imp:p=1 $tr leg
541 305 -2.7 (-531 -322 543 545 -503 -525):(-531 -322 503 545 -523 -505) &
imp:n=1 imp:p=1 $bl thick leg
542 305 -2.7 (-531 -322 524 -544 545 -505):(-531 -322 504 -544 545 -525) &
imp:n=1 imp:p=1 $br thick leg
543 305 -2.7 (-531 -322 543 -546 -503 526):(-531 -322 503 -546 -523 506) &
imp:n=1 imp:p=1 $tl thick leg
544 305 -2.7 (-531 -322 524 -544 -546 506):(-531 -322 504 -544 -546 526) &
imp:n=1 imp:p=1 $tr thick leg
551 305 -2.7 501 -553 551 -552 imp:n=1 imp:p=1 $Al stabilizer ring
c **

c Surface Cards
c Cylinder and planes to define the theaded portion of the
c     secondary capsule
c
1 CX 0.2413
2 PX 1.8542
3 PX 1.3462
c
c Cylinders to define the secondary encapsulation
c
4 CX 0.4699
5 CX 0.4115
6 CX 0.2972
c
c planes and cone to define the seconday encapsulation
c
7 PX 1.143
8 PX -1.778
9 PX -1.905
10 KX 1.720611544 0.007654266 -1
c
c Cylinders to define the primary encapsulation
c
11 CX 0.2769
12 CX 0.1636
13 CX 0.1524
c
c Planes to define the primary encapsulation
c
14 PX 1.0859
15 PX 0.6922
16 PX 0.5144
17 PX 0.1588
18 PX -0.1588
19 PX -0.4763
20 PX -0.8319
21 PX -0.9970
22 PX -1.3907
23 PX -1.4478
35 PX -1.6764
c **Pb Sphere **
301  SO 19.3675  $Outer surface of Pb Sphere (bot hem)
302  SO 3.05   $inner void for source (bot hem)
303 PZ 0 $top of bottom hemisphere
304 S -.02338 0 0.95135 19.3675 $Pb top hemisphere sphere
```

```
305 S -.02338 0 0.95135 3.05 $inner void for source (top hem)
306  SO 500     $Edge of the Universe
307 P -19.3675 0 0 -.02338 0 .95135 -.02338 1 .95135
322 SO 100      $100cm tally sphere around source
c **
c *Al table top*
501  pz -19.3675 $top of Al table top
502  pz -19.9675 $bot of Al table top
503  px -25.325 $left of Al table top
504  px 25.325 $right of Al table top
505  py -25.325 $front of Al table top
506  py 25.325 $back of Al table top
513  px -25.475 $left of Al table leg
514  px 25.475 $right of Al table leg
515  py -25.475 $front of Al table leg
516  py 25.475 $back of Al table leg
523  px -20.575 $cutoff of Al table top
524  px 20.575 $cutoff of Al table top
525  py -20.575 $cutoff of Al table top
526  py 20.575 $cutoff of Al table top
531  pz -35.9675 $bot of thin legs/top of thick legs
543  px -26.075 $left of Al table thick leg
544  px 26.075 $right of Al table thick leg
545  py -26.075 $front of Al table thick leg
546  py 26.075 $back of Al table thick leg
551  cz 6.25 $inner radius of Al stabilizer
552  cz 8.75 $outer radius of Al stabilizer
553  pz -18.7175 $top of Al stablizer
c **
c  The next set of planes will be used to segment surface 22 to do the angular
c  dependent tally.  They do not have to be used in the cell descriptions.
c
324 PZ 98.7688340595138
325 PZ 95.1056516295154
326 PZ 89.1006524188368
327 PZ 80.9016994374947
328 PZ 70.7106781186548
329 PZ 58.7785252292473
330 PZ 45.3990499739547
331 PZ 30.9016994374947
332 PZ 15.6434465040231
333 PZ 0
334 PZ -15.6434465040231
335 PZ -30.9016994374947
336 PZ -45.3990499739547
337 PZ -58.7785252292473
338 PZ -70.7106781186547
339 PZ -80.9016994374947
340 PZ -89.1006524188368
341 PZ -95.1056516295154
342 PZ -98.7688340595138
c **

c Material Cards
c
c Materials: M1 is the porous filter, M2 is the 90% Pt, 10% Rh
c    and M4 is the Zircalloy-2
c
M1 78000 1.0
M2 78000 -0.9 45103 -0.1
M3 50000 -0.015 26000 -0.0012 24000 -0.001 28000 -0.0005 &
40090 -.5053934 40091 -.1102141 40092 -.1684645 40094 -.1707237 &
40096 -.0275044
c ** Pb Sphere **
m301 82204 .014 82206 .241 82207 .221 82208 .524
c **
m304 7014 -.7558 8016 -.2314 18000 -.0128 $air
c **
m305 13027 1.0 $Al
```

```
c
c the source is input in cell one region using a Maxwellian with
c   temperature of 1.42 MeV
c
c old syntax -- SRC4 3J 1 1 0.0 0.1636 0.1588 0. 0. 1.
SDEF ERG=D1 CEL=1 PAR =1 POS=0 0 0 AXS=0 0 1 EXT=D3 RAD=D2
SI3 -0.159 0.159
SI2 0 0.164
SP2 -21 1
SP1 -2 1.42
c
c Tallies
F2:N  322
FC2  Neutron Flux
FS2 -334 -332 T $plus/minus 15.6cm cutoffs
c Current Tally of whole sphere
F1:N  322
FC1 number of neutrons per spherical surface segments at 100 cm
c Segmented Tally across z plans of the sphere
FS1  -342 -341 -340 -339 -338 -337 -336 -335 -334 -333 -332 -331 &
-330 -329 -328 -327 -326 -325 -324
c
F12:N 322
FC12  Icrp 74 ambient dose equivalent on spherical surface at 100 cm
c Segmented Tally across z plans of the sphere
FS12  -342 -341 -340 -339 -338 -337 -336 -335 -334 -333 -332 -331 &
-330 -329 -328 -327 -326 -325 -324
c
c  gamma fluence tally at 100 cm
F22:P  322
FC22  Gamma Ray Fluence induced by neutrons at 100 cm
FS22 -334 -332 T $plus/minus 15.6cm cutoffs
c
F32:P   322
FC32  Gamma Ray Dose rate at 100 cm
FS32 -334 -332 T $plus/minus 15.6cm cutoffs
c
F5:N -100.0001 0 0 .1
FC5 Point Neutron Detector at 100cm
c
F25:N -100.0001 0 0 .1
FC25 ICRP 74 ambient dose equivalent on Point Neutron Detector at 100cm
c Energy groups used to bin fluence
e1   1.00E-09   2.15E-09   4.64E-09   1.00E-08   2.15E-08   4.64E-08
     1.00E-07   2.15E-07   4.64E-07   1.00E-06   2.15E-06   4.64E-06
     1.00E-05   2.15E-05   4.64E-05   1.00E-04   2.15E-04   4.64E-04
     1.00E-03   2.15E-03   4.64E-03   1.00E-02   1.25E-02   1.58E-02
     1.99E-02   2.51E-02   3.16E-02   3.98E-02   5.01E-02   6.30E-02
     7.94E-02   1.00E-01   1.25E-01   1.58E-01   1.99E-01   2.51E-01
     3.16E-01   3.98E-01   5.01E-01   6.30E-01   7.94E-01   1.00E+00
     1.25E+00   1.58E+00   1.99E+00   2.51E+00   3.16E+00   3.98E+00
     5.01E+00   6.30E+00   7.94E+00   1.00E+01   1.15E+01   25.
c
e2   1.00E-09   2.15E-09   4.64E-09   1.00E-08   2.15E-08   4.64E-08
     1.00E-07   2.15E-07   4.64E-07   1.00E-06   2.15E-06   4.64E-06
     1.00E-05   2.15E-05   4.64E-05   1.00E-04   2.15E-04   4.64E-04
     1.00E-03   2.15E-03   4.64E-03   1.00E-02   1.25E-02   1.58E-02
     1.99E-02   2.51E-02   3.16E-02   3.98E-02   5.01E-02   6.30E-02
     7.94E-02   1.00E-01   1.25E-01   1.58E-01   1.99E-01   2.51E-01
     3.16E-01   3.98E-01   5.01E-01   6.30E-01   7.94E-01   1.00E+00
     1.25E+00   1.58E+00   1.99E+00   2.51E+00   3.16E+00   3.98E+00
     5.01E+00   6.30E+00   7.94E+00   1.00E+01   1.15E+01   25.
c
e5   1.00E-09   2.15E-09   4.64E-09   1.00E-08   2.15E-08   4.64E-08
     1.00E-07   2.15E-07   4.64E-07   1.00E-06   2.15E-06   4.64E-06
     1.00E-05   2.15E-05   4.64E-05   1.00E-04   2.15E-04   4.64E-04
     1.00E-03   2.15E-03   4.64E-03   1.00E-02   1.25E-02   1.58E-02
     1.99E-02   2.51E-02   3.16E-02   3.98E-02   5.01E-02   6.30E-02
     7.94E-02   1.00E-01   1.25E-01   1.58E-01   1.99E-01   2.51E-01
```

```
     3.16E-01   3.98E-01   5.01E-01   6.30E-01   7.94E-01   1.00E+00
     1.25E+00   1.58E+00   1.99E+00   2.51E+00   3.16E+00   3.98E+00
     5.01E+00   6.30E+00   7.94E+00   1.00E+01   1.15E+01   25.
c
e12   1.00E-09   2.15E-09   4.64E-09   1.00E-08   2.15E-08   4.64E-08
     1.00E-07   2.15E-07   4.64E-07   1.00E-06   2.15E-06   4.64E-06
     1.00E-05   2.15E-05   4.64E-05   1.00E-04   2.15E-04   4.64E-04
     1.00E-03   2.15E-03   4.64E-03   1.00E-02   1.25E-02   1.58E-02
     1.99E-02   2.51E-02   3.16E-02   3.98E-02   5.01E-02   6.30E-02
     7.94E-02   1.00E-01   1.25E-01   1.58E-01   1.99E-01   2.51E-01
     3.16E-01   3.98E-01   5.01E-01   6.30E-01   7.94E-01   1.00E+00
     1.25E+00   1.58E+00   1.99E+00   2.51E+00   3.16E+00   3.98E+00
     5.01E+00   6.30E+00   7.94E+00   1.00E+01   1.15E+01   25.
c
e25   1.00E-09   2.15E-09   4.64E-09   1.00E-08   2.15E-08   4.64E-08
     1.00E-07   2.15E-07   4.64E-07   1.00E-06   2.15E-06   4.64E-06
     1.00E-05   2.15E-05   4.64E-05   1.00E-04   2.15E-04   4.64E-04
     1.00E-03   2.15E-03   4.64E-03   1.00E-02   1.25E-02   1.58E-02
     1.99E-02   2.51E-02   3.16E-02   3.98E-02   5.01E-02   6.30E-02
     7.94E-02   1.00E-01   1.25E-01   1.58E-01   1.99E-01   2.51E-01
     3.16E-01   3.98E-01   5.01E-01   6.30E-01   7.94E-01   1.00E+00
     1.25E+00   1.58E+00   1.99E+00   2.51E+00   3.16E+00   3.98E+00
     5.01E+00   6.30E+00   7.94E+00   1.00E+01   1.15E+01   25.
c
c  for gammas
e22  0.01   0.015   0.02   0.03   0.04   0.05   0.06   0.08   0.1
     0.15   0.2      0.3    0.4    0.5    0.6    0.8     1.   1.5
       2.    3.       4.     5.     6.     8.   10.0    12.    15.
c
c  ICRP 74 Dose Conversion coeffients
DE12  1.00E-09  1.00E-08  2.53E-08  1.00E-07  2.00E-07  5.00E-07
      1.00E-06  2.00E-06  5.00E-06  1.00E-05  2.00E-05  5.00E-05
      1.00E-04  2.00E-04  5.00E-04  1.00E-03  2.00E-03  5.00E-03
      1.00E-02  2.00E-02  3.00E-02  5.00E-02  7.00E-02  1.00E-01
      1.50E-01  2.00E-01  3.00E-01  5.00E-01  7.00E-01  9.00E-01
      1.00E+00  1.20E+00  2.00E+00  3.00E+00  4.00E+00  5.00E+00
      6.00E+00  7.00E+00  8.00E+00  9.00E+00  1.00E+01  1.20E+01
      1.40E+01  1.50E+01  1.60E+01  1.80E+01  2.00E+01  3.00E+01
      5.00E+01  7.50E+01  1.00E+02  1.25E+02  1.50E+02  1.75E+02
      2.01E+02
c
DF12  6.6  9   10.6  12.9  13.5  13.6  13.3  12.9   12   11.3  10.6
      9.9  9.4  8.9   8.3   7.9   7.7     8  10.5  16.6  23.7  41.1
       60   88  132   170   233   322   375   400   416   425   420
      412  408  405   400   405   409   420   440   480   520   540
      555  570  600   515   400   330   285   260   245   250   260
c
c  ICRP 74 Dose Conversion coeffients
DE25  1.00E-09  1.00E-08  2.53E-08  1.00E-07  2.00E-07  5.00E-07
      1.00E-06  2.00E-06  5.00E-06  1.00E-05  2.00E-05  5.00E-05
      1.00E-04  2.00E-04  5.00E-04  1.00E-03  2.00E-03  5.00E-03
      1.00E-02  2.00E-02  3.00E-02  5.00E-02  7.00E-02  1.00E-01
      1.50E-01  2.00E-01  3.00E-01  5.00E-01  7.00E-01  9.00E-01
      1.00E+00  1.20E+00  2.00E+00  3.00E+00  4.00E+00  5.00E+00
      6.00E+00  7.00E+00  8.00E+00  9.00E+00  1.00E+01  1.20E+01
      1.40E+01  1.50E+01  1.60E+01  1.80E+01  2.00E+01  3.00E+01
      5.00E+01  7.50E+01  1.00E+02  1.25E+02  1.50E+02  1.75E+02
      2.01E+02
c
DF25  6.6  9   10.6  12.9  13.5  13.6  13.3  12.9   12   11.3  10.6
      9.9  9.4  8.9   8.3   7.9   7.7     8  10.5  16.6  23.7  41.1
       60   88  132   170   233   322   375   400   416   425   420
      412  408  405   400   405   409   420   440   480   520   540
      555  570  600   515   400   330   285   260   245   250   260
c
c ICRP 74 DCCs for photons (pSv-cm2)
de32  0.01   0.015   0.02   0.03   0.04   0.05   0.06   0.08   0.1
     0.15   0.2      0.3    0.4    0.5    0.6    0.8     1.   1.5
       2.    3.       4.     5.     6.     8.   10.0
```

```
df32   0.061   0.83   1.05   0.81   0.64   0.55   0.51   0.53  0.61
       0.89    1.2    1.8    2.38   2.93   3.44   4.38    5.2   6.9
        8.6   11.1   13.4    15.5   17.6   21.6   25.6
c
mode n p
CUT:N  1J  1.e-10
CUT:P  1J   0.01
nps 1E7
```

B.4 ^{252}Cf in Iron MCNP Input

```
Cf in 30" Fe sphere
c by Pete Exline
c Cell Cards
c cells for bare source with no PNL rabbit
c
c ***PRIMARY ENCAPSULATION***
c
c CF oxide source volume (no material assumed for the moment**
c
1 0      -12 -18 17 imp:n=1 imp:p=1
c
c Lower porous platinum filter (1/2 full density assumed)
c
2 1 -10.68 -12 -17 16 imp:n=1 imp:p=1
c
c Lower void
c
3 0      -13 -16 15 imp:n=1 imp:p=1
c
c Middle void
c
4 0      -12 -19 18 imp:n=1 imp:p=1
c
c upper porous platinum filter (1/2 full density assumed)
c
5 1 -10.68 -12 19 -20 imp:n=1 imp:p=1
c
c Upper void
c
6 0      -12 20 -21 imp:n=1 imp:p=1
c
c Primary capsule container (90% Pt and 10% Rh)
c
7 2 -19.9541 #(15 -13 -16:16 -12 -21) -22 -11 14 imp:n=1 imp:p=1
c
c Gap between the primnary and secondary capsules
c
8 0       #(-22 -11 14) (-23 -6 7):(-6 10 23 -35) imp:n=1 imp:p=1
c
c **SECONDARY CAPSULE OF ZIRCALLOY-2***
c
9 3 -6.415 #(7 -6 -35) (-4 -8 3):8 -9 -5:-10 23 -35 imp:n=1 imp:p=1
c
c The threads of the secondary capsule
c
10 3 -6.415 2 -1 -3 imp:n=1 imp:p=1
c
c ** Fe Sphere **
301 304 -1.24e-3      -322 301 #(501 -502 -503 504 505 -506) &
  #(502 -507 505 -510 -508 509) &
  #(502 -507 -506 511 -508 509) &
  #(507 -518 -512 -513 514 -516 528) &
  #(507 -518 -512 -513 515 -517 528) &
  #((514 -516 518 525 -526 -519 528):(514 -516 519 -524 520 &
  -521 -523 -522 528)) &
  #((515 -517 518 525 -526 -519 528):(515 -517 519 -524 520 &
  -521 -523 -522 528)) &
  #(529 -516 303 -528 301) &
  #(-530 515 303 -528 301) &
  #(-533:(-535 524 -537)) &
  #(-534:(-536 524 -537)) &
  #(507 -540 516 -510 541 538 -539) &
  #(507 -540 511 -515 542 538 -539) &
  #(-312 313 -314) imp:n=1 imp:p=1 $air from Fe surface to tally sph
302 304 -1.24e-3      322 -306  imp:n=1 imp:p=1 $air
c 302 0     322 -306  imp:n=1 imp:p=1 $void from sphere to edge of univ
```

```
303 301 -7.874  -301 302 307 (303:309) (305:311) (310:304) (308:-311) &
  imp:n=1 imp:p=1 $Fe sphere
304 0      306                    imp:n=0 imp:p=0 $Void space outside universe
305 301 -7.874 -301 -307             imp:n=1 imp:p=1 $plugged right tube
306 304 -1.24e-3 -303 302 -301 -309 #(-312 313 -314) imp:n=1 imp:p=1 $left tube
307 301 -7.874  (-301 -305 -311 302):(-301 -310 -304 302) &
  imp:n=1 imp:p=1 $plugged bottom tube
308 301 -7.874 -301 302 -308 311      imp:n=1 imp:p=1 $plugged top tube
309 301 -7.874 -312 313 -314 imp:n=1 imp:p=1 $smaller plug for left tube
c **
c
c ** Fe Stand **
501 301 -7.874 501 -502 -503 504 505 -506 imp:n=1 imp:p=1 $base plate
502 301 -7.874 502 -507 505 -510 -508 509 imp:n=1 imp:p=1 $l upp base
503 301 -7.874 502 -507 -506 511 -508 509 imp:n=1 imp:p=1 $r upp base
504 301 -7.874 507 -518 -512 -513 514 -516 528 imp:n=1 imp:p=1 $l support
505 301 -7.874 507 -518 -512 -513 515 -517 528 imp:n=1 imp:p=1 $r support
506 301 -7.874 (514 -516 518 525 -526 -519 528):(514 -516 519 -524 520 &
  -521 -523 -522 528) imp:n=1 imp:p=1 $left support cap
507 301 -7.874 (515 -517 518 525 -526 -519 528):(515 -517 519 -524 520 &
  -521 -523 -522 528) imp:n=1 imp:p=1 $right support cap
508 301 -7.874 529 -516 303 -528 301 imp:n=1 imp:p=1 $left cap ring
509 301 -7.874 -530 515 303 -528 301 imp:n=1 imp:p=1 $right cap ring
510 301 -7.874 -533:(-535 524 -537) imp:n=1 imp:p=1 $left eyelet
511 301 -7.874 -534:(-536 524 -537) imp:n=1 imp:p=1 $right eyelet
512 301 -7.874 507 -540 516 -510 541 538 -539 imp:n=1 imp:p=1 $left flange
513 301 -7.874 507 -540 511 -515 542 538 -539 imp:n=1 imp:p=1 $right flange
c **
c ** Air to combine for Fe Sphere **
401 304 -1.24e-3  (-302 1 2 -3):(-302 4 3 -8):(-302 5 8 -9):(-302 -2):(-302 9)&
   imp:n=1 imp:p=1

c Surface Cards
c Cylinder and planes to define the theaded portion of the
c     secondary capsule
c
1 CX 0.2413
2 PX -1.8542
3 PX -1.3462
c
c Cylinders to define the secondary encapsulation
c
4 CX 0.4699
5 CX 0.4115
6 CX 0.2972
c
c planes and cone to define the seconday encapsulation
c
7 PX -1.143
8 PX 1.778
9 PX 1.905
10 KX -1.720611544 0.007654266 +1
c
c Cylinders to define the primary encapsulation
c
11 CX 0.2769
12 CX 0.1636
13 CX 0.1524
c
c Planes to define the primary encapsulation
c
14 PX -1.0859
15 PX -0.6922
16 PX -0.5144
17 PX -0.1588
18 PX 0.1588
19 PX 0.4763
20 PX 0.8319
21 PX 0.9970
```

```
22 PX 1.3907
23 PX 1.4478
35 PX 1.6764
c **Fe Sphere **
301  SO 38.1  $Outer surface of Fe Sphere
306  SO 500     $Edge of the Universe
302  SO 7.62   $inner void for source
303  CX 4.7625   $constant radius tube from left
304  PY -19.05  $plane to define radius change point in bottom entry
305 CY 5.08   $tube from bottom (smaller radius)
310 CY 6.35   $tube from bottom (larger radius)
307 C/Y 22.86 0 2.54    $tube on right side
308 CY 1.27   $used to define upper half for plug geometries
309 PX 0 $used to stop tubes on left/right of origin
311 PY 0 $used to stop tubes on top/bottom of origin
312 PX -17.5838 $top of shape used to move left plug out due to Cf attachment
313 PX -48.0638 $bottom of left plug cylinder
314 CX 4.25 $smaller left plug
322 SO 100      $100cm Sphere around source
c **
c
c **Fe Stand**
501 PZ -44.1325 $bottom of base plate
502 PZ -41.91 $top of base plate and bot of upper base
503 PY 40.64 $top edge of base plate
504 PY -40.64 $bottom edge of base plate
505 PX -45.72 $left edge of base plate and upper base
506 PX 45.72 $right edge of base plate and upper base
507 PZ -40.3225 $top of upper base
508 PY 17.78 $top edge of upper base
509 PY -17.78 $bot edge of upper base
510 PX -29.36875 $right edge of l upper base
511 PX 29.36875 $left edge of r upper base
512 P 0 -17.78 -40.3225 0 -12.7 0 1 -12.7 0
513 P 0 17.78 -40.3225 0 12.7 0 1 12.7 0
514 PX -41.5925 $left support left edge
515 PX 37.62375 $right support left edge
516 PX -37.62375 $left support right edge
517 PX 41.5925 $right support right edge
518 PZ 0 $supports top edge
519 PZ 1.11125 $cap screw flange top
520 PY -10.16 $cap left vert
521 PY 10.16 $cap right vert
522 P 0 -10.16 3.81 0 -2.8575 12.065 1 -2.8575 12.065 $cap left diagonal
523 P 0 10.16 3.81 0 2.8575 12.065 1 2.8575 12.065 $cap right diagonal
524 PZ 12.065 $cap top
525 PY -12.7 $cap left edge
526 PY 12.7 $cap right edge
c 527 CX 4.683125 $inner radius cap ring {set to match port radius}
528 CX 8.41375 $outer radius cap rin
529 PX -40.16375 $outer edge of left cap ring
530 PX 40.16375 $outer edge of right cap ring
c 531 PX -37.8138 $inner edge of left cap ring {adjusted to fit imperfect sphere}
c 532 PX 37.8138 $inner edge of right cap ring {adjusted to fit imperfect sphere}
533 TX -39.60813 0 15.5575 2.420938 .595313 .595313 $left eyelet
534 TX 39.60813 0 15.5575 2.420938 .595313 .595313 $right eyelet
535 C/Z -39.60813 0 .79375 $left eyelet connector walls
536 C/Z 39.60813 0 .79375 $right eyelet connector walls
537 PZ 12.7 $eyelet connector top cutoff
538 PY -.635 $bottom edge of flagnes
539 PY .635 $top edge of flanges
540 PZ -8.41375 $top of flanges (tapered completely off)
541 P -29.36875 0 -40.3225 -37.62375 0 -8.41375 -37.62375 1 -8.41375
542 P 29.36875 0 -40.3225 37.62375 0 -8.41375 37.62375 1 -8.41375
c **
c  The next set of planes will be used to segment surface 22 to do the angular
c  dependent tally.  They do not have to be used in the cell descriptions.
c
324 PZ 98.7688340595138
```

```
325 PZ 95.1056516295154
326 PZ 89.1006524188368
327 PZ 80.9016994374947
328 PZ 70.7106781186548
329 PZ 58.7785252292473
330 PZ 45.3990499739547
331 PZ 30.9016994374947
332 PZ 15.6434465040231
333 PZ 0
334 PZ -15.6434465040231
335 PZ -30.9016994374947
336 PZ -45.3990499739547
337 PZ -58.7785252292473
338 PZ -70.7106781186547
339 PZ -80.9016994374947
340 PZ -89.1006524188368
341 PZ -95.1056516295154
342 PZ -98.7688340595138
c **

c Material Cards
c
c Materials: M1 is the porous filter, M2 is the 90% Pt, 10% Rh
c    and M4 is the Zircalloy-2
c
M1 78000 1.0
M2 78000 -0.9 45103 -0.1
M3 50000 -0.015 26000 -0.0012 24000 -0.001 28000 -0.0005 &
40090 -.5053934 40091 -.1102141 40092 -.1684645 40094 -.1707237 &
40096 -.0275044
c ** Fe Sphere **
m301 26000. -.99283 6000 -.0021 25055.61c -.0047 &
   15031 -.00013 16000 -.00024
c
m304 7014 -.7558 8016 -.2314 18000 -.0128 $air
c **
c
c the source is input in cell one region using a Maxwellian with
c   temperature of 1.42 MeV
c
c old syntax -- SRC4 3J 1 1 0.0 0.1636 0.1588 0. 0. 1.
SDEF ERG=D1 CEL=1 PAR =1 POS=0 0 0 AXS=0 0 1 EXT=D3 RAD=D2
SI3 -0.159 0.159
SI2 0 0.164
SP2 -21 1
SP1 -2 1.42
c
c Tallies
F2:N  322
FC2  Neutron Flux
FS2 -334 -332 T $plus/minus 15.6cm cutoffs
c Current Tally of whole sphere
F1:N  322
FC1 number of neutrons per spherical surface segments at 100 cm
c Segmented Tally across z plans of the sphere
FS1  -342 -341 -340 -339 -338 -337 -336 -335 -334 -333 -332 -331 &
-330 -329 -328 -327 -326 -325 -324
c
F12:N 322
FC12  Icrp 74 ambient dose equivalent on spherical surface at 100 cm
c Segmented Tally across z plans of the sphere
FS12  -342 -341 -340 -339 -338 -337 -336 -335 -334 -333 -332 -331 &
-330 -329 -328 -327 -326 -325 -324
c
c  gamma fluence tally at 100 cm
F22:P  322
FC22  Gamma Ray Fluence induced by neutrons at 100 cm
FS22 -334 -332 T $plus/minus 15.6cm cutoffs
c
```

```
F32:P   322
FC32  Gamma Ray Dose rate at 100 cm
FS32 -334 -332 T $plus/minus 15.6cm cutoffs
c
F5:N -100.0001 0 0 .1
FC5 Point Neutron Detector at 100cm
c
F25:N -100.0001 0 0 .1
FC25 ICRP 74 ambient dose equivalent on Point Neutron Detector at 100cm
c Energy groups used to bin fluence
e1   1.00E-09   2.15E-09   4.64E-09   1.00E-08   2.15E-08   4.64E-08
     1.00E-07   2.15E-07   4.64E-07   1.00E-06   2.15E-06   4.64E-06
     1.00E-05   2.15E-05   4.64E-05   1.00E-04   2.15E-04   4.64E-04
     1.00E-03   2.15E-03   4.64E-03   1.00E-02   1.25E-02   1.58E-02
     1.99E-02   2.51E-02   3.16E-02   3.98E-02   5.01E-02   6.30E-02
     7.94E-02   1.00E-01   1.25E-01   1.58E-01   1.99E-01   2.51E-01
     3.16E-01   3.98E-01   5.01E-01   6.30E-01   7.94E-01   1.00E+00
     1.25E+00   1.58E+00   1.99E+00   2.51E+00   3.16E+00   3.98E+00
     5.01E+00   6.30E+00   7.94E+00   1.00E+01   1.15E+01   25.
c
e2   1.00E-09   2.15E-09   4.64E-09   1.00E-08   2.15E-08   4.64E-08
     1.00E-07   2.15E-07   4.64E-07   1.00E-06   2.15E-06   4.64E-06
     1.00E-05   2.15E-05   4.64E-05   1.00E-04   2.15E-04   4.64E-04
     1.00E-03   2.15E-03   4.64E-03   1.00E-02   1.25E-02   1.58E-02
     1.99E-02   2.51E-02   3.16E-02   3.98E-02   5.01E-02   6.30E-02
     7.94E-02   1.00E-01   1.25E-01   1.58E-01   1.99E-01   2.51E-01
     3.16E-01   3.98E-01   5.01E-01   6.30E-01   7.94E-01   1.00E+00
     1.25E+00   1.58E+00   1.99E+00   2.51E+00   3.16E+00   3.98E+00
     5.01E+00   6.30E+00   7.94E+00   1.00E+01   1.15E+01   25.
c
e5   1.00E-09   2.15E-09   4.64E-09   1.00E-08   2.15E-08   4.64E-08
     1.00E-07   2.15E-07   4.64E-07   1.00E-06   2.15E-06   4.64E-06
     1.00E-05   2.15E-05   4.64E-05   1.00E-04   2.15E-04   4.64E-04
     1.00E-03   2.15E-03   4.64E-03   1.00E-02   1.25E-02   1.58E-02
     1.99E-02   2.51E-02   3.16E-02   3.98E-02   5.01E-02   6.30E-02
     7.94E-02   1.00E-01   1.25E-01   1.58E-01   1.99E-01   2.51E-01
     3.16E-01   3.98E-01   5.01E-01   6.30E-01   7.94E-01   1.00E+00
     1.25E+00   1.58E+00   1.99E+00   2.51E+00   3.16E+00   3.98E+00
     5.01E+00   6.30E+00   7.94E+00   1.00E+01   1.15E+01   25.
c
e12   1.00E-09   2.15E-09   4.64E-09   1.00E-08   2.15E-08   4.64E-08
     1.00E-07   2.15E-07   4.64E-07   1.00E-06   2.15E-06   4.64E-06
     1.00E-05   2.15E-05   4.64E-05   1.00E-04   2.15E-04   4.64E-04
     1.00E-03   2.15E-03   4.64E-03   1.00E-02   1.25E-02   1.58E-02
     1.99E-02   2.51E-02   3.16E-02   3.98E-02   5.01E-02   6.30E-02
     7.94E-02   1.00E-01   1.25E-01   1.58E-01   1.99E-01   2.51E-01
     3.16E-01   3.98E-01   5.01E-01   6.30E-01   7.94E-01   1.00E+00
     1.25E+00   1.58E+00   1.99E+00   2.51E+00   3.16E+00   3.98E+00
     5.01E+00   6.30E+00   7.94E+00   1.00E+01   1.15E+01   25.
c
e25   1.00E-09   2.15E-09   4.64E-09   1.00E-08   2.15E-08   4.64E-08
     1.00E-07   2.15E-07   4.64E-07   1.00E-06   2.15E-06   4.64E-06
     1.00E-05   2.15E-05   4.64E-05   1.00E-04   2.15E-04   4.64E-04
     1.00E-03   2.15E-03   4.64E-03   1.00E-02   1.25E-02   1.58E-02
     1.99E-02   2.51E-02   3.16E-02   3.98E-02   5.01E-02   6.30E-02
     7.94E-02   1.00E-01   1.25E-01   1.58E-01   1.99E-01   2.51E-01
     3.16E-01   3.98E-01   5.01E-01   6.30E-01   7.94E-01   1.00E+00
     1.25E+00   1.58E+00   1.99E+00   2.51E+00   3.16E+00   3.98E+00
     5.01E+00   6.30E+00   7.94E+00   1.00E+01   1.15E+01   25.
c
c  for gammas
e22  0.01   0.015   0.02   0.03   0.04   0.05   0.06   0.08   0.1
     0.15   0.2      0.3    0.4    0.5    0.6    0.8     1.   1.5
       2.    3.       4.     5.     6.     8.   10.0    12.    15.
c
c  ICRP 74 Dose Conversion coeffients
DE12  1.00E-09  1.00E-08  2.53E-08  1.00E-07  2.00E-07  5.00E-07
      1.00E-06  2.00E-06  5.00E-06  1.00E-05  2.00E-05  5.00E-05
      1.00E-04  2.00E-04  5.00E-04  1.00E-03  2.00E-03  5.00E-03
```

```
      1.00E-02  2.00E-02  3.00E-02  5.00E-02  7.00E-02  1.00E-01
      1.50E-01  2.00E-01  3.00E-01  5.00E-01  7.00E-01  9.00E-01
      1.00E+00  1.20E+00  2.00E+00  3.00E+00  4.00E+00  5.00E+00
      6.00E+00  7.00E+00  8.00E+00  9.00E+00  1.00E+01  1.20E+01
      1.40E+01  1.50E+01  1.60E+01  1.80E+01  2.00E+01  3.00E+01
      5.00E+01  7.50E+01  1.00E+02  1.25E+02  1.50E+02  1.75E+02
      2.01E+02
c
DF12  6.6  9   10.6  12.9  13.5  13.6  13.3  12.9   12   11.3  10.6
      9.9  9.4  8.9   8.3   7.9   7.7     8  10.5  16.6  23.7  41.1
       60   88  132   170   233   322   375   400   416   425   420
      412  408  405   400   405   409   420   440   480   520   540
      555  570  600   515   400   330   285   260   245   250   260
c
c  ICRP 74 Dose Conversion coeffients
DE25  1.00E-09  1.00E-08  2.53E-08  1.00E-07  2.00E-07  5.00E-07
      1.00E-06  2.00E-06  5.00E-06  1.00E-05  2.00E-05  5.00E-05
      1.00E-04  2.00E-04  5.00E-04  1.00E-03  2.00E-03  5.00E-03
      1.00E-02  2.00E-02  3.00E-02  5.00E-02  7.00E-02  1.00E-01
      1.50E-01  2.00E-01  3.00E-01  5.00E-01  7.00E-01  9.00E-01
      1.00E+00  1.20E+00  2.00E+00  3.00E+00  4.00E+00  5.00E+00
      6.00E+00  7.00E+00  8.00E+00  9.00E+00  1.00E+01  1.20E+01
      1.40E+01  1.50E+01  1.60E+01  1.80E+01  2.00E+01  3.00E+01
      5.00E+01  7.50E+01  1.00E+02  1.25E+02  1.50E+02  1.75E+02
      2.01E+02
c
DF25  6.6  9   10.6  12.9  13.5  13.6  13.3  12.9   12   11.3  10.6
      9.9  9.4  8.9   8.3   7.9   7.7     8  10.5  16.6  23.7  41.1
       60   88  132   170   233   322   375   400   416   425   420
      412  408  405   400   405   409   420   440   480   520   540
      555  570  600   515   400   330   285   260   245   250   260
c
c ICRP 74 DCCs for photons (pSv-cm2)
de32  0.01   0.015   0.02   0.03   0.04   0.05   0.06   0.08   0.1
     0.15   0.2      0.3    0.4    0.5    0.6    0.8     1.   1.5
       2.    3.       4.     5.     6.     8.   10.0
df32   0.061   0.83   1.05   0.81   0.64   0.55   0.51   0.53  0.61
       0.89    1.2    1.8    2.38   2.93   3.44   4.38    5.2   6.9
        8.6   11.1   13.4    15.5   17.6   21.6   25.6
c
mode n p
CUT:N  1J  1.e-10
CUT:P  1J   0.01
nps 1E7
```

B.5 ^{252}Cf in Tantalum MCNP Input

```
Cf in Ta
c by Pete Exline
c Cell Cards
c cells for bare source with no PNL rabbit
c
c ***PRIMARY ENCAPSULATION***
c
c CF oxide source volume (no material assumed for the moment**
c
1 0      -12 18 -17 imp:n=1 imp:p=1
c
c Lower porous platinum filter (1/2 full density assumed)
c
2 1 -10.68 -12 17 -16 imp:n=1 imp:p=1
c
c Lower void
c
3 0      -13 16 -15 imp:n=1 imp:p=1
c
c Middle void
c
4 0      -12 19 -18 imp:n=1 imp:p=1
c
c upper porous platinum filter (1/2 full density assumed)
c
5 1 -10.68 -12 -19 20 imp:n=1 imp:p=1
c
c Upper void
c
6 0      -12 -20 21 imp:n=1 imp:p=1
c
c Primary capsule container (90% Pt and 10% Rh)
c
7 2 -19.9541 #(-15 -13 16:-16 -12 21) 22 -11 -14 imp:n=1 imp:p=1
c
c Gap between the primnary and secondary capsules
c
8 0       #(22 -11 -14) (23 -6 -7):(-6 10 -23 35) imp:n=1 imp:p=1
c
c **SECONDARY CAPSULE OF ZIRCALLOY-2***
c
9 3 -6.415 #(-7 -6 35) (-4 8 -3):-8 9 -5:-10 -23 35 imp:n=1 imp:p=1
c
c The threads of the secondary capsule
c
10 3 -6.415 -2 -1 3 imp:n=1 imp:p=1
c
c ** Ta Sphere **
304 304 -1.24e-3 (307 -322 #((316 -312 314 -313):(312 -311 310 -313):&
(-317 318 -360 361 313 -312 315):&
(-317 318 -312 315 -320):&
(-317 318 -312 315 -319):(-501 502 503 -504 505 -506):&
((-501 531 513 515 -503 -525):(-501 531 503 515 -523 -505))&
:((-501 531 524 -514 515 -505):(-501 531 504 -514 515 -525))&
:((-501 531 513 -516 -503 526):(-501 531 503 -516 -523 506))&
:((-501 531 524 -514 -516 506):(-501 531 504 -514 -516 526))&
:((-531 543 545 -503 -525):(-531 503 545 -523 -505))&
:((-531 524 -544 545 -505):(-531 504 -544 545 -525))&
:((-531 543 -546 -503 526):(-531 503 -546 -523 506))&
:((-531 524 -544 -546 506):(-531 504 -544 -546 526))&
:((501 -553 551 -552))&
))&
:(-308 #(310 -313 -311 312) &
#(314 -313 -312 315)):-309 &
 imp:n=1   imp:p=1 $air from Ta surface to tally sphere
305 304 -1.24e-3 322 -306   imp:n=1 imp:p=1 $air from sphere to edge of universe
```

```
306 303 -16.69  -307 301 308 309 imp:n=1 imp:p=1 $Ta Sphere
307 0      306                  imp:n=0 imp:p=0 $Void space outside universe
308 305 -2.7 310 -313 -311 312 imp:n=1 imp:p=1 $aluminum ring 1 (in groove)
309 305 -2.7 (314 -313 -312 315):(-317 318 -360 361 313 -312 315):&
(-317 318 -312 315 -320):&
(-317 318 -312 315 -319)  imp:n=1 imp:p=1 $aluminum ring 2
310 305 -2.7 314 -313 -315 316 imp:n=1 imp:p=1 $aluminum ring 3
c * Al table top*
501 305 -2.7 -501 502 503 -504 505 -506 imp:n=1 imp:p=1 $Al table top
511 305 -2.7 (-501 531 513 515 -503 -525):(-501 531 503 515 -523 -505) &
imp:n=1 imp:p=1 $bl leg
512 305 -2.7 (-501 531 524 -514 515 -505):(-501 531 504 -514 515 -525) &
imp:n=1 imp:p=1 $br leg
513 305 -2.7 (-501 531 513 -516 -503 526):(-501 531 503 -516 -523 506) &
imp:n=1 imp:p=1 $tl leg
514 305 -2.7 (-501 531 524 -514 -516 506):(-501 531 504 -514 -516 526) &
imp:n=1 imp:p=1 $tr leg
541 305 -2.7 (-531 -322 543 545 -503 -525):(-531 -322 503 545 -523 -505) &
imp:n=1 imp:p=1 $bl thick leg
542 305 -2.7 (-531 -322 524 -544 545 -505):(-531 -322 504 -544 545 -525) &
imp:n=1 imp:p=1 $br thick leg
543 305 -2.7 (-531 -322 543 -546 -503 526):(-531 -322 503 -546 -523 506) &
imp:n=1 imp:p=1 $tl thick leg
544 305 -2.7 (-531 -322 524 -544 -546 506):(-531 -322 504 -544 -546 526) &
imp:n=1 imp:p=1 $tr thick leg
551 305 -2.7 501 -553 551 -552 imp:n=1 imp:p=1 $Al stabilizer ring
c **
c ** air to combine for Ta Sphere **
401 304 -1.24e-3  (-301 1 -2 3):(-301 4 -3 8):(-301 5 -8 9):(-301 2):(-301 -9) &
imp:n=1 imp:p=1

c Surface Cards
c Cylinder and planes to define the theaded portion of the
c     secondary capsule
c
1 CY 0.2413
2 PY 1.8542
3 PY 1.3462
c
c Cylinders to define the secondary encapsulation
c
4 CY 0.4699
5 CY 0.4115
6 CY 0.2972
c
c planes and cone to define the seconday encapsulation
c
7 PY 1.143
8 PY -1.778
9 PY -1.905
10 KY 1.720611544 0.007654266 -1
c
c Cylinders to define the primary encapsulation
c
11 CY 0.2769
12 CY 0.1636
13 CY 0.1524
c
c Planes to define the primary encapsulation
c
14 PY 1.0859
15 PY 0.6922
16 PY 0.5144
17 PY 0.1588
18 PY -0.1588
19 PY -0.4763
20 PY -0.8319
21 PY -0.9970
22 PY -1.3907
```

```
23 PY -1.4478
35 PY -1.6764
c **Ta Sphere **
301  SO 3.048   $Outer surface of source sphere
306  SO 500     $Edge of the Universe
307  SO 12   $radius of Ta spherical shell
308  tz 0 0 .75 12 .45 .45 $top groove
309  tz 0 0 -.75 12 .45 .45 $bottom groove
322  SO 100     $100cm Sphere around source
310  cz 11.7  $Al ring inner radius in groove
313  cz 14.1  $Al ring outer radius (all)
311  pz .9 $top of Al ring in groove
312  pz .6 $bottom of Al Ring in groove / top of ring 2
314  cz 12.1  $Al ring inner radius (ring 2/3)
315  pz .3 $bottom of ring 2 / top of ring 3
316  pz 0  $bottom of ring 3
317  py 1.9 $top of lift arms
318  py -1.9 $bot of lift arms
319  C/Z -32.7 0 1.9 $l round edge of lift arm
320  C/Z 32.7 0 1.9 $r round edge of lift arm
360  px 32.7 $cutoff of straight part of lift arm
361  px -32.7 $cutoff of straight part of lift arm
c *Al table top*
501  pz -12.0 $top of Al table top
502  pz -12.6 $bot of Al table top
503  px -25.325 $left of Al table top
504  px 25.325 $right of Al table top
505  py -25.325 $front of Al table top
506  py 25.325 $back of Al table top
513  px -25.475 $left of Al table leg
514  px 25.475 $right of Al table leg
515  py -25.475 $front of Al table leg
516  py 25.475 $back of Al table leg
523  px -20.575 $cutoff of Al table top
524  px 20.575 $cutoff of Al table top
525  py -20.575 $cutoff of Al table top
526  py 20.575 $cutoff of Al table top
531  pz -28.6 $bot of thin legs/top of thick legs
543  px -26.075 $left of Al table thick leg
544  px 26.075 $right of Al table thick leg
545  py -26.075 $front of Al table thick leg
546  py 26.075 $back of Al table thick leg
551  cz 6.25 $inner radius of Al stabilizer
552  cz 8.75 $outer radius of Al stabilizer
553  pz -11.35 $top of Al stablizer
c **
c  The next set of planes will be used to segment surface 22 to do the angular
c  dependent tally.  They do not have to be used in the cell descriptions.
c
324 PZ 98.7688340595138
325 PZ 95.1056516295154
326 PZ 89.1006524188368
327 PZ 80.9016994374947
328 PZ 70.7106781186548
329 PZ 58.7785252292473
330 PZ 45.3990499739547
331 PZ 30.9016994374947
332 PZ 15.6434465040231
333 PZ 0
334 PZ -15.6434465040231
335 PZ -30.9016994374947
336 PZ -45.3990499739547
337 PZ -58.7785252292473
338 PZ -70.7106781186547
339 PZ -80.9016994374947
340 PZ -89.1006524188368
341 PZ -95.1056516295154
342 PZ -98.7688340595138
c **
```

```
c Material Cards
c
c Materials: M1 is the porous filter, M2 is the 90% Pt, 10% Rh
c    and M4 is the Zircalloy-2
c
M1 78000 1.0
M2 78000 -0.9 45103 -0.1
M3 50000 -0.015 26000 -0.0012 24000 -0.001 28000 -0.0005 &
40090 -.5053934 40091 -.1102141 40092 -.1684645 40094 -.1707237 &
40096 -.0275044
c ** Ta Sphere **
m303 73181  1.0 $Ta
m305 13027 1.0 $Al
c **
m304 7014 -.7558 8016 -.2314 18000 -.0128 $air
c **
c
c the source is input in cell one region using a Maxwellian with
c   temperature of 1.42 MeV
c
c old syntax -- SRC4 3J 1 1 0.0 0.1636 0.1588 0. 0. 1.
SDEF ERG=D1 CEL=1 PAR =1 POS=0 0 0 AXS=0 0 1 EXT=D3 RAD=D2
SI3 -0.159 0.159
SI2 0 0.164
SP2 -21 1
SP1 -2 1.42
c
c Tallies
F2:N  322
FC2  Neutron Flux
FS2 -334 -332 T $plus/minus 15.6cm cutoffs
c Current Tally of whole sphere
F1:N  322
FC1 number of neutrons per spherical surface segments at 100 cm
c Segmented Tally across z plans of the sphere
FS1  -342 -341 -340 -339 -338 -337 -336 -335 -334 -333 -332 -331 &
-330 -329 -328 -327 -326 -325 -324
c
F12:N 322
FC12  Icrp 74 ambient dose equivalent on spherical surface at 100 cm
c Segmented Tally across z plans of the sphere
FS12  -342 -341 -340 -339 -338 -337 -336 -335 -334 -333 -332 -331 &
-330 -329 -328 -327 -326 -325 -324
c
c  gamma fluence tally at 100 cm
F22:P  322
FC22  Gamma Ray Fluence induced by neutrons at 100 cm
FS22 -334 -332 T $plus/minus 15.6cm cutoffs
c
F32:P   322
FC32  Gamma Ray Dose rate at 100 cm
FS32 -334 -332 T $plus/minus 15.6cm cutoffs
c
F5:N -100.0001 0 0 .1
FC5 Point Neutron Detector at 100cm
c
F25:N -100.0001 0 0 .1
FC25 ICRP 74 ambient dose equivalent on Point Neutron Detector at 100cm
c Energy groups used to bin fluence
e1   1.00E-09   2.15E-09   4.64E-09   1.00E-08   2.15E-08   4.64E-08
     1.00E-07   2.15E-07   4.64E-07   1.00E-06   2.15E-06   4.64E-06
     1.00E-05   2.15E-05   4.64E-05   1.00E-04   2.15E-04   4.64E-04
     1.00E-03   2.15E-03   4.64E-03   1.00E-02   1.25E-02   1.58E-02
     1.99E-02   2.51E-02   3.16E-02   3.98E-02   5.01E-02   6.30E-02
     7.94E-02   1.00E-01   1.25E-01   1.58E-01   1.99E-01   2.51E-01
     3.16E-01   3.98E-01   5.01E-01   6.30E-01   7.94E-01   1.00E+00
     1.25E+00   1.58E+00   1.99E+00   2.51E+00   3.16E+00   3.98E+00
     5.01E+00   6.30E+00   7.94E+00   1.00E+01   1.15E+01   25.
```

```
c
e2   1.00E-09   2.15E-09   4.64E-09   1.00E-08   2.15E-08   4.64E-08
     1.00E-07   2.15E-07   4.64E-07   1.00E-06   2.15E-06   4.64E-06
     1.00E-05   2.15E-05   4.64E-05   1.00E-04   2.15E-04   4.64E-04
     1.00E-03   2.15E-03   4.64E-03   1.00E-02   1.25E-02   1.58E-02
     1.99E-02   2.51E-02   3.16E-02   3.98E-02   5.01E-02   6.30E-02
     7.94E-02   1.00E-01   1.25E-01   1.58E-01   1.99E-01   2.51E-01
     3.16E-01   3.98E-01   5.01E-01   6.30E-01   7.94E-01   1.00E+00
     1.25E+00   1.58E+00   1.99E+00   2.51E+00   3.16E+00   3.98E+00
     5.01E+00   6.30E+00   7.94E+00   1.00E+01   1.15E+01   25.
c
e5   1.00E-09   2.15E-09   4.64E-09   1.00E-08   2.15E-08   4.64E-08
     1.00E-07   2.15E-07   4.64E-07   1.00E-06   2.15E-06   4.64E-06
     1.00E-05   2.15E-05   4.64E-05   1.00E-04   2.15E-04   4.64E-04
     1.00E-03   2.15E-03   4.64E-03   1.00E-02   1.25E-02   1.58E-02
     1.99E-02   2.51E-02   3.16E-02   3.98E-02   5.01E-02   6.30E-02
     7.94E-02   1.00E-01   1.25E-01   1.58E-01   1.99E-01   2.51E-01
     3.16E-01   3.98E-01   5.01E-01   6.30E-01   7.94E-01   1.00E+00
     1.25E+00   1.58E+00   1.99E+00   2.51E+00   3.16E+00   3.98E+00
     5.01E+00   6.30E+00   7.94E+00   1.00E+01   1.15E+01   25.
c
e12   1.00E-09   2.15E-09   4.64E-09   1.00E-08   2.15E-08   4.64E-08
     1.00E-07   2.15E-07   4.64E-07   1.00E-06   2.15E-06   4.64E-06
     1.00E-05   2.15E-05   4.64E-05   1.00E-04   2.15E-04   4.64E-04
     1.00E-03   2.15E-03   4.64E-03   1.00E-02   1.25E-02   1.58E-02
     1.99E-02   2.51E-02   3.16E-02   3.98E-02   5.01E-02   6.30E-02
     7.94E-02   1.00E-01   1.25E-01   1.58E-01   1.99E-01   2.51E-01
     3.16E-01   3.98E-01   5.01E-01   6.30E-01   7.94E-01   1.00E+00
     1.25E+00   1.58E+00   1.99E+00   2.51E+00   3.16E+00   3.98E+00
     5.01E+00   6.30E+00   7.94E+00   1.00E+01   1.15E+01   25.
c
e25   1.00E-09   2.15E-09   4.64E-09   1.00E-08   2.15E-08   4.64E-08
     1.00E-07   2.15E-07   4.64E-07   1.00E-06   2.15E-06   4.64E-06
     1.00E-05   2.15E-05   4.64E-05   1.00E-04   2.15E-04   4.64E-04
     1.00E-03   2.15E-03   4.64E-03   1.00E-02   1.25E-02   1.58E-02
     1.99E-02   2.51E-02   3.16E-02   3.98E-02   5.01E-02   6.30E-02
     7.94E-02   1.00E-01   1.25E-01   1.58E-01   1.99E-01   2.51E-01
     3.16E-01   3.98E-01   5.01E-01   6.30E-01   7.94E-01   1.00E+00
     1.25E+00   1.58E+00   1.99E+00   2.51E+00   3.16E+00   3.98E+00
     5.01E+00   6.30E+00   7.94E+00   1.00E+01   1.15E+01   25.
c
c  for gammas
e22  0.01   0.015   0.02   0.03   0.04   0.05   0.06   0.08   0.1
     0.15   0.2      0.3    0.4    0.5    0.6    0.8     1.   1.5
       2.    3.       4.     5.     6.     8.   10.0    12.    15.
c
c  ICRP 74 Dose Conversion coeffients
DE12  1.00E-09  1.00E-08  2.53E-08  1.00E-07  2.00E-07  5.00E-07
      1.00E-06  2.00E-06  5.00E-06  1.00E-05  2.00E-05  5.00E-05
      1.00E-04  2.00E-04  5.00E-04  1.00E-03  2.00E-03  5.00E-03
      1.00E-02  2.00E-02  3.00E-02  5.00E-02  7.00E-02  1.00E-01
      1.50E-01  2.00E-01  3.00E-01  5.00E-01  7.00E-01  9.00E-01
      1.00E+00  1.20E+00  2.00E+00  3.00E+00  4.00E+00  5.00E+00
      6.00E+00  7.00E+00  8.00E+00  9.00E+00  1.00E+01  1.20E+01
      1.40E+01  1.50E+01  1.60E+01  1.80E+01  2.00E+01  3.00E+01
      5.00E+01  7.50E+01  1.00E+02  1.25E+02  1.50E+02  1.75E+02
      2.01E+02
c
DF12  6.6  9   10.6  12.9  13.5  13.6  13.3  12.9   12   11.3  10.6
      9.9  9.4  8.9   8.3   7.9   7.7     8  10.5  16.6  23.7  41.1
       60   88  132   170   233   322   375   400   416   425   420
      412  408  405   400   405   409   420   440   480   520   540
      555  570  600   515   400   330   285   260   245   250   260
c
c  ICRP 74 Dose Conversion coeffients
DE25  1.00E-09  1.00E-08  2.53E-08  1.00E-07  2.00E-07  5.00E-07
      1.00E-06  2.00E-06  5.00E-06  1.00E-05  2.00E-05  5.00E-05
      1.00E-04  2.00E-04  5.00E-04  1.00E-03  2.00E-03  5.00E-03
      1.00E-02  2.00E-02  3.00E-02  5.00E-02  7.00E-02  1.00E-01
```

```
      1.50E-01  2.00E-01  3.00E-01  5.00E-01  7.00E-01  9.00E-01
      1.00E+00  1.20E+00  2.00E+00  3.00E+00  4.00E+00  5.00E+00
      6.00E+00  7.00E+00  8.00E+00  9.00E+00  1.00E+01  1.20E+01
      1.40E+01  1.50E+01  1.60E+01  1.80E+01  2.00E+01  3.00E+01
      5.00E+01  7.50E+01  1.00E+02  1.25E+02  1.50E+02  1.75E+02
      2.01E+02
c
DF25  6.6  9   10.6  12.9  13.5  13.6  13.3  12.9   12   11.3  10.6
      9.9  9.4  8.9   8.3   7.9   7.7     8  10.5  16.6  23.7  41.1
       60   88  132   170   233   322   375   400   416   425   420
      412  408  405   400   405   409   420   440   480   520   540
      555  570  600   515   400   330   285   260   245   250   260
c
c ICRP 74 DCCs for photons (pSv-cm2)
de32  0.01   0.015   0.02   0.03   0.04   0.05   0.06   0.08   0.1
     0.15   0.2      0.3    0.4    0.5    0.6    0.8     1.   1.5
       2.    3.       4.     5.     6.     8.   10.0
df32   0.061   0.83   1.05   0.81   0.64   0.55   0.51   0.53  0.61
       0.89    1.2    1.8    2.38   2.93   3.44   4.38    5.2   6.9
        8.6   11.1   13.4    15.5   17.6   21.6   25.6
c
mode n p
CUT:N  1J  1.e-10
CUT:P  1J   0.01
nps 1E7
```

B.6 ^{252}Cf in Polyethylene MCNP Input

```
Cf in 12" poly
c by Pete Exline
c Cell Cards
c cells for bare source with no PNL rabbit
c
c ***PRIMARY ENCAPSULATION***
c
c CF oxide source volume (no material assumed for the moment**
c
1 0      -12 18 -17 imp:n=1 imp:p=1
c
c Lower porous platinum filter (1/2 full density assumed)
c
2 1 -10.68 -12 17 -16 imp:n=1 imp:p=1
c
c Lower void
c
3 0      -13 16 -15 imp:n=1 imp:p=1
c
c Middle void
c
4 0      -12 19 -18 imp:n=1 imp:p=1
c
c upper porous platinum filter (1/2 full density assumed)
c
5 1 -10.68 -12 -19 20 imp:n=1 imp:p=1
c
c Upper void
c
6 0      -12 -20 21 imp:n=1 imp:p=1
c
c Primary capsule container (90% Pt and 10% Rh)
c
7 2 -19.9541 #(-15 -13 16:-16 -12 21) 22 -11 -14 imp:n=1 imp:p=1
c
c Gap between the primnary and secondary capsules
c
8 0       #(22 -11 -14) (23 -6 -7):(-6 10 -23 35) imp:n=1 imp:p=1
c
c **SECONDARY CAPSULE OF ZIRCALLOY-2***
c
9 3 -6.415 #(-7 -6 35) (-4 8 -3):-8 9 -5:-10 -23 35 imp:n=1 imp:p=1
c
c The threads of the secondary capsule
c
10 3 -6.415 -2 -1 3 imp:n=1 imp:p=1
c
c ** Poly Sphere **
301 304 -1.24e-3 -322 301              imp:n=1 imp:p=1 $air from Poly surface to tally
sph
302 304 -1.24e-3 322 -306              imp:n=1 imp:p=1 $air from sphere to edge of univ
303 301 -0.93  -301 (302:-303)         imp:n=1 imp:p=1 $Poly sphere
304 0      306                    imp:n=0 imp:p=0 $Void space outside universe
c **
c ** Air to combine for Poly Sphere **
401 304 -1.24e-3  (303 -301 -302 1 2 -3):(303 -301 -302 4 3 -8):(303 -301 &
-302 5 8 -9):(303 -301 -302 -2):(303 -301 -302 9) imp:n=1 imp:p=1

c Surface Cards
c Cylinder and planes to define the theaded portion of the
c     secondary capsule
c
1 CZ 0.2413
2 PZ 1.8542
3 PZ 1.3462
c
c Cylinders to define the secondary encapsulation
```

```
c
4 CZ 0.4699
5 CZ 0.4115
6 CZ 0.2972
c
c planes and cone to define the seconday encapsulation
c
7 PZ 1.143
8 PZ -1.778
9 PZ -1.905
10 KZ 1.720611544 0.007654266 -1
c
c Cylinders to define the primary encapsulation
c
11 CZ 0.2769
12 CZ 0.1636
13 CZ 0.1524
c
c Planes to define the primary encapsulation
c
14 PZ 1.0859
15 PZ 0.6922
16 PZ 0.5144
17 PZ 0.1588
18 PZ -0.1588
19 PZ -0.4763
20 PZ -0.8319
21 PZ -0.9970
22 PZ -1.3907
23 PZ -1.4478
35 PZ -1.6764
c **Poly Sphere **
301  SO 15  $Outer surface of Poly Sphere
306  SO 500     $Edge of the Universe
302  CZ .75   $hole for source
303 PZ -2    $bottom of hole
322 SO 100      $100cm Sphere around source
c
c  The next set of planes will be used to segment surface 22 to do the angular
c  dependent tally.  They do not have to be used in the cell descriptions.
c
324 PZ 98.7688340595138
325 PZ 95.1056516295154
326 PZ 89.1006524188368
327 PZ 80.9016994374947
328 PZ 70.7106781186548
329 PZ 58.7785252292473
330 PZ 45.3990499739547
331 PZ 30.9016994374947
332 PZ 15.6434465040231
333 PZ 0
334 PZ -15.6434465040231
335 PZ -30.9016994374947
336 PZ -45.3990499739547
337 PZ -58.7785252292473
338 PZ -70.7106781186547
339 PZ -80.9016994374947
340 PZ -89.1006524188368
341 PZ -95.1056516295154
342 PZ -98.7688340595138
c **

c Material Cards
c
c Materials: M1 is the porous filter, M2 is the 90% Pt, 10% Rh
c    and M4 is the Zircalloy-2
c
M1 78000 1.0
M2 78000 -0.9 45103 -0.1
```

```
M3 50000 -0.015 26000 -0.0012 24000 -0.001 28000 -0.0005 &
40090 -.5053934 40091 -.1102141 40092 -.1684645 40094 -.1707237 &
40096 -.0275044
c ** Poly Sphere **
m301 001001 .666662 006000 .333338 $from PNNL-15870.pdf
mt301 poly.10t $H in poly at 293k
c **
m304 7014 -.7558 8016 -.2314 18000 -.0128 $air
c **
c
c the source is input in cell one region using a Maxwellian with
c   temperature of 1.42 MeV
c
c old syntax -- SRC4 3J 1 1 0.0 0.1636 0.1588 0. 0. 1.
SDEF ERG=D1 CEL=1 PAR =1 POS=0 0 0 AXS=0 0 1 EXT=D3 RAD=D2
SI3 -0.159 0.159
SI2 0 0.164
SP2 -21 1
SP1 -2 1.42
c
c Tallies
F2:N  322
FC2  Neutron Flux
FS2 -334 -332 T $plus/minus 15.6cm cutoffs
c Current Tally of whole sphere
F1:N  322
FC1 number of neutrons per spherical surface segments at 100 cm
c Segmented Tally across z plans of the sphere
FS1  -342 -341 -340 -339 -338 -337 -336 -335 -334 -333 -332 -331 &
-330 -329 -328 -327 -326 -325 -324
c
F12:N 322
FC12  Icrp 74 ambient dose equivalent on spherical surface at 100 cm
c Segmented Tally across z plans of the sphere
FS12  -342 -341 -340 -339 -338 -337 -336 -335 -334 -333 -332 -331 &
-330 -329 -328 -327 -326 -325 -324
c
c  gamma fluence tally at 100 cm
F22:P  322
FC22  Gamma Ray Fluence induced by neutrons at 100 cm
FS22 -334 -332 T $plus/minus 15.6cm cutoffs
c
F32:P   322
FC32  Gamma Ray Dose rate at 100 cm
FS32 -334 -332 T $plus/minus 15.6cm cutoffs
c
F5:N -100.0001 0 0 .1
FC5 Point Neutron Detector at 100cm
c
F25:N -100.0001 0 0 .1
FC25 ICRP 74 ambient dose equivalent on Point Neutron Detector at 100cm
c Energy groups used to bin fluence
e1   1.00E-09   2.15E-09   4.64E-09   1.00E-08   2.15E-08   4.64E-08
     1.00E-07   2.15E-07   4.64E-07   1.00E-06   2.15E-06   4.64E-06
     1.00E-05   2.15E-05   4.64E-05   1.00E-04   2.15E-04   4.64E-04
     1.00E-03   2.15E-03   4.64E-03   1.00E-02   1.25E-02   1.58E-02
     1.99E-02   2.51E-02   3.16E-02   3.98E-02   5.01E-02   6.30E-02
     7.94E-02   1.00E-01   1.25E-01   1.58E-01   1.99E-01   2.51E-01
     3.16E-01   3.98E-01   5.01E-01   6.30E-01   7.94E-01   1.00E+00
     1.25E+00   1.58E+00   1.99E+00   2.51E+00   3.16E+00   3.98E+00
     5.01E+00   6.30E+00   7.94E+00   1.00E+01   1.15E+01   25.
c
e2   1.00E-09   2.15E-09   4.64E-09   1.00E-08   2.15E-08   4.64E-08
     1.00E-07   2.15E-07   4.64E-07   1.00E-06   2.15E-06   4.64E-06
     1.00E-05   2.15E-05   4.64E-05   1.00E-04   2.15E-04   4.64E-04
     1.00E-03   2.15E-03   4.64E-03   1.00E-02   1.25E-02   1.58E-02
     1.99E-02   2.51E-02   3.16E-02   3.98E-02   5.01E-02   6.30E-02
     7.94E-02   1.00E-01   1.25E-01   1.58E-01   1.99E-01   2.51E-01
     3.16E-01   3.98E-01   5.01E-01   6.30E-01   7.94E-01   1.00E+00
```

```
     1.25E+00   1.58E+00   1.99E+00   2.51E+00   3.16E+00   3.98E+00
     5.01E+00   6.30E+00   7.94E+00   1.00E+01   1.15E+01   25.
c
e5   1.00E-09   2.15E-09   4.64E-09   1.00E-08   2.15E-08   4.64E-08
     1.00E-07   2.15E-07   4.64E-07   1.00E-06   2.15E-06   4.64E-06
     1.00E-05   2.15E-05   4.64E-05   1.00E-04   2.15E-04   4.64E-04
     1.00E-03   2.15E-03   4.64E-03   1.00E-02   1.25E-02   1.58E-02
     1.99E-02   2.51E-02   3.16E-02   3.98E-02   5.01E-02   6.30E-02
     7.94E-02   1.00E-01   1.25E-01   1.58E-01   1.99E-01   2.51E-01
     3.16E-01   3.98E-01   5.01E-01   6.30E-01   7.94E-01   1.00E+00
     1.25E+00   1.58E+00   1.99E+00   2.51E+00   3.16E+00   3.98E+00
     5.01E+00   6.30E+00   7.94E+00   1.00E+01   1.15E+01   25.
c
e12   1.00E-09   2.15E-09   4.64E-09   1.00E-08   2.15E-08   4.64E-08
     1.00E-07   2.15E-07   4.64E-07   1.00E-06   2.15E-06   4.64E-06
     1.00E-05   2.15E-05   4.64E-05   1.00E-04   2.15E-04   4.64E-04
     1.00E-03   2.15E-03   4.64E-03   1.00E-02   1.25E-02   1.58E-02
     1.99E-02   2.51E-02   3.16E-02   3.98E-02   5.01E-02   6.30E-02
     7.94E-02   1.00E-01   1.25E-01   1.58E-01   1.99E-01   2.51E-01
     3.16E-01   3.98E-01   5.01E-01   6.30E-01   7.94E-01   1.00E+00
     1.25E+00   1.58E+00   1.99E+00   2.51E+00   3.16E+00   3.98E+00
     5.01E+00   6.30E+00   7.94E+00   1.00E+01   1.15E+01   25.
c
e25   1.00E-09   2.15E-09   4.64E-09   1.00E-08   2.15E-08   4.64E-08
     1.00E-07   2.15E-07   4.64E-07   1.00E-06   2.15E-06   4.64E-06
     1.00E-05   2.15E-05   4.64E-05   1.00E-04   2.15E-04   4.64E-04
     1.00E-03   2.15E-03   4.64E-03   1.00E-02   1.25E-02   1.58E-02
     1.99E-02   2.51E-02   3.16E-02   3.98E-02   5.01E-02   6.30E-02
     7.94E-02   1.00E-01   1.25E-01   1.58E-01   1.99E-01   2.51E-01
     3.16E-01   3.98E-01   5.01E-01   6.30E-01   7.94E-01   1.00E+00
     1.25E+00   1.58E+00   1.99E+00   2.51E+00   3.16E+00   3.98E+00
     5.01E+00   6.30E+00   7.94E+00   1.00E+01   1.15E+01   25.
c
c  for gammas
e22  0.01   0.015   0.02   0.03   0.04   0.05   0.06   0.08   0.1
     0.15   0.2      0.3    0.4    0.5    0.6    0.8     1.   1.5
       2.    3.       4.     5.     6.     8.   10.0    12.    15.
c
c  ICRP 74 Dose Conversion coeffients
DE12  1.00E-09  1.00E-08  2.53E-08  1.00E-07  2.00E-07  5.00E-07
      1.00E-06  2.00E-06  5.00E-06  1.00E-05  2.00E-05  5.00E-05
      1.00E-04  2.00E-04  5.00E-04  1.00E-03  2.00E-03  5.00E-03
      1.00E-02  2.00E-02  3.00E-02  5.00E-02  7.00E-02  1.00E-01
      1.50E-01  2.00E-01  3.00E-01  5.00E-01  7.00E-01  9.00E-01
      1.00E+00  1.20E+00  2.00E+00  3.00E+00  4.00E+00  5.00E+00
      6.00E+00  7.00E+00  8.00E+00  9.00E+00  1.00E+01  1.20E+01
      1.40E+01  1.50E+01  1.60E+01  1.80E+01  2.00E+01  3.00E+01
      5.00E+01  7.50E+01  1.00E+02  1.25E+02  1.50E+02  1.75E+02
      2.01E+02
c
DF12  6.6  9   10.6  12.9  13.5  13.6  13.3  12.9   12   11.3  10.6
      9.9  9.4  8.9   8.3   7.9   7.7     8  10.5  16.6  23.7  41.1
       60   88  132   170   233   322   375   400   416   425   420
      412  408  405   400   405   409   420   440   480   520   540
      555  570  600   515   400   330   285   260   245   250   260
c
c  ICRP 74 Dose Conversion coeffients
DE25  1.00E-09  1.00E-08  2.53E-08  1.00E-07  2.00E-07  5.00E-07
      1.00E-06  2.00E-06  5.00E-06  1.00E-05  2.00E-05  5.00E-05
      1.00E-04  2.00E-04  5.00E-04  1.00E-03  2.00E-03  5.00E-03
      1.00E-02  2.00E-02  3.00E-02  5.00E-02  7.00E-02  1.00E-01
      1.50E-01  2.00E-01  3.00E-01  5.00E-01  7.00E-01  9.00E-01
      1.00E+00  1.20E+00  2.00E+00  3.00E+00  4.00E+00  5.00E+00
      6.00E+00  7.00E+00  8.00E+00  9.00E+00  1.00E+01  1.20E+01
      1.40E+01  1.50E+01  1.60E+01  1.80E+01  2.00E+01  3.00E+01
      5.00E+01  7.50E+01  1.00E+02  1.25E+02  1.50E+02  1.75E+02
      2.01E+02
c
DF25  6.6  9   10.6  12.9  13.5  13.6  13.3  12.9   12   11.3  10.6
```

```
      9.9  9.4  8.9   8.3   7.9   7.7     8  10.5  16.6  23.7  41.1
       60   88  132   170   233   322   375   400   416   425   420
      412  408  405   400   405   409   420   440   480   520   540
      555  570  600   515   400   330   285   260   245   250   260
c
c ICRP 74 DCCs for photons (pSv-cm2)
de32  0.01   0.015   0.02   0.03   0.04   0.05   0.06   0.08   0.1
     0.15   0.2      0.3    0.4    0.5    0.6    0.8     1.   1.5
       2.    3.       4.     5.     6.     8.   10.0
df32   0.061   0.83   1.05   0.81   0.64   0.55   0.51   0.53  0.61
       0.89    1.2    1.8    2.38   2.93   3.44   4.38    5.2   6.9
        8.6   11.1   13.4    15.5   17.6   21.6   25.6
c
mode n p
CUT:N  1J  1.e-10
CUT:P  1J   0.01
nps 1E7
```

B.7 ^{252}Cf in D_2O MCNP Input

```
Cf in D2O Sphere w/ Cd Cover
c by Pete Exline
c Cell Cards
c cells for bare source with no PNL rabbit
c
c ***PRIMARY ENCAPSULATION***
c
c CF oxide source volume (no material assumed for the moment**
c
1 0      -12 18 -17 imp:n=1 imp:p=1
c
c Lower porous platinum filter (1/2 full density assumed)
c
2 1 -10.68 -12 17 -16 imp:n=1 imp:p=1
c
c Lower void
c
3 0      -13 16 -15 imp:n=1 imp:p=1
c
c Middle void
c
4 0      -12 19 -18 imp:n=1 imp:p=1
c
c upper porous platinum filter (1/2 full density assumed)
c
5 1 -10.68 -12 -19 20 imp:n=1 imp:p=1
c
c Upper void
c
6 0      -12 -20 21 imp:n=1 imp:p=1
c
c Primary capsule container (90% Pt and 10% Rh)
c
7 2 -19.9541 #(-15 -13 16:-16 -12 21) 22 -11 -14 imp:n=1 imp:p=1
c
c Gap between the primnary and secondary capsules
c
8 0       #(22 -11 -14) (23 -6 -7):(-6 10 -23 35) imp:n=1 imp:p=1
c
c **SECONDARY CAPSULE OF ZIRCALLOY-2***
c
9 3 -6.415 #(-7 -6 35) (-4 8 -3):-8 9 -5:-10 -23 35 imp:n=1 imp:p=1
c
c The threads of the secondary capsule
c
10 3 -6.415 -2 -1 3 imp:n=1 imp:p=1
c
c ** D2O Sphere **
301 304 -1.24e-3 -322 305:(-305 301 -302 303) imp:n=1 imp:p=1 $air from D2O &
c surface to tally sph
302 304 -1.24e-3  322 -306               imp:n=1 imp:p=1 $air from tally to edge of univ
303 301 -1.107  -301 #(-307 308)         imp:n=1 imp:p=1 $D2O sphere
304 0      306                    imp:n=0 imp:p=0 $Void space outside universe
305 302 -7.94 -304 301 #(-302 303) imp:n=1 imp:p=1 $steel wall
306 302 -7.94 (302 -307 308 -301):(-307 -303 308) imp:n=1 imp:p=1 $steel hole wall
307 303 -8.65 -305 304 #(-302 303) imp:n=1 imp:p=1 $Cd cover
c **
c ** Air to combine for D2O Sphere **
401 304 -1.24e-3  (303 -301 -302 1 -2 3):(303 -301 -302 4 -3 8):(303 -301 &
-302 5 -8 9):(303 -301 -302 2):(303 -301 -302 -9) imp:n=1 imp:p=1

c Surface Cards
c Cylinder and planes to define the theaded portion of the
c     secondary capsule
c
1 CZ 0.2413
```

```
2 PZ 1.8542
3 PZ 1.3462
c
c Cylinders to define the secondary encapsulation
c
4 CZ 0.4699
5 CZ 0.4115
6 CZ 0.2972
c
c planes and cone to define the seconday encapsulation
c
7 PZ 1.143
8 PZ -1.778
9 PZ -1.905
10 KZ 1.720611544 0.007654266 -1
c
c Cylinders to define the primary encapsulation
c
11 CZ 0.2769
12 CZ 0.1636
13 CZ 0.1524
c
c Planes to define the primary encapsulation
c
14 PZ 1.0859
15 PZ 0.6922
16 PZ 0.5144
17 PZ 0.1588
18 PZ -0.1588
19 PZ -0.4763
20 PZ -0.8319
21 PZ -0.9970
22 PZ -1.3907
23 PZ -1.4478
35 PZ -1.6764
c **D2O Sphere **
301  SO 15  $Outer surface of D2O Sphere
304  SO 15.08    $Outer surface of Steel sphere
305  SO 15.13    $Outer surface of the Cd Sphere
306  SO 500     $Edge of the Universe
302  CZ .5   $hole for source
307  CZ .54   $Steel wall of hole for source
303 PZ -2    $bottom of hole
308 PZ -2.04  $bottom of Steel cover of hole
322 SO 100      $100cm Sphere around source
c **
c  The next set of planes will be used to segment surface 22 to do the angular
c  dependent tally.  They do not have to be used in the cell descriptions.
c
324 PZ 98.7688340595138
325 PZ 95.1056516295154
326 PZ 89.1006524188368
327 PZ 80.9016994374947
328 PZ 70.7106781186548
329 PZ 58.7785252292473
330 PZ 45.3990499739547
331 PZ 30.9016994374947
332 PZ 15.6434465040231
333 PZ 0
334 PZ -15.6434465040231
335 PZ -30.9016994374947
336 PZ -45.3990499739547
337 PZ -58.7785252292473
338 PZ -70.7106781186547
339 PZ -80.9016994374947
340 PZ -89.1006524188368
341 PZ -95.1056516295154
342 PZ -98.7688340595138
c **
```

```
c Material Cards
c
c Materials: M1 is the porous filter, M2 is the 90% Pt, 10% Rh
c    and M4 is the Zircalloy-2
c
M1 78000 1.0
M2 78000 -0.9 45103 -0.1
M3 50000 -0.015 26000 -0.0012 24000 -0.001 28000 -0.0005 &
40090 -.5053934 40091 -.1102141 40092 -.1684645 40094 -.1707237 &
40096 -.0275044
c ** D2O Sphere **
m301 001002 .667 008016 .333 $heavy water
mt301 hwtr.10t $heavy water H-2 treatment at 293K
m302 26000. -.99283 6000 -.0021 25055.61c -.0047 &
  15031 -.00013 16000 -.00024 $stainless steel
m303 048106 .0125 048108 0.0089 048110 .1249 048111 .128 &
 048112 .2413 048113 .1222 048114 .2873 048116 .0749 $Cd
m304 7014 -.7558 8016 -.2314 18000 -.0128 $air
c **
c
c the source is input in cell one region using a Maxwellian with
c   temperature of 1.42 MeV
c
c old syntax -- SRC4 3J 1 1 0.0 0.1636 0.1588 0. 0. 1.
SDEF ERG=D1 CEL=1 PAR =1 POS=0 0 0 AXS=0 0 1 EXT=D3 RAD=D2
SI3 -0.159 0.159
SI2 0 0.164
SP2 -21 1
SP1 -2 1.42
c
c Tallies
F2:N  322
FC2  Neutron Flux
FS2 -334 -332 T $plus/minus 15.6cm cutoffs
c Current Tally of whole sphere
F1:N  322
FC1 number of neutrons per spherical surface segments at 100 cm
c Segmented Tally across z plans of the sphere
FS1  -342 -341 -340 -339 -338 -337 -336 -335 -334 -333 -332 -331 &
-330 -329 -328 -327 -326 -325 -324
c
F12:N 322
FC12  Icrp 74 ambient dose equivalent on spherical surface at 100 cm
c Segmented Tally across z plans of the sphere
FS12  -342 -341 -340 -339 -338 -337 -336 -335 -334 -333 -332 -331 &
-330 -329 -328 -327 -326 -325 -324
c
c  gamma fluence tally at 100 cm
F22:P  322
FC22  Gamma Ray Fluence induced by neutrons at 100 cm
FS22 -334 -332 T $plus/minus 15.6cm cutoffs
c
F32:P   322
FC32  Gamma Ray Dose rate at 100 cm
FS32 -334 -332 T $plus/minus 15.6cm cutoffs
c
F5:N -100.0001 0 0 .1
FC5 Point Neutron Detector at 100cm
c
F25:N -100.0001 0 0 .1
FC25 ICRP 74 ambient dose equivalent on Point Neutron Detector at 100cm
c Energy groups used to bin fluence
e1   1.00E-09   2.15E-09   4.64E-09   1.00E-08   2.15E-08   4.64E-08
     1.00E-07   2.15E-07   4.64E-07   1.00E-06   2.15E-06   4.64E-06
     1.00E-05   2.15E-05   4.64E-05   1.00E-04   2.15E-04   4.64E-04
     1.00E-03   2.15E-03   4.64E-03   1.00E-02   1.25E-02   1.58E-02
     1.99E-02   2.51E-02   3.16E-02   3.98E-02   5.01E-02   6.30E-02
     7.94E-02   1.00E-01   1.25E-01   1.58E-01   1.99E-01   2.51E-01
```

```
     3.16E-01   3.98E-01   5.01E-01   6.30E-01   7.94E-01   1.00E+00
     1.25E+00   1.58E+00   1.99E+00   2.51E+00   3.16E+00   3.98E+00
     5.01E+00   6.30E+00   7.94E+00   1.00E+01   1.15E+01   25.
c
e2   1.00E-09   2.15E-09   4.64E-09   1.00E-08   2.15E-08   4.64E-08
     1.00E-07   2.15E-07   4.64E-07   1.00E-06   2.15E-06   4.64E-06
     1.00E-05   2.15E-05   4.64E-05   1.00E-04   2.15E-04   4.64E-04
     1.00E-03   2.15E-03   4.64E-03   1.00E-02   1.25E-02   1.58E-02
     1.99E-02   2.51E-02   3.16E-02   3.98E-02   5.01E-02   6.30E-02
     7.94E-02   1.00E-01   1.25E-01   1.58E-01   1.99E-01   2.51E-01
     3.16E-01   3.98E-01   5.01E-01   6.30E-01   7.94E-01   1.00E+00
     1.25E+00   1.58E+00   1.99E+00   2.51E+00   3.16E+00   3.98E+00
     5.01E+00   6.30E+00   7.94E+00   1.00E+01   1.15E+01   25.
c
e5   1.00E-09   2.15E-09   4.64E-09   1.00E-08   2.15E-08   4.64E-08
     1.00E-07   2.15E-07   4.64E-07   1.00E-06   2.15E-06   4.64E-06
     1.00E-05   2.15E-05   4.64E-05   1.00E-04   2.15E-04   4.64E-04
     1.00E-03   2.15E-03   4.64E-03   1.00E-02   1.25E-02   1.58E-02
     1.99E-02   2.51E-02   3.16E-02   3.98E-02   5.01E-02   6.30E-02
     7.94E-02   1.00E-01   1.25E-01   1.58E-01   1.99E-01   2.51E-01
     3.16E-01   3.98E-01   5.01E-01   6.30E-01   7.94E-01   1.00E+00
     1.25E+00   1.58E+00   1.99E+00   2.51E+00   3.16E+00   3.98E+00
     5.01E+00   6.30E+00   7.94E+00   1.00E+01   1.15E+01   25.
c
e12   1.00E-09   2.15E-09   4.64E-09   1.00E-08   2.15E-08   4.64E-08
     1.00E-07   2.15E-07   4.64E-07   1.00E-06   2.15E-06   4.64E-06
     1.00E-05   2.15E-05   4.64E-05   1.00E-04   2.15E-04   4.64E-04
     1.00E-03   2.15E-03   4.64E-03   1.00E-02   1.25E-02   1.58E-02
     1.99E-02   2.51E-02   3.16E-02   3.98E-02   5.01E-02   6.30E-02
     7.94E-02   1.00E-01   1.25E-01   1.58E-01   1.99E-01   2.51E-01
     3.16E-01   3.98E-01   5.01E-01   6.30E-01   7.94E-01   1.00E+00
     1.25E+00   1.58E+00   1.99E+00   2.51E+00   3.16E+00   3.98E+00
     5.01E+00   6.30E+00   7.94E+00   1.00E+01   1.15E+01   25.
c
e25   1.00E-09   2.15E-09   4.64E-09   1.00E-08   2.15E-08   4.64E-08
     1.00E-07   2.15E-07   4.64E-07   1.00E-06   2.15E-06   4.64E-06
     1.00E-05   2.15E-05   4.64E-05   1.00E-04   2.15E-04   4.64E-04
     1.00E-03   2.15E-03   4.64E-03   1.00E-02   1.25E-02   1.58E-02
     1.99E-02   2.51E-02   3.16E-02   3.98E-02   5.01E-02   6.30E-02
     7.94E-02   1.00E-01   1.25E-01   1.58E-01   1.99E-01   2.51E-01
     3.16E-01   3.98E-01   5.01E-01   6.30E-01   7.94E-01   1.00E+00
     1.25E+00   1.58E+00   1.99E+00   2.51E+00   3.16E+00   3.98E+00
     5.01E+00   6.30E+00   7.94E+00   1.00E+01   1.15E+01   25.
c
c  for gammas
e22  0.01   0.015   0.02   0.03   0.04   0.05   0.06   0.08   0.1
     0.15   0.2      0.3    0.4    0.5    0.6    0.8     1.   1.5
       2.    3.       4.     5.     6.     8.   10.0    12.    15.
c
c  ICRP 74 Dose Conversion coeffients
DE12  1.00E-09  1.00E-08  2.53E-08  1.00E-07  2.00E-07  5.00E-07
      1.00E-06  2.00E-06  5.00E-06  1.00E-05  2.00E-05  5.00E-05
      1.00E-04  2.00E-04  5.00E-04  1.00E-03  2.00E-03  5.00E-03
      1.00E-02  2.00E-02  3.00E-02  5.00E-02  7.00E-02  1.00E-01
      1.50E-01  2.00E-01  3.00E-01  5.00E-01  7.00E-01  9.00E-01
      1.00E+00  1.20E+00  2.00E+00  3.00E+00  4.00E+00  5.00E+00
      6.00E+00  7.00E+00  8.00E+00  9.00E+00  1.00E+01  1.20E+01
      1.40E+01  1.50E+01  1.60E+01  1.80E+01  2.00E+01  3.00E+01
      5.00E+01  7.50E+01  1.00E+02  1.25E+02  1.50E+02  1.75E+02
      2.01E+02
c
DF12  6.6  9   10.6  12.9  13.5  13.6  13.3  12.9   12   11.3  10.6
      9.9  9.4  8.9   8.3   7.9   7.7     8  10.5  16.6  23.7  41.1
       60   88  132   170   233   322   375   400   416   425   420
      412  408  405   400   405   409   420   440   480   520   540
      555  570  600   515   400   330   285   260   245   250   260
c
c  ICRP 74 Dose Conversion coeffients
DE25  1.00E-09  1.00E-08  2.53E-08  1.00E-07  2.00E-07  5.00E-07
```

```
      1.00E-06  2.00E-06  5.00E-06  1.00E-05  2.00E-05  5.00E-05
      1.00E-04  2.00E-04  5.00E-04  1.00E-03  2.00E-03  5.00E-03
      1.00E-02  2.00E-02  3.00E-02  5.00E-02  7.00E-02  1.00E-01
      1.50E-01  2.00E-01  3.00E-01  5.00E-01  7.00E-01  9.00E-01
      1.00E+00  1.20E+00  2.00E+00  3.00E+00  4.00E+00  5.00E+00
      6.00E+00  7.00E+00  8.00E+00  9.00E+00  1.00E+01  1.20E+01
      1.40E+01  1.50E+01  1.60E+01  1.80E+01  2.00E+01  3.00E+01
      5.00E+01  7.50E+01  1.00E+02  1.25E+02  1.50E+02  1.75E+02
      2.01E+02
c
DF25  6.6  9   10.6  12.9  13.5  13.6  13.3  12.9   12   11.3  10.6
      9.9  9.4  8.9   8.3   7.9   7.7     8  10.5  16.6  23.7  41.1
       60   88  132   170   233   322   375   400   416   425   420
      412  408  405   400   405   409   420   440   480   520   540
      555  570  600   515   400   330   285   260   245   250   260
c
c ICRP 74 DCCs for photons (pSv-cm2)
de32  0.01   0.015   0.02   0.03   0.04   0.05   0.06   0.08   0.1
     0.15   0.2      0.3    0.4    0.5    0.6    0.8     1.   1.5
       2.    3.       4.     5.     6.     8.   10.0
df32   0.061   0.83   1.05   0.81   0.64   0.55   0.51   0.53  0.61
       0.89    1.2    1.8    2.38   2.93   3.44   4.38    5.2   6.9
        8.6   11.1   13.4    15.5   17.6   21.6   25.6
c
mode n p
CUT:N  1J  1.e-10
CUT:P  1J   0.01
nps 1E7
```

B.8 AmBe Bare MCNP Input

```
AmBe bare
c by Pete Exline
c Cell Cards
1 1 -1.214 (-2 -3 4):(-2 -5) imp:n=1 imp:p=1 $AmBe Source Region
2 0 -2 -4 5 #((72 -73 -63 66 -78 -77 5):&
(72 -73 67 -64 78 74 -76):(72 -73 67 -64 78 -71 -74):&
(72 -73 68 -65 77 -75):(72 -73 68 -65 75 -71)) imp:n=1 imp:p=1 $void spring area
3 2 -7.94 (-1 2):(3 -1)      imp:n=1 imp:p=1 $SS304 Shell
c leaf spring - center:left:far left:right:far right
60 2 -7.94 (72 -73 -63 66 -78 -77 5):(72 -73 67 -64 78 74 -76):&
(72 -73 67 -64 78 -71 -74):(72 -73 68 -65 77 -75):&
(72 -73 68 -65 75 -71) imp:n=1 imp:p=1
c ** air to combine for Bare **
401 304 -1.24e-3  1 -322 imp:n=1 imp:p=1 $air from AmBe to tally sphere
402 304 -1.24e-3  322 -306 imp:n=1 imp:p=1 $air from tally sphere to edge of uni
403 0 306 imp:n=0 imp:p=0 $vac past edge of universe

c Surface Cards
1  SO 3.048   $Outer surface of source sphere
2  SO 2.7305  $Inner Radius of SS304 Layer
3  PZ 2.3876  $Upper Bound on AmBe Material
4  PZ 0.3175  $Upper Bound on Void Space
5  PZ -0.3175 $Lower Bound on Void Space
63 C/Y 0 -.83185 1.149349  $leaf spring middle circle outer
64 C/Y -1.12299 .0381 0.35559 $leaf spring left circle outer
65 C/Y 1.12299 .0381 0.35559 $leaf spring right circle outer
66 C/Y 0 -.83185 1.07315  $leaf spring middle circle inner
67 C/Y -1.12299 .0381 0.2794 $leaf spring left circle inner
68 C/Y 1.12299 .0381 0.2794 $leaf spring right circle inner
71 PZ -.15875 $end spring l/r
72 PY -1.27 $edge of width of spring
73 PY 1.27 $edge of width of spring
74 PX -1.12299 $used to treat inner half of small curve different for cutoffs
75 PX 1.12299 $used to treat inner half of small curve different for cutoffs
76 PZ 0.01 $used to fix what 75 does in allowing top of circles
77 p 1 0 -1 .9525
78 p -1 0 -1 .9525
306  SO 500     $Edge of the Universe
322 SO 100     $100cm Sphere around source
c **
c
c  The next set of planes will be used to segment surface 22 to do the angular
c  dependent tally.  They do not have to be used in the cell descriptions.
c
324 PZ 98.7688340595138
325 PZ 95.1056516295154
326 PZ 89.1006524188368
327 PZ 80.9016994374947
328 PZ 70.7106781186548
329 PZ 58.7785252292473
330 PZ 45.3990499739547
331 PZ 30.9016994374947
332 PZ 15.6434465040231
333 PZ 0
334 PZ -15.6434465040231
335 PZ -30.9016994374947
336 PZ -45.3990499739547
337 PZ -58.7785252292473
338 PZ -70.7106781186547
339 PZ -80.9016994374947
340 PZ -89.1006524188368
341 PZ -95.1056516295154
342 PZ -98.7688340595138
c **

c Material Cards
```

```
c
c
m1 95241.66c -.2 4009.62c -.8 $AmBe
c SS304
m2 6000 -.0008 14000 -.01 15031 -.00045 24000 -.19 &
   25055.61c -.02 26000 -.68375 28000 -.095
m304 7014 -.7558 8016 -.2314 18000 -.0128 $air
c **
c
c Source
sdef par=1 erg=d1  RAD=D2  CEL=1
c
SI1   4.14e-7  0.11  0.166  0.224  0.302  0.369   0.45   0.55         &
      0.672  0.821   1.003  1.108  1.225  1.353  1.496  1.653   1.827 &
      2.019  2.123   2.231  2.346  2.466  2.592  2.725  2.865   3.012 &
      3.166  3.329   3.499  3.679  3.867  4.066  4.274  4.493   4.724 &
      4.966  5.221   5.488  5.627  5.770  5.916  6.065  6.219   6.376 &
      6.538  6.703   6.873  7.047  7.225  7.408  7.596  7.788   7.985 &
      8.187  8.395   8.607  8.825  9.048  9.277  9.512  9.753   10.0  &
     10.253 10.513  10.779 11.052 11.331
c
sp1  0 .014036  .006889  .007264  .009769  .008391  .010163  .012457  &
       .015032  .016573  .017775  .00844   .00773   .006091  .006321  &
       .006287  .006968  .011401  .00702   .00804   .0099    .012154  &
       .013445  .015515  .018104  .021269  .023188  .0267    .0324    &
       .0337    .029836  .031177  .034159  .036369  .038848  .037056  &
       .038803  .037562  .017426  .0172    .01537   .013832  .013948  &
       .013378  .013805  .014282  .014806  .014082  .011839  .012698  &
       .014484  .01617   .01612   .014402  .013867  .012271  .014014  &
       .006684  .004591  .005624  .007721  .008642  .007526  .006221  &
       .00401   .001699  .00033
sb1 0 1 65R
c
SI2  0.0   2.7305
SP2  -21 2
c
c Tallies
F2:N  322
FC2  Neutron Flux
FS2 -334 -332 T $plus/minus 15.6cm cutoffs
c Current Tally of whole sphere
F1:N  322
FC1 number of neutrons per spherical surface segments at 100 cm
c Segmented Tally across z plans of the sphere
FS1  -342 -341 -340 -339 -338 -337 -336 -335 -334 -333 -332 -331 &
-330 -329 -328 -327 -326 -325 -324
c
F12:N 322
FC12  Icrp 74 ambient dose equivalent on spherical surface at 100 cm
c Segmented Tally across z plans of the sphere
FS12  -342 -341 -340 -339 -338 -337 -336 -335 -334 -333 -332 -331 &
-330 -329 -328 -327 -326 -325 -324
c
c  gamma fluence tally at 100 cm
F22:P  322
FC22  Gamma Ray Fluence induced by neutrons at 100 cm
FS22 -334 -332 T $plus/minus 15.6cm cutoffs
c
F32:P   322
FC32  Gamma Ray Dose rate at 100 cm
FS32 -334 -332 T $plus/minus 15.6cm cutoffs
c
F5:N -100.0001 0 0 .1
FC5 Point Neutron Detector at 100cm
c
F25:N -100.0001 0 0 .1
FC25 ICRP 74 ambient dose equivalent on Point Neutron Detector at 100cm
c Energy groups used to bin fluence
e1   1.00E-09   2.15E-09   4.64E-09   1.00E-08   2.15E-08   4.64E-08
```

```
     1.00E-07   2.15E-07   4.64E-07   1.00E-06   2.15E-06   4.64E-06
     1.00E-05   2.15E-05   4.64E-05   1.00E-04   2.15E-04   4.64E-04
     1.00E-03   2.15E-03   4.64E-03   1.00E-02   1.25E-02   1.58E-02
     1.99E-02   2.51E-02   3.16E-02   3.98E-02   5.01E-02   6.30E-02
     7.94E-02   1.00E-01   1.25E-01   1.58E-01   1.99E-01   2.51E-01
     3.16E-01   3.98E-01   5.01E-01   6.30E-01   7.94E-01   1.00E+00
     1.25E+00   1.58E+00   1.99E+00   2.51E+00   3.16E+00   3.98E+00
     5.01E+00   6.30E+00   7.94E+00   1.00E+01   1.15E+01   25.
c
e2   1.00E-09   2.15E-09   4.64E-09   1.00E-08   2.15E-08   4.64E-08
     1.00E-07   2.15E-07   4.64E-07   1.00E-06   2.15E-06   4.64E-06
     1.00E-05   2.15E-05   4.64E-05   1.00E-04   2.15E-04   4.64E-04
     1.00E-03   2.15E-03   4.64E-03   1.00E-02   1.25E-02   1.58E-02
     1.99E-02   2.51E-02   3.16E-02   3.98E-02   5.01E-02   6.30E-02
     7.94E-02   1.00E-01   1.25E-01   1.58E-01   1.99E-01   2.51E-01
     3.16E-01   3.98E-01   5.01E-01   6.30E-01   7.94E-01   1.00E+00
     1.25E+00   1.58E+00   1.99E+00   2.51E+00   3.16E+00   3.98E+00
     5.01E+00   6.30E+00   7.94E+00   1.00E+01   1.15E+01   25.
c
e5   1.00E-09   2.15E-09   4.64E-09   1.00E-08   2.15E-08   4.64E-08
     1.00E-07   2.15E-07   4.64E-07   1.00E-06   2.15E-06   4.64E-06
     1.00E-05   2.15E-05   4.64E-05   1.00E-04   2.15E-04   4.64E-04
     1.00E-03   2.15E-03   4.64E-03   1.00E-02   1.25E-02   1.58E-02
     1.99E-02   2.51E-02   3.16E-02   3.98E-02   5.01E-02   6.30E-02
     7.94E-02   1.00E-01   1.25E-01   1.58E-01   1.99E-01   2.51E-01
     3.16E-01   3.98E-01   5.01E-01   6.30E-01   7.94E-01   1.00E+00
     1.25E+00   1.58E+00   1.99E+00   2.51E+00   3.16E+00   3.98E+00
     5.01E+00   6.30E+00   7.94E+00   1.00E+01   1.15E+01   25.
c
e12   1.00E-09   2.15E-09   4.64E-09   1.00E-08   2.15E-08   4.64E-08
     1.00E-07   2.15E-07   4.64E-07   1.00E-06   2.15E-06   4.64E-06
     1.00E-05   2.15E-05   4.64E-05   1.00E-04   2.15E-04   4.64E-04
     1.00E-03   2.15E-03   4.64E-03   1.00E-02   1.25E-02   1.58E-02
     1.99E-02   2.51E-02   3.16E-02   3.98E-02   5.01E-02   6.30E-02
     7.94E-02   1.00E-01   1.25E-01   1.58E-01   1.99E-01   2.51E-01
     3.16E-01   3.98E-01   5.01E-01   6.30E-01   7.94E-01   1.00E+00
     1.25E+00   1.58E+00   1.99E+00   2.51E+00   3.16E+00   3.98E+00
     5.01E+00   6.30E+00   7.94E+00   1.00E+01   1.15E+01   25.
c
e25   1.00E-09   2.15E-09   4.64E-09   1.00E-08   2.15E-08   4.64E-08
     1.00E-07   2.15E-07   4.64E-07   1.00E-06   2.15E-06   4.64E-06
     1.00E-05   2.15E-05   4.64E-05   1.00E-04   2.15E-04   4.64E-04
     1.00E-03   2.15E-03   4.64E-03   1.00E-02   1.25E-02   1.58E-02
     1.99E-02   2.51E-02   3.16E-02   3.98E-02   5.01E-02   6.30E-02
     7.94E-02   1.00E-01   1.25E-01   1.58E-01   1.99E-01   2.51E-01
     3.16E-01   3.98E-01   5.01E-01   6.30E-01   7.94E-01   1.00E+00
     1.25E+00   1.58E+00   1.99E+00   2.51E+00   3.16E+00   3.98E+00
     5.01E+00   6.30E+00   7.94E+00   1.00E+01   1.15E+01   25.
c
c  for gammas
e22  0.01   0.015   0.02   0.03   0.04   0.05   0.06   0.08   0.1
     0.15   0.2      0.3    0.4    0.5    0.6    0.8     1.   1.5
       2.    3.       4.     5.     6.     8.   10.0    12.    15.
c
c  ICRP 74 Dose Conversion coeffients
DE12  1.00E-09  1.00E-08  2.53E-08  1.00E-07  2.00E-07  5.00E-07
      1.00E-06  2.00E-06  5.00E-06  1.00E-05  2.00E-05  5.00E-05
      1.00E-04  2.00E-04  5.00E-04  1.00E-03  2.00E-03  5.00E-03
      1.00E-02  2.00E-02  3.00E-02  5.00E-02  7.00E-02  1.00E-01
      1.50E-01  2.00E-01  3.00E-01  5.00E-01  7.00E-01  9.00E-01
      1.00E+00  1.20E+00  2.00E+00  3.00E+00  4.00E+00  5.00E+00
      6.00E+00  7.00E+00  8.00E+00  9.00E+00  1.00E+01  1.20E+01
      1.40E+01  1.50E+01  1.60E+01  1.80E+01  2.00E+01  3.00E+01
      5.00E+01  7.50E+01  1.00E+02  1.25E+02  1.50E+02  1.75E+02
      2.01E+02
c
DF12  6.6  9   10.6  12.9  13.5  13.6  13.3  12.9   12   11.3  10.6
      9.9  9.4  8.9   8.3   7.9   7.7     8  10.5  16.6  23.7  41.1
       60   88  132   170   233   322   375   400   416   425   420
```

```
      412  408  405   400   405   409   420   440   480   520   540
      555  570  600   515   400   330   285   260   245   250   260
c
c  ICRP 74 Dose Conversion coeffients
DE25  1.00E-09  1.00E-08  2.53E-08  1.00E-07  2.00E-07  5.00E-07
      1.00E-06  2.00E-06  5.00E-06  1.00E-05  2.00E-05  5.00E-05
      1.00E-04  2.00E-04  5.00E-04  1.00E-03  2.00E-03  5.00E-03
      1.00E-02  2.00E-02  3.00E-02  5.00E-02  7.00E-02  1.00E-01
      1.50E-01  2.00E-01  3.00E-01  5.00E-01  7.00E-01  9.00E-01
      1.00E+00  1.20E+00  2.00E+00  3.00E+00  4.00E+00  5.00E+00
      6.00E+00  7.00E+00  8.00E+00  9.00E+00  1.00E+01  1.20E+01
      1.40E+01  1.50E+01  1.60E+01  1.80E+01  2.00E+01  3.00E+01
      5.00E+01  7.50E+01  1.00E+02  1.25E+02  1.50E+02  1.75E+02
      2.01E+02
c
DF25  6.6  9   10.6  12.9  13.5  13.6  13.3  12.9   12   11.3  10.6
      9.9  9.4  8.9   8.3   7.9   7.7     8  10.5  16.6  23.7  41.1
       60   88  132   170   233   322   375   400   416   425   420
      412  408  405   400   405   409   420   440   480   520   540
      555  570  600   515   400   330   285   260   245   250   260
c
c ICRP 74 DCCs for photons (pSv-cm2)
de32  0.01   0.015   0.02   0.03   0.04   0.05   0.06   0.08   0.1
     0.15   0.2     0.3    0.4    0.5    0.6    0.8     1.   1.5
       2.    3.       4.     5.     6.     8.   10.0
df32   0.061   0.83   1.05   0.81   0.64   0.55   0.51   0.53  0.61
       0.89    1.2    1.8    2.38   2.93   3.44   4.38    5.2   6.9
        8.6   11.1   13.4    15.5   17.6   21.6   25.6
c
mode n p
CUT:N  1J  1.e-10
CUT:P  1J   0.01
nps 1E7
```

B.9 AmBe in Beryllium MCNP Input

```
AmBe in 10.16 cm r Be sphere
c by Pete Exline
c Cell Cards
1 1 -1.214 (-2 -3 4):(-2 -5) imp:n=1 imp:p=1 $AmBe Source Region
2 0 -2 -4 5 #((72 -73 -63 66 -78 -77 5):&
(72 -73 67 -64 78 74 -76):(72 -73 67 -64 78 -71 -74):&
(72 -73 68 -65 77 -75):(72 -73 68 -65 75 -71)) imp:n=1 imp:p=1 $void spring area
3 2 -7.94 (-1 2):(3 -1)      imp:n=1 imp:p=1 $SS304 Shell
c leaf spring - center:left:far left:right:far right
60 2 -7.94 (72 -73 -63 66 -78 -77 5):(72 -73 67 -64 78 74 -76):&
(72 -73 67 -64 78 -71 -74):(72 -73 68 -65 77 -75):&
(72 -73 68 -65 75 -71) imp:n=1 imp:p=1
c ** Be Sphere **
304 304 -1.24e-3 (-322 307 #(&
(-501 502 503 -504 505 -506):&
((-501 531 513 515 -503 -525):(-501 531 503 515 -523 -505))&
:((-501 531 524 -514 515 -505):(-501 531 504 -514 515 -525))&
:((-501 531 513 -516 -503 526):(-501 531 503 -516 -523 506))&
:((-501 531 524 -514 -516 506):(-501 531 504 -514 -516 526))&
:((-531 543 545 -503 -525):(-531 503 545 -523 -505))&
:((-531 524 -544 545 -505):(-531 504 -544 545 -525))&
:((-531 543 -546 -503 526):(-531 503 -546 -523 506))&
:((-531 524 -544 -546 506):(-531 504 -544 -546 526))&
:((501 -553 551 -552))))&
  imp:n=1 imp:p=1 $air from Be surface to tally sphere
305 304 -1.24e-3 322 -306   imp:n=1 imp:p=1 $air from sphere to edge of universe
c Be sphere (with last two terms removing plug)
306 303 -1.84  -307 301 (308:-312) (309:-311) imp:n=1 imp:p=1
307 0      306                  imp:n=0 imp:p=0 $Void space outside universe
c plug in place
308 303 -1.84 -307 301 (-308 312 -307 301):(-309 311 -307 301) &
 imp:n=1 imp:p=1
c ** air to combine for Be Sphere **
c 401 304 -1.24e-3  (-301 1 2 -3):(-301 4 3 -8):(-301 5 8 -9):(-301 -2):(-301 9) &
c imp:n=1 imp:p=1
c * Al table top*
501 305 -2.7 -501 502 503 -504 505 -506 imp:n=1 imp:p=1 $Al table top
511 305 -2.7 (-501 531 513 515 -503 -525):(-501 531 503 515 -523 -505) &
imp:n=1 imp:p=1 $bl leg
512 305 -2.7 (-501 531 524 -514 515 -505):(-501 531 504 -514 515 -525) &
imp:n=1 imp:p=1 $br leg
513 305 -2.7 (-501 531 513 -516 -503 526):(-501 531 503 -516 -523 506) &
imp:n=1 imp:p=1 $tl leg
514 305 -2.7 (-501 531 524 -514 -516 506):(-501 531 504 -514 -516 526) &
imp:n=1 imp:p=1 $tr leg
541 305 -2.7 (-531 -322 543 545 -503 -525):(-531 -322 503 545 -523 -505) &
imp:n=1 imp:p=1 $bl thick leg
542 305 -2.7 (-531 -322 524 -544 545 -505):(-531 -322 504 -544 545 -525) &
imp:n=1 imp:p=1 $br thick leg
543 305 -2.7 (-531 -322 543 -546 -503 526):(-531 -322 503 -546 -523 506) &
imp:n=1 imp:p=1 $tl thick leg
544 305 -2.7 (-531 -322 524 -544 -546 506):(-531 -322 504 -544 -546 526) &
imp:n=1 imp:p=1 $tr thick leg
551 305 -2.7 501 -553 551 -552 imp:n=1 imp:p=1 $Al stabilizer ring
c **

c Surface Cards
1  SO 3.048   $Outer surface of source sphere
2  SO 2.7305  $Inner Radius of SS304 Layer
3  PZ 2.3876  $Upper Bound on AmBe Material
4  PZ 0.3175  $Upper Bound on Void Space
5  PZ -0.3175 $Lower Bound on Void Space
63 C/Y 0 -.83185 1.149349  $leaf spring middle circle outer
64 C/Y -1.12299 .0381 0.35559 $leaf spring left circle outer
65 C/Y 1.12299 .0381 0.35559 $leaf spring right circle outer
66 C/Y 0 -.83185 1.07315  $leaf spring middle circle inner
```

```
67 C/Y -1.12299 .0381 0.2794 $leaf spring left circle inner
68 C/Y 1.12299 .0381 0.2794 $leaf spring right circle inner
71 PZ -.15875 $end spring l/r
72 PY -1.27 $edge of width of spring
73 PY 1.27 $edge of width of spring
74 PX -1.12299 $used to treat inner half of small curve different for cutoffs
75 PX 1.12299 $used to treat inner half of small curve different for cutoffs
76 PZ 0.01 $used to fix what 75 does in allowing top of circles
77 p 1 0 -1 .9525
78 p -1 0 -1 .9525
c **Be Sphere **
301  SO 3.048   $Outer surface of source sphere
306  SO 500     $Edge of the Universe
307  SO 10.16   $radius of Be spherical shell
308  CZ 0.635   $small radius of plug
309  CZ 0.9525  $larger radius of plug lip
310 PZ 3.175   $bottom of plug
311 PZ 8.89    $bottom of plug lip
312 PZ 0.001   $used to define upper half for plug geometries
322 SO 100     $100cm Sphere around source
c **
c *Al table top*
501  pz -10.16 $top of Al table top
502  pz -10.76 $bot of Al table top
503  px -25.325 $left of Al table top
504  px 25.325 $right of Al table top
505  py -25.325 $front of Al table top
506  py 25.325 $back of Al table top
513  px -25.475 $left of Al table leg
514  px 25.475 $right of Al table leg
515  py -25.475 $front of Al table leg
516  py 25.475 $back of Al table leg
523  px -20.575 $cutoff of Al table top
524  px 20.575 $cutoff of Al table top
525  py -20.575 $cutoff of Al table top
526  py 20.575 $cutoff of Al table top
531  pz -35.9675 $bot of thin legs/top of thick legs
543  px -26.075 $left of Al table thick leg
544  px 26.075 $right of Al table thick leg
545  py -26.075 $front of Al table thick leg
546  py 26.075 $back of Al table thick leg
551  cz 6.25 $inner radius of Al stabilizer
552  cz 8.75 $outer radius of Al stabilizer
553  pz -9.51 $top of Al stablizer
c **
c
c  The next set of planes will be used to segment surface 22 to do the angular
c  dependent tally.  They do not have to be used in the cell descriptions.
c
324 PZ 98.7688340595138
325 PZ 95.1056516295154
326 PZ 89.1006524188368
327 PZ 80.9016994374947
328 PZ 70.7106781186548
329 PZ 58.7785252292473
330 PZ 45.3990499739547
331 PZ 30.9016994374947
332 PZ 15.6434465040231
333 PZ 0
334 PZ -15.6434465040231
335 PZ -30.9016994374947
336 PZ -45.3990499739547
337 PZ -58.7785252292473
338 PZ -70.7106781186547
339 PZ -80.9016994374947
340 PZ -89.1006524188368
341 PZ -95.1056516295154
342 PZ -98.7688340595138
c **
```

```
c Material Cards
c
m1 95241.66c -.2 4009.62c -.8 $AmBe
c SS304
m2 6000 -.0008 14000 -.01 15031 -.00045 24000 -.19 &
   25055.61c -.02 26000 -.68375 28000 -.095
c ** Be Sphere **
m303 4009.62  1.0
c **
m304 7014 -.7558 8016 -.2314 18000 -.0128 $air
c **
m305 13027 1.0 $Al
c
c Source
sdef par=1 erg=d1  RAD=D2  CEL=1
c
SI1   4.14e-7  0.11  0.166  0.224  0.302  0.369   0.45   0.55         &
      0.672  0.821   1.003  1.108  1.225  1.353  1.496  1.653   1.827 &
      2.019  2.123   2.231  2.346  2.466  2.592  2.725  2.865   3.012 &
      3.166  3.329   3.499  3.679  3.867  4.066  4.274  4.493   4.724 &
      4.966  5.221   5.488  5.627  5.770  5.916  6.065  6.219   6.376 &
      6.538  6.703   6.873  7.047  7.225  7.408  7.596  7.788   7.985 &
      8.187  8.395   8.607  8.825  9.048  9.277  9.512  9.753   10.0  &
     10.253 10.513  10.779 11.052 11.331
c
sp1  0 .014036  .006889  .007264  .009769  .008391  .010163  .012457  &
       .015032  .016573  .017775  .00844   .00773   .006091  .006321  &
       .006287  .006968  .011401  .00702   .00804   .0099    .012154  &
       .013445  .015515  .018104  .021269  .023188  .0267    .0324    &
       .0337    .029836  .031177  .034159  .036369  .038848  .037056  &
       .038803  .037562  .017426  .0172    .01537   .013832  .013948  &
       .013378  .013805  .014282  .014806  .014082  .011839  .012698  &
       .014484  .01617   .01612   .014402  .013867  .012271  .014014  &
       .006684  .004591  .005624  .007721  .008642  .007526  .006221  &
       .00401   .001699  .00033
sb1 0 1 65R
c
SI2  0.0   2.7305
SP2  -21 2
c
c Tallies
F2:N  322
FC2  Neutron Flux
FS2 -334 -332 T $plus/minus 15.6cm cutoffs
c Current Tally of whole sphere
F1:N  322
FC1 number of neutrons per spherical surface segments at 100 cm
c Segmented Tally across z plans of the sphere
FS1  -342 -341 -340 -339 -338 -337 -336 -335 -334 -333 -332 -331 &
-330 -329 -328 -327 -326 -325 -324
c
F12:N 322
FC12  Icrp 74 ambient dose equivalent on spherical surface at 100 cm
c Segmented Tally across z plans of the sphere
FS12  -342 -341 -340 -339 -338 -337 -336 -335 -334 -333 -332 -331 &
-330 -329 -328 -327 -326 -325 -324
c
c  gamma fluence tally at 100 cm
F22:P  322
FC22  Gamma Ray Fluence induced by neutrons at 100 cm
FS22 -334 -332 T $plus/minus 15.6cm cutoffs
c
F32:P   322
FC32  Gamma Ray Dose rate at 100 cm
FS32 -334 -332 T $plus/minus 15.6cm cutoffs
c
F5:N -100.0001 0 0 .1
FC5 Point Neutron Detector at 100cm
```

```
c
F25:N -100.0001 0 0 .1
FC25 ICRP 74 ambient dose equivalent on Point Neutron Detector at 100cm
c Energy groups used to bin fluence
e1   1.00E-09   2.15E-09   4.64E-09   1.00E-08   2.15E-08   4.64E-08
     1.00E-07   2.15E-07   4.64E-07   1.00E-06   2.15E-06   4.64E-06
     1.00E-05   2.15E-05   4.64E-05   1.00E-04   2.15E-04   4.64E-04
     1.00E-03   2.15E-03   4.64E-03   1.00E-02   1.25E-02   1.58E-02
     1.99E-02   2.51E-02   3.16E-02   3.98E-02   5.01E-02   6.30E-02
     7.94E-02   1.00E-01   1.25E-01   1.58E-01   1.99E-01   2.51E-01
     3.16E-01   3.98E-01   5.01E-01   6.30E-01   7.94E-01   1.00E+00
     1.25E+00   1.58E+00   1.99E+00   2.51E+00   3.16E+00   3.98E+00
     5.01E+00   6.30E+00   7.94E+00   1.00E+01   1.15E+01   25.
c
e2   1.00E-09   2.15E-09   4.64E-09   1.00E-08   2.15E-08   4.64E-08
     1.00E-07   2.15E-07   4.64E-07   1.00E-06   2.15E-06   4.64E-06
     1.00E-05   2.15E-05   4.64E-05   1.00E-04   2.15E-04   4.64E-04
     1.00E-03   2.15E-03   4.64E-03   1.00E-02   1.25E-02   1.58E-02
     1.99E-02   2.51E-02   3.16E-02   3.98E-02   5.01E-02   6.30E-02
     7.94E-02   1.00E-01   1.25E-01   1.58E-01   1.99E-01   2.51E-01
     3.16E-01   3.98E-01   5.01E-01   6.30E-01   7.94E-01   1.00E+00
     1.25E+00   1.58E+00   1.99E+00   2.51E+00   3.16E+00   3.98E+00
     5.01E+00   6.30E+00   7.94E+00   1.00E+01   1.15E+01   25.
c
e5   1.00E-09   2.15E-09   4.64E-09   1.00E-08   2.15E-08   4.64E-08
     1.00E-07   2.15E-07   4.64E-07   1.00E-06   2.15E-06   4.64E-06
     1.00E-05   2.15E-05   4.64E-05   1.00E-04   2.15E-04   4.64E-04
     1.00E-03   2.15E-03   4.64E-03   1.00E-02   1.25E-02   1.58E-02
     1.99E-02   2.51E-02   3.16E-02   3.98E-02   5.01E-02   6.30E-02
     7.94E-02   1.00E-01   1.25E-01   1.58E-01   1.99E-01   2.51E-01
     3.16E-01   3.98E-01   5.01E-01   6.30E-01   7.94E-01   1.00E+00
     1.25E+00   1.58E+00   1.99E+00   2.51E+00   3.16E+00   3.98E+00
     5.01E+00   6.30E+00   7.94E+00   1.00E+01   1.15E+01   25.
c
e12   1.00E-09   2.15E-09   4.64E-09   1.00E-08   2.15E-08   4.64E-08
     1.00E-07   2.15E-07   4.64E-07   1.00E-06   2.15E-06   4.64E-06
     1.00E-05   2.15E-05   4.64E-05   1.00E-04   2.15E-04   4.64E-04
     1.00E-03   2.15E-03   4.64E-03   1.00E-02   1.25E-02   1.58E-02
     1.99E-02   2.51E-02   3.16E-02   3.98E-02   5.01E-02   6.30E-02
     7.94E-02   1.00E-01   1.25E-01   1.58E-01   1.99E-01   2.51E-01
     3.16E-01   3.98E-01   5.01E-01   6.30E-01   7.94E-01   1.00E+00
     1.25E+00   1.58E+00   1.99E+00   2.51E+00   3.16E+00   3.98E+00
     5.01E+00   6.30E+00   7.94E+00   1.00E+01   1.15E+01   25.
c
e25   1.00E-09   2.15E-09   4.64E-09   1.00E-08   2.15E-08   4.64E-08
     1.00E-07   2.15E-07   4.64E-07   1.00E-06   2.15E-06   4.64E-06
     1.00E-05   2.15E-05   4.64E-05   1.00E-04   2.15E-04   4.64E-04
     1.00E-03   2.15E-03   4.64E-03   1.00E-02   1.25E-02   1.58E-02
     1.99E-02   2.51E-02   3.16E-02   3.98E-02   5.01E-02   6.30E-02
     7.94E-02   1.00E-01   1.25E-01   1.58E-01   1.99E-01   2.51E-01
     3.16E-01   3.98E-01   5.01E-01   6.30E-01   7.94E-01   1.00E+00
     1.25E+00   1.58E+00   1.99E+00   2.51E+00   3.16E+00   3.98E+00
     5.01E+00   6.30E+00   7.94E+00   1.00E+01   1.15E+01   25.
c
c  for gammas
e22  0.01   0.015   0.02   0.03   0.04   0.05   0.06   0.08   0.1
     0.15   0.2      0.3    0.4    0.5    0.6    0.8     1.   1.5
       2.    3.       4.     5.     6.     8.   10.0    12.    15.
c
c  ICRP 74 Dose Conversion coeffients
DE12  1.00E-09  1.00E-08  2.53E-08  1.00E-07  2.00E-07  5.00E-07
      1.00E-06  2.00E-06  5.00E-06  1.00E-05  2.00E-05  5.00E-05
      1.00E-04  2.00E-04  5.00E-04  1.00E-03  2.00E-03  5.00E-03
      1.00E-02  2.00E-02  3.00E-02  5.00E-02  7.00E-02  1.00E-01
      1.50E-01  2.00E-01  3.00E-01  5.00E-01  7.00E-01  9.00E-01
      1.00E+00  1.20E+00  2.00E+00  3.00E+00  4.00E+00  5.00E+00
      6.00E+00  7.00E+00  8.00E+00  9.00E+00  1.00E+01  1.20E+01
      1.40E+01  1.50E+01  1.60E+01  1.80E+01  2.00E+01  3.00E+01
      5.00E+01  7.50E+01  1.00E+02  1.25E+02  1.50E+02  1.75E+02
```

```
      2.01E+02
c
DF12  6.6  9   10.6  12.9  13.5  13.6  13.3  12.9   12   11.3  10.6
      9.9  9.4  8.9   8.3   7.9   7.7     8  10.5  16.6  23.7  41.1
       60   88  132   170   233   322   375   400   416   425   420
      412  408  405   400   405   409   420   440   480   520   540
      555  570  600   515   400   330   285   260   245   250   260
c
c  ICRP 74 Dose Conversion coeffients
DE25  1.00E-09  1.00E-08  2.53E-08  1.00E-07  2.00E-07  5.00E-07
      1.00E-06  2.00E-06  5.00E-06  1.00E-05  2.00E-05  5.00E-05
      1.00E-04  2.00E-04  5.00E-04  1.00E-03  2.00E-03  5.00E-03
      1.00E-02  2.00E-02  3.00E-02  5.00E-02  7.00E-02  1.00E-01
      1.50E-01  2.00E-01  3.00E-01  5.00E-01  7.00E-01  9.00E-01
      1.00E+00  1.20E+00  2.00E+00  3.00E+00  4.00E+00  5.00E+00
      6.00E+00  7.00E+00  8.00E+00  9.00E+00  1.00E+01  1.20E+01
      1.40E+01  1.50E+01  1.60E+01  1.80E+01  2.00E+01  3.00E+01
      5.00E+01  7.50E+01  1.00E+02  1.25E+02  1.50E+02  1.75E+02
      2.01E+02
c
DF25  6.6  9   10.6  12.9  13.5  13.6  13.3  12.9   12   11.3  10.6
      9.9  9.4  8.9   8.3   7.9   7.7     8  10.5  16.6  23.7  41.1
       60   88  132   170   233   322   375   400   416   425   420
      412  408  405   400   405   409   420   440   480   520   540
      555  570  600   515   400   330   285   260   245   250   260
c
c ICRP 74 DCCs for photons (pSv-cm2)
de32  0.01   0.015   0.02   0.03   0.04   0.05   0.06   0.08   0.1
     0.15   0.2      0.3    0.4    0.5    0.6    0.8     1.   1.5
       2.    3.       4.     5.     6.     8.   10.0
df32   0.061   0.83   1.05   0.81   0.64   0.55   0.51   0.53  0.61
       0.89    1.2    1.8    2.38   2.93   3.44   4.38    5.2   6.9
        8.6   11.1   13.4    15.5   17.6   21.6   25.6
c
mode n p
CUT:N  1J  1.e-10
CUT:P  1J   0.01
nps 1E7
```

B.10 AmBe in Lead MCNP Input

```
AmBe in 19.3675cm r Pb sphere
c by Pete Exline
c Cell Cards
1 1 -1.214 (-2 -3 4):(-2 -5) imp:n=1 imp:p=1 $AmBe Source Region
2 0 -2 -4 5 #((72 -73 -63 66 -78 -77 5):&
(72 -73 67 -64 78 74 -76):(72 -73 67 -64 78 -71 -74):&
(72 -73 68 -65 77 -75):(72 -73 68 -65 75 -71)) imp:n=1 imp:p=1 $void spring area
3 2 -7.94 (-1 2):(3 -1)      imp:n=1 imp:p=1 $SS304 Shell
c leaf spring - center:left:far left:right:far right
60 2 -7.94 (72 -73 -63 66 -78 -77 5):(72 -73 67 -64 78 74 -76):&
(72 -73 67 -64 78 -71 -74):(72 -73 68 -65 77 -75):&
(72 -73 68 -65 75 -71) imp:n=1 imp:p=1
c ** Pb Sphere **
301 304 -1.24e-3 (301 -322 #(&
(-501 502 503 -504 505 -506):&
((-501 531 513 515 -503 -525):(-501 531 503 515 -523 -505))&
:((-501 531 524 -514 515 -505):(-501 531 504 -514 515 -525))&
:((-501 531 513 -516 -503 526):(-501 531 503 -516 -523 506))&
:((-501 531 524 -514 -516 506):(-501 531 504 -514 -516 526))&
:((-531 543 545 -503 -525):(-531 503 545 -523 -505))&
:((-531 524 -544 545 -505):(-531 504 -544 545 -525))&
:((-531 543 -546 -503 526):(-531 503 -546 -523 506))&
:((-531 524 -544 -546 506):(-531 504 -544 -546 526))&
:((501 -553 551 -552))))&
imp:n=1 imp:p=1 $air from Pb surface to tally sph
302 304 -1.24e-3 322 -306         imp:n=1 imp:p=1 $air from tally to edge of univ
303 301 -11.34  -301 302          imp:n=1 imp:p=1 $Pb sphere
304 0      306                    imp:n=0 imp:p=0 $Void space outside universe
c 305 301 -11.34 -304 305 307       imp:n=1 imp:p=1 $Pb sphere top
c **
c * Al table top*
501 305 -2.7 -501 502 503 -504 505 -506 imp:n=1 imp:p=1 $Al table top
511 305 -2.7 (-501 531 513 515 -503 -525):(-501 531 503 515 -523 -505) &
imp:n=1 imp:p=1 $bl leg
512 305 -2.7 (-501 531 524 -514 515 -505):(-501 531 504 -514 515 -525) &
imp:n=1 imp:p=1 $br leg
513 305 -2.7 (-501 531 513 -516 -503 526):(-501 531 503 -516 -523 506) &
imp:n=1 imp:p=1 $tl leg
514 305 -2.7 (-501 531 524 -514 -516 506):(-501 531 504 -514 -516 526) &
imp:n=1 imp:p=1 $tr leg
541 305 -2.7 (-531 -322 543 545 -503 -525):(-531 -322 503 545 -523 -505) &
imp:n=1 imp:p=1 $bl thick leg
542 305 -2.7 (-531 -322 524 -544 545 -505):(-531 -322 504 -544 545 -525) &
imp:n=1 imp:p=1 $br thick leg
543 305 -2.7 (-531 -322 543 -546 -503 526):(-531 -322 503 -546 -523 506) &
imp:n=1 imp:p=1 $tl thick leg
544 305 -2.7 (-531 -322 524 -544 -546 506):(-531 -322 504 -544 -546 526) &
imp:n=1 imp:p=1 $tr thick leg
551 305 -2.7 501 -553 551 -552 imp:n=1 imp:p=1 $Al stabilizer ring
c **

c Surface Cards
1  SO 3.048   $Outer surface of source sphere
2  SO 2.7305  $Inner Radius of SS304 Layer
3  PZ 2.3876  $Upper Bound on AmBe Material
4  PZ 0.3175  $Upper Bound on Void Space
5  PZ -0.3175 $Lower Bound on Void Space
63 C/Y 0 -.83185 1.149349  $leaf spring middle circle outer
64 C/Y -1.12299 .0381 0.35559 $leaf spring left circle outer
65 C/Y 1.12299 .0381 0.35559 $leaf spring right circle outer
66 C/Y 0 -.83185 1.07315  $leaf spring middle circle inner
67 C/Y -1.12299 .0381 0.2794 $leaf spring left circle inner
68 C/Y 1.12299 .0381 0.2794 $leaf spring right circle inner
71 PZ -.15875 $end spring l/r
72 PY -1.27 $edge of width of spring
73 PY 1.27 $edge of width of spring
```

```
74 PX -1.12299 $used to treat inner half of small curve different for cutoffs
75 PX 1.12299 $used to treat inner half of small curve different for cutoffs
76 PZ 0.01 $used to fix what 75 does in allowing top of circles
77 p 1 0 -1 .9525
78 p -1 0 -1 .9525
c **Pb Sphere **
301  SO 19.3675  $Outer surface of Pb Sphere (bot hem)
302  SO 3.048   $inner void for source (bot hem)
c 303 PZ 0 $top of bottom hemisphere
c 304 S -.02338 0 0.95135 19.3675 $Pb top hemisphere sphere
c 305 S -.02338 0 0.95135 3.05 $inner void for source (top hem)
306  SO 500     $Edge of the Universe
c 307 P -19.3675 0 0 -.02338 0 .95135 -.02338 1 .95135
322 SO 100      $100cm tally sphere around source
c **
c *Al table top*
501  pz -19.3675 $top of Al table top
502  pz -19.9675 $bot of Al table top
503  px -25.325 $left of Al table top
504  px 25.325 $right of Al table top
505  py -25.325 $front of Al table top
506  py 25.325 $back of Al table top
513  px -25.475 $left of Al table leg
514  px 25.475 $right of Al table leg
515  py -25.475 $front of Al table leg
516  py 25.475 $back of Al table leg
523  px -20.575 $cutoff of Al table top
524  px 20.575 $cutoff of Al table top
525  py -20.575 $cutoff of Al table top
526  py 20.575 $cutoff of Al table top
531  pz -35.9675 $bot of thin legs/top of thick legs
543  px -26.075 $left of Al table thick leg
544  px 26.075 $right of Al table thick leg
545  py -26.075 $front of Al table thick leg
546  py 26.075 $back of Al table thick leg
551  cz 6.25 $inner radius of Al stabilizer
552  cz 8.75 $outer radius of Al stabilizer
553  pz -18.7175 $top of Al stablizer
c **
c
c  The next set of planes will be used to segment surface 22 to do the angular
c  dependent tally.  They do not have to be used in the cell descriptions.
c
324 PZ 98.7688340595138
325 PZ 95.1056516295154
326 PZ 89.1006524188368
327 PZ 80.9016994374947
328 PZ 70.7106781186548
329 PZ 58.7785252292473
330 PZ 45.3990499739547
331 PZ 30.9016994374947
332 PZ 15.6434465040231
333 PZ 0
334 PZ -15.6434465040231
335 PZ -30.9016994374947
336 PZ -45.3990499739547
337 PZ -58.7785252292473
338 PZ -70.7106781186547
339 PZ -80.9016994374947
340 PZ -89.1006524188368
341 PZ -95.1056516295154
342 PZ -98.7688340595138
c **

c Material Cards
c
m1 95241.66c -.2 4009.62c -.8 $AmBe
c SS304
m2 6000 -.0008 14000 -.01 15031 -.00045 24000 -.19 &
```

```
   25055.61c -.02 26000 -.68375 28000 -.095
c ** Pb Sphere **
m301 82204 .014 82206 .241 82207 .221 82208 .524
c **
m304 7014 -.7558 8016 -.2314 18000 -.0128 $air
c **
m305 13027 1.0 $Al
c
c Source
sdef par=1 erg=d1  RAD=D2  CEL=1
c
SI1   4.14e-7  0.11  0.166  0.224  0.302  0.369   0.45   0.55         &
      0.672  0.821   1.003  1.108  1.225  1.353  1.496  1.653   1.827 &
      2.019  2.123   2.231  2.346  2.466  2.592  2.725  2.865   3.012 &
      3.166  3.329   3.499  3.679  3.867  4.066  4.274  4.493   4.724 &
      4.966  5.221   5.488  5.627  5.770  5.916  6.065  6.219   6.376 &
      6.538  6.703   6.873  7.047  7.225  7.408  7.596  7.788   7.985 &
      8.187  8.395   8.607  8.825  9.048  9.277  9.512  9.753   10.0  &
     10.253 10.513  10.779 11.052 11.331
c
sp1  0 .014036  .006889  .007264  .009769  .008391  .010163  .012457  &
       .015032  .016573  .017775  .00844   .00773   .006091  .006321  &
       .006287  .006968  .011401  .00702   .00804   .0099    .012154  &
       .013445  .015515  .018104  .021269  .023188  .0267    .0324    &
       .0337    .029836  .031177  .034159  .036369  .038848  .037056  &
       .038803  .037562  .017426  .0172    .01537   .013832  .013948  &
       .013378  .013805  .014282  .014806  .014082  .011839  .012698  &
       .014484  .01617   .01612   .014402  .013867  .012271  .014014  &
       .006684  .004591  .005624  .007721  .008642  .007526  .006221  &
       .00401   .001699  .00033
sb1 0 1 65R
c
SI2  0.0   2.7305
SP2  -21 2
c
c Tallies
F2:N  322
FC2  Neutron Flux
FS2 -334 -332 T $plus/minus 15.6cm cutoffs
c Current Tally of whole sphere
F1:N  322
FC1 number of neutrons per spherical surface segments at 100 cm
c Segmented Tally across z plans of the sphere
FS1  -342 -341 -340 -339 -338 -337 -336 -335 -334 -333 -332 -331 &
-330 -329 -328 -327 -326 -325 -324
c
F12:N 322
FC12  Icrp 74 ambient dose equivalent on spherical surface at 100 cm
c Segmented Tally across z plans of the sphere
FS12  -342 -341 -340 -339 -338 -337 -336 -335 -334 -333 -332 -331 &
-330 -329 -328 -327 -326 -325 -324
c
c  gamma fluence tally at 100 cm
F22:P  322
FC22  Gamma Ray Fluence induced by neutrons at 100 cm
FS22 -334 -332 T $plus/minus 15.6cm cutoffs
c
F32:P   322
FC32  Gamma Ray Dose rate at 100 cm
FS32 -334 -332 T $plus/minus 15.6cm cutoffs
c
F5:N -100.0001 0 0 .1
FC5 Point Neutron Detector at 100cm
c
F25:N -100.0001 0 0 .1
FC25 ICRP 74 ambient dose equivalent on Point Neutron Detector at 100cm
c Energy groups used to bin fluence
e1   1.00E-09   2.15E-09   4.64E-09   1.00E-08   2.15E-08   4.64E-08
     1.00E-07   2.15E-07   4.64E-07   1.00E-06   2.15E-06   4.64E-06
```

```
     1.00E-05   2.15E-05   4.64E-05   1.00E-04   2.15E-04   4.64E-04
     1.00E-03   2.15E-03   4.64E-03   1.00E-02   1.25E-02   1.58E-02
     1.99E-02   2.51E-02   3.16E-02   3.98E-02   5.01E-02   6.30E-02
     7.94E-02   1.00E-01   1.25E-01   1.58E-01   1.99E-01   2.51E-01
     3.16E-01   3.98E-01   5.01E-01   6.30E-01   7.94E-01   1.00E+00
     1.25E+00   1.58E+00   1.99E+00   2.51E+00   3.16E+00   3.98E+00
     5.01E+00   6.30E+00   7.94E+00   1.00E+01   1.15E+01   25.
c
e2   1.00E-09   2.15E-09   4.64E-09   1.00E-08   2.15E-08   4.64E-08
     1.00E-07   2.15E-07   4.64E-07   1.00E-06   2.15E-06   4.64E-06
     1.00E-05   2.15E-05   4.64E-05   1.00E-04   2.15E-04   4.64E-04
     1.00E-03   2.15E-03   4.64E-03   1.00E-02   1.25E-02   1.58E-02
     1.99E-02   2.51E-02   3.16E-02   3.98E-02   5.01E-02   6.30E-02
     7.94E-02   1.00E-01   1.25E-01   1.58E-01   1.99E-01   2.51E-01
     3.16E-01   3.98E-01   5.01E-01   6.30E-01   7.94E-01   1.00E+00
     1.25E+00   1.58E+00   1.99E+00   2.51E+00   3.16E+00   3.98E+00
     5.01E+00   6.30E+00   7.94E+00   1.00E+01   1.15E+01   25.
c
e5   1.00E-09   2.15E-09   4.64E-09   1.00E-08   2.15E-08   4.64E-08
     1.00E-07   2.15E-07   4.64E-07   1.00E-06   2.15E-06   4.64E-06
     1.00E-05   2.15E-05   4.64E-05   1.00E-04   2.15E-04   4.64E-04
     1.00E-03   2.15E-03   4.64E-03   1.00E-02   1.25E-02   1.58E-02
     1.99E-02   2.51E-02   3.16E-02   3.98E-02   5.01E-02   6.30E-02
     7.94E-02   1.00E-01   1.25E-01   1.58E-01   1.99E-01   2.51E-01
     3.16E-01   3.98E-01   5.01E-01   6.30E-01   7.94E-01   1.00E+00
     1.25E+00   1.58E+00   1.99E+00   2.51E+00   3.16E+00   3.98E+00
     5.01E+00   6.30E+00   7.94E+00   1.00E+01   1.15E+01   25.
c
e12   1.00E-09   2.15E-09   4.64E-09   1.00E-08   2.15E-08   4.64E-08
     1.00E-07   2.15E-07   4.64E-07   1.00E-06   2.15E-06   4.64E-06
     1.00E-05   2.15E-05   4.64E-05   1.00E-04   2.15E-04   4.64E-04
     1.00E-03   2.15E-03   4.64E-03   1.00E-02   1.25E-02   1.58E-02
     1.99E-02   2.51E-02   3.16E-02   3.98E-02   5.01E-02   6.30E-02
     7.94E-02   1.00E-01   1.25E-01   1.58E-01   1.99E-01   2.51E-01
     3.16E-01   3.98E-01   5.01E-01   6.30E-01   7.94E-01   1.00E+00
     1.25E+00   1.58E+00   1.99E+00   2.51E+00   3.16E+00   3.98E+00
     5.01E+00   6.30E+00   7.94E+00   1.00E+01   1.15E+01   25.
c
e25   1.00E-09   2.15E-09   4.64E-09   1.00E-08   2.15E-08   4.64E-08
     1.00E-07   2.15E-07   4.64E-07   1.00E-06   2.15E-06   4.64E-06
     1.00E-05   2.15E-05   4.64E-05   1.00E-04   2.15E-04   4.64E-04
     1.00E-03   2.15E-03   4.64E-03   1.00E-02   1.25E-02   1.58E-02
     1.99E-02   2.51E-02   3.16E-02   3.98E-02   5.01E-02   6.30E-02
     7.94E-02   1.00E-01   1.25E-01   1.58E-01   1.99E-01   2.51E-01
     3.16E-01   3.98E-01   5.01E-01   6.30E-01   7.94E-01   1.00E+00
     1.25E+00   1.58E+00   1.99E+00   2.51E+00   3.16E+00   3.98E+00
     5.01E+00   6.30E+00   7.94E+00   1.00E+01   1.15E+01   25.
c
c  for gammas
e22  0.01   0.015   0.02   0.03   0.04   0.05   0.06   0.08   0.1
     0.15   0.2      0.3    0.4    0.5    0.6    0.8     1.   1.5
       2.    3.       4.     5.     6.     8.   10.0    12.    15.
c
c  ICRP 74 Dose Conversion coeffients
DE12  1.00E-09  1.00E-08  2.53E-08  1.00E-07  2.00E-07  5.00E-07
      1.00E-06  2.00E-06  5.00E-06  1.00E-05  2.00E-05  5.00E-05
      1.00E-04  2.00E-04  5.00E-04  1.00E-03  2.00E-03  5.00E-03
      1.00E-02  2.00E-02  3.00E-02  5.00E-02  7.00E-02  1.00E-01
      1.50E-01  2.00E-01  3.00E-01  5.00E-01  7.00E-01  9.00E-01
      1.00E+00  1.20E+00  2.00E+00  3.00E+00  4.00E+00  5.00E+00
      6.00E+00  7.00E+00  8.00E+00  9.00E+00  1.00E+01  1.20E+01
      1.40E+01  1.50E+01  1.60E+01  1.80E+01  2.00E+01  3.00E+01
      5.00E+01  7.50E+01  1.00E+02  1.25E+02  1.50E+02  1.75E+02
      2.01E+02
c
DF12  6.6  9   10.6  12.9  13.5  13.6  13.3  12.9   12   11.3  10.6
      9.9  9.4  8.9   8.3   7.9   7.7     8  10.5  16.6  23.7  41.1
       60   88  132   170   233   322   375   400   416   425   420
      412  408  405   400   405   409   420   440   480   520   540
```

```
      555  570  600   515   400   330   285   260   245   250   260
c
c  ICRP 74 Dose Conversion coeffients
DE25  1.00E-09  1.00E-08  2.53E-08  1.00E-07  2.00E-07  5.00E-07
      1.00E-06  2.00E-06  5.00E-06  1.00E-05  2.00E-05  5.00E-05
      1.00E-04  2.00E-04  5.00E-04  1.00E-03  2.00E-03  5.00E-03
      1.00E-02  2.00E-02  3.00E-02  5.00E-02  7.00E-02  1.00E-01
      1.50E-01  2.00E-01  3.00E-01  5.00E-01  7.00E-01  9.00E-01
      1.00E+00  1.20E+00  2.00E+00  3.00E+00  4.00E+00  5.00E+00
      6.00E+00  7.00E+00  8.00E+00  9.00E+00  1.00E+01  1.20E+01
      1.40E+01  1.50E+01  1.60E+01  1.80E+01  2.00E+01  3.00E+01
      5.00E+01  7.50E+01  1.00E+02  1.25E+02  1.50E+02  1.75E+02
      2.01E+02
c
DF25  6.6  9   10.6  12.9  13.5  13.6  13.3  12.9   12   11.3  10.6
      9.9  9.4  8.9   8.3   7.9   7.7     8  10.5  16.6  23.7  41.1
       60   88  132   170   233   322   375   400   416   425   420
      412  408  405   400   405   409   420   440   480   520   540
      555  570  600   515   400   330   285   260   245   250   260
c
c ICRP 74 DCCs for photons (pSv-cm2)
de32  0.01   0.015   0.02   0.03   0.04   0.05   0.06   0.08   0.1
     0.15   0.2      0.3    0.4    0.5    0.6    0.8     1.   1.5
       2.    3.       4.     5.     6.     8.   10.0
df32   0.061   0.83   1.05   0.81   0.64   0.55   0.51   0.53  0.61
       0.89    1.2    1.8    2.38   2.93   3.44   4.38    5.2   6.9
        8.6   11.1   13.4    15.5   17.6   21.6   25.6
c
mode n p
CUT:N  1J  1.e-10
CUT:P  1J   0.01
nps 1E7
```

B.11 AmBe in Iron MCNP Input

```
AmBe in 30" d Fe sphere
c by Pete Exline
c Cell Cards
1 1 -1.214 (-2 -3 4):(-2 -5) imp:n=1 imp:p=1 $AmBe Source Region
2 0 -2 -4 5 #((72 -73 -63 66 -78 -77 5):&
(72 -73 67 -64 78 74 -76):(72 -73 67 -64 78 -71 -74):&
(72 -73 68 -65 77 -75):(72 -73 68 -65 75 -71)) imp:n=1 imp:p=1 $void spring area
3 2 -7.94 (-301 2):(3 -301)      imp:n=1 imp:p=1 $SS304 Shell
60 2 -7.94 (72 -73 -63 66 -78 -77 5):(72 -73 67 -64 78 74 -76):&
(72 -73 67 -64 78 -71 -74):(72 -73 68 -65 77 -75):&
(72 -73 68 -65 75 -71) imp:n=1 imp:p=1
c ** Fe Sphere **
301 304 -1.24e-3      -322 355 #(501 -502 -503 504 505 -506) &
  #(502 -507 505 -510 -508 509) &
  #(502 -507 -506 511 -508 509) &
  #(507 -518 -512 -513 514 -516 528) &
  #(507 -518 -512 -513 515 -517 528) &
  #((514 -516 518 525 -526 -519 528):(514 -516 519 -524 520 &
  -521 -523 -522 528)) &
  #((515 -517 518 525 -526 -519 528):(515 -517 519 -524 520 &
  -521 -523 -522 528)) &
  #(529 -516 303 -528 301) &
  #(-530 515 303 -528 301) &
  #(-533:(-535 524 -537)) &
  #(-534:(-536 524 -537)) &
  #(507 -540 516 -510 541 538 -539) &
  #(507 -540 511 -515 542 538 -539) &
  #(-312 313 -314) imp:n=1 imp:p=1 $air from Fe surface to tally sph
302 304 -1.24e-3      322 -306  imp:n=1 imp:p=1 $air
c 302 0     322 -306  imp:n=1 imp:p=1 $void from sphere to edge of univ
303 301 -7.874  -355 302 307 (303:309) (305:311) (310:304) (308:-311) &
  imp:n=1 imp:p=1 $Fe sphere
304 0      306                  imp:n=0 imp:p=0 $Void space outside universe
305 301 -7.874 -355 -307             imp:n=1 imp:p=1 $plugged right tube
306 304 -1.24e-3 -303 302 -355 -309 #(-312 313 -314) imp:n=1 imp:p=1 $left tube
307 301 -7.874  (-355 -305 -311 302):(-355 -310 -304 302) &
  imp:n=1 imp:p=1 $plugged bottom tube
308 301 -7.874 -355 302 -308 311      imp:n=1 imp:p=1 $plugged top tube
309 301 -7.874 -312 313 -314 imp:n=1 imp:p=1 $smaller plug for left tube
c ** Air to combine for Fe Sphere **
401 304 -1.24e-3  301 -302 imp:n=1 imp:p=1 $air/styrofoam from source to sphere
c **
c
c ** Fe Stand **
501 301 -7.874 501 -502 -503 504 505 -506 imp:n=1 imp:p=1 $base plate
502 301 -7.874 502 -507 505 -510 -508 509 imp:n=1 imp:p=1 $l upp base
503 301 -7.874 502 -507 -506 511 -508 509 imp:n=1 imp:p=1 $r upp base
504 301 -7.874 507 -518 -512 -513 514 -516 528 imp:n=1 imp:p=1 $l support
505 301 -7.874 507 -518 -512 -513 515 -517 528 imp:n=1 imp:p=1 $r support
506 301 -7.874 (514 -516 518 525 -526 -519 528):(514 -516 519 -524 520 &
  -521 -523 -522 528) imp:n=1 imp:p=1 $left support cap
507 301 -7.874 (515 -517 518 525 -526 -519 528):(515 -517 519 -524 520 &
  -521 -523 -522 528) imp:n=1 imp:p=1 $right support cap
508 301 -7.874 529 -516 303 -528 355 imp:n=1 imp:p=1 $left cap ring
509 301 -7.874 -530 515 303 -528 355 imp:n=1 imp:p=1 $right cap ring
510 301 -7.874 -533:(-535 524 -537) imp:n=1 imp:p=1 $left eyelet
511 301 -7.874 -534:(-536 524 -537) imp:n=1 imp:p=1 $right eyelet
512 301 -7.874 507 -540 516 -510 541 538 -539 imp:n=1 imp:p=1 $left flange
513 301 -7.874 507 -540 511 -515 542 538 -539 imp:n=1 imp:p=1 $right flange
c **

c Surface Cards
301  SO 3.048   $Outer surface of source sphere
2  SO 2.7305  $Inner Radius of SS304 Layer
3  PZ 2.3876  $Upper Bound on AmBe Material
4  PZ 0.3175  $Upper Bound on Void Space
```

```
5  PZ -0.3175 $Lower Bound on Void Space
63 C/Y 0 -.83185 1.149349  $leaf spring middle circle outer
64 C/Y -1.12299 .0381 0.35559 $leaf spring left circle outer
65 C/Y 1.12299 .0381 0.35559 $leaf spring right circle outer
66 C/Y 0 -.83185 1.07315  $leaf spring middle circle inner
67 C/Y -1.12299 .0381 0.2794 $leaf spring left circle inner
68 C/Y 1.12299 .0381 0.2794 $leaf spring right circle inner
71 PZ -.15875 $end spring l/r
72 PY -1.27 $edge of width of spring
73 PY 1.27 $edge of width of spring
74 PX -1.12299 $used to treat inner half of small curve different for cutoffs
75 PX 1.12299 $used to treat inner half of small curve different for cutoffs
76 PZ 0.01 $used to fix what 75 does in allowing top of circles
77 p 1 0 -1 .9525
78 p -1 0 -1 .9525
c
c **Fe Sphere **
355  SO 38.1 $outer surface of Fe Sphere
306  SO 500     $Edge of the Universe
302  SO 7.62   $inner void for source
303  CX 4.7625   $constant radius tube from left
304  PY -19.05  $plane to define radius change point in bottom entry
305 CY 5.08   $tube from bottom (smaller radius)
310 CY 6.35   $tube from bottom (larger radius)
307 C/Y 22.86 0 2.54    $tube on right side
308 CY 1.27   $used to define upper half for plug geometries
309 PX 0 $used to stop tubes on left/right of origin
311 PY 0 $used to stop tubes on top/bottom of origin
312 PX -17.5838 $top of shape used to move left plug out due to Cf attachment
313 PX -48.0638 $bottom of left plug cylinder
314 CX 4.25 $smaller left plug
322 SO 100      $100cm Sphere around source
c **
c
c **Fe Stand**
501 PZ -44.1325 $bottom of base plate
502 PZ -41.91 $top of base plate and bot of upper base
503 PY 40.64 $top edge of base plate
504 PY -40.64 $bottom edge of base plate
505 PX -45.72 $left edge of base plate and upper base
506 PX 45.72 $right edge of base plate and upper base
507 PZ -40.3225 $top of upper base
508 PY 17.78 $top edge of upper base
509 PY -17.78 $bot edge of upper base
510 PX -29.36875 $right edge of l upper base
511 PX 29.36875 $left edge of r upper base
512 P 0 -17.78 -40.3225 0 -12.7 0 1 -12.7 0
513 P 0 17.78 -40.3225 0 12.7 0 1 12.7 0
514 PX -41.5925 $left support left edge
515 PX 37.62375 $right support left edge
516 PX -37.62375 $left support right edge
517 PX 41.5925 $right support right edge
518 PZ 0 $supports top edge
519 PZ 1.11125 $cap screw flange top
520 PY -10.16 $cap left vert
521 PY 10.16 $cap right vert
522 P 0 -10.16 3.81 0 -2.8575 12.065 1 -2.8575 12.065 $cap left diagonal
523 P 0 10.16 3.81 0 2.8575 12.065 1 2.8575 12.065 $cap right diagonal
524 PZ 12.065 $cap top
525 PY -12.7 $cap left edge
526 PY 12.7 $cap right edge
c 527 CX 4.683125 $inner radius cap ring {set to match port radius}
528 CX 8.41375 $outer radius cap rin
529 PX -40.16375 $outer edge of left cap ring
530 PX 40.16375 $outer edge of right cap ring
c 531 PX -37.8138 $inner edge of left cap ring {adjusted to fit imperfect sphere}
c 532 PX 37.8138 $inner edge of right cap ring {adjusted to fit imperfect sphere}
533 TX -39.60813 0 15.5575 2.420938 .595313 .595313 $left eyelet
534 TX 39.60813 0 15.5575 2.420938 .595313 .595313 $right eyelet
```

```
535 C/Z -39.60813 0 .79375 $left eyelet connector walls
536 C/Z 39.60813 0 .79375 $right eyelet connector walls
537 PZ 12.7 $eyelet connector top cutoff
538 PY -.635 $bottom edge of flagnes
539 PY .635 $top edge of flanges
540 PZ -8.41375 $top of flanges (tapered completely off)
541 P -29.36875 0 -40.3225 -37.62375 0 -8.41375 -37.62375 1 -8.41375
542 P 29.36875 0 -40.3225 37.62375 0 -8.41375 37.62375 1 -8.41375
c **
c  The next set of planes will be used to segment surface 22 to do the angular
c  dependent tally.  They do not have to be used in the cell descriptions.
c
324 PZ 98.7688340595138
325 PZ 95.1056516295154
326 PZ 89.1006524188368
327 PZ 80.9016994374947
328 PZ 70.7106781186548
329 PZ 58.7785252292473
330 PZ 45.3990499739547
331 PZ 30.9016994374947
332 PZ 15.6434465040231
333 PZ 0
334 PZ -15.6434465040231
335 PZ -30.9016994374947
336 PZ -45.3990499739547
337 PZ -58.7785252292473
338 PZ -70.7106781186547
339 PZ -80.9016994374947
340 PZ -89.1006524188368
341 PZ -95.1056516295154
342 PZ -98.7688340595138
c **

c Material Cards
m1 95241.66c -.2 4009.62c -.8 $AmBe
c SS304
m2 6000 -.0008 14000 -.01 15031 -.00045 24000 -.19 &
   25055.61c -.02 26000 -.68375 28000 -.095
c ** Fe Sphere **
m301 26000. -.99283 6000 -.0021 25055.61c -.0047 &
   15031 -.00013 16000 -.00024
c **
m304 7014 -.7558 8016 -.2314 18000 -.0128 $air
c **
c
c Source
sdef par=1 erg=d1  RAD=D2  CEL=1
c
SI1   4.14e-7  0.11  0.166  0.224  0.302  0.369   0.45   0.55         &
      0.672  0.821   1.003  1.108  1.225  1.353  1.496  1.653   1.827 &
      2.019  2.123   2.231  2.346  2.466  2.592  2.725  2.865   3.012 &
      3.166  3.329   3.499  3.679  3.867  4.066  4.274  4.493   4.724 &
      4.966  5.221   5.488  5.627  5.770  5.916  6.065  6.219   6.376 &
      6.538  6.703   6.873  7.047  7.225  7.408  7.596  7.788   7.985 &
      8.187  8.395   8.607  8.825  9.048  9.277  9.512  9.753   10.0  &
     10.253 10.513  10.779 11.052 11.331
c
sp1  0 .014036  .006889  .007264  .009769  .008391  .010163  .012457  &
       .015032  .016573  .017775  .00844   .00773   .006091  .006321  &
       .006287  .006968  .011401  .00702   .00804   .0099    .012154  &
       .013445  .015515  .018104  .021269  .023188  .0267    .0324    &
       .0337    .029836  .031177  .034159  .036369  .038848  .037056  &
       .038803  .037562  .017426  .0172    .01537   .013832  .013948  &
       .013378  .013805  .014282  .014806  .014082  .011839  .012698  &
       .014484  .01617   .01612   .014402  .013867  .012271  .014014  &
       .006684  .004591  .005624  .007721  .008642  .007526  .006221  &
       .00401   .001699  .00033
sb1 0 1 65R
c
```

```
SI2  0.0   2.7305
SP2  -21 2
c
c Tallies
F2:N  322
FC2  Neutron Flux
FS2 -334 -332 T $plus/minus 15.6cm cutoffs
c Current Tally of whole sphere
F1:N  322
FC1 number of neutrons per spherical surface segments at 100 cm
c Segmented Tally across z plans of the sphere
FS1  -342 -341 -340 -339 -338 -337 -336 -335 -334 -333 -332 -331 &
-330 -329 -328 -327 -326 -325 -324
c
F12:N 322
FC12  Icrp 74 ambient dose equivalent on spherical surface at 100 cm
c Segmented Tally across z plans of the sphere
FS12  -342 -341 -340 -339 -338 -337 -336 -335 -334 -333 -332 -331 &
-330 -329 -328 -327 -326 -325 -324
c
c  gamma fluence tally at 100 cm
F22:P  322
FC22  Gamma Ray Fluence induced by neutrons at 100 cm
FS22 -334 -332 T $plus/minus 15.6cm cutoffs
c
F32:P   322
FC32  Gamma Ray Dose rate at 100 cm
FS32 -334 -332 T $plus/minus 15.6cm cutoffs
c
F5:N -100.0001 0 0 .1
FC5 Point Neutron Detector at 100cm
c
F25:N -100.0001 0 0 .1
FC25 ICRP 74 ambient dose equivalent on Point Neutron Detector at 100cm
c Energy groups used to bin fluence
e1   1.00E-09   2.15E-09   4.64E-09   1.00E-08   2.15E-08   4.64E-08
     1.00E-07   2.15E-07   4.64E-07   1.00E-06   2.15E-06   4.64E-06
     1.00E-05   2.15E-05   4.64E-05   1.00E-04   2.15E-04   4.64E-04
     1.00E-03   2.15E-03   4.64E-03   1.00E-02   1.25E-02   1.58E-02
     1.99E-02   2.51E-02   3.16E-02   3.98E-02   5.01E-02   6.30E-02
     7.94E-02   1.00E-01   1.25E-01   1.58E-01   1.99E-01   2.51E-01
     3.16E-01   3.98E-01   5.01E-01   6.30E-01   7.94E-01   1.00E+00
     1.25E+00   1.58E+00   1.99E+00   2.51E+00   3.16E+00   3.98E+00
     5.01E+00   6.30E+00   7.94E+00   1.00E+01   1.15E+01   25.
c
e2   1.00E-09   2.15E-09   4.64E-09   1.00E-08   2.15E-08   4.64E-08
     1.00E-07   2.15E-07   4.64E-07   1.00E-06   2.15E-06   4.64E-06
     1.00E-05   2.15E-05   4.64E-05   1.00E-04   2.15E-04   4.64E-04
     1.00E-03   2.15E-03   4.64E-03   1.00E-02   1.25E-02   1.58E-02
     1.99E-02   2.51E-02   3.16E-02   3.98E-02   5.01E-02   6.30E-02
     7.94E-02   1.00E-01   1.25E-01   1.58E-01   1.99E-01   2.51E-01
     3.16E-01   3.98E-01   5.01E-01   6.30E-01   7.94E-01   1.00E+00
     1.25E+00   1.58E+00   1.99E+00   2.51E+00   3.16E+00   3.98E+00
     5.01E+00   6.30E+00   7.94E+00   1.00E+01   1.15E+01   25.
c
e5   1.00E-09   2.15E-09   4.64E-09   1.00E-08   2.15E-08   4.64E-08
     1.00E-07   2.15E-07   4.64E-07   1.00E-06   2.15E-06   4.64E-06
     1.00E-05   2.15E-05   4.64E-05   1.00E-04   2.15E-04   4.64E-04
     1.00E-03   2.15E-03   4.64E-03   1.00E-02   1.25E-02   1.58E-02
     1.99E-02   2.51E-02   3.16E-02   3.98E-02   5.01E-02   6.30E-02
     7.94E-02   1.00E-01   1.25E-01   1.58E-01   1.99E-01   2.51E-01
     3.16E-01   3.98E-01   5.01E-01   6.30E-01   7.94E-01   1.00E+00
     1.25E+00   1.58E+00   1.99E+00   2.51E+00   3.16E+00   3.98E+00
     5.01E+00   6.30E+00   7.94E+00   1.00E+01   1.15E+01   25.
c
e12   1.00E-09   2.15E-09   4.64E-09   1.00E-08   2.15E-08   4.64E-08
     1.00E-07   2.15E-07   4.64E-07   1.00E-06   2.15E-06   4.64E-06
     1.00E-05   2.15E-05   4.64E-05   1.00E-04   2.15E-04   4.64E-04
     1.00E-03   2.15E-03   4.64E-03   1.00E-02   1.25E-02   1.58E-02
```

```
     1.99E-02   2.51E-02   3.16E-02   3.98E-02   5.01E-02   6.30E-02
     7.94E-02   1.00E-01   1.25E-01   1.58E-01   1.99E-01   2.51E-01
     3.16E-01   3.98E-01   5.01E-01   6.30E-01   7.94E-01   1.00E+00
     1.25E+00   1.58E+00   1.99E+00   2.51E+00   3.16E+00   3.98E+00
     5.01E+00   6.30E+00   7.94E+00   1.00E+01   1.15E+01   25.
c
e25   1.00E-09   2.15E-09   4.64E-09   1.00E-08   2.15E-08   4.64E-08
     1.00E-07   2.15E-07   4.64E-07   1.00E-06   2.15E-06   4.64E-06
     1.00E-05   2.15E-05   4.64E-05   1.00E-04   2.15E-04   4.64E-04
     1.00E-03   2.15E-03   4.64E-03   1.00E-02   1.25E-02   1.58E-02
     1.99E-02   2.51E-02   3.16E-02   3.98E-02   5.01E-02   6.30E-02
     7.94E-02   1.00E-01   1.25E-01   1.58E-01   1.99E-01   2.51E-01
     3.16E-01   3.98E-01   5.01E-01   6.30E-01   7.94E-01   1.00E+00
     1.25E+00   1.58E+00   1.99E+00   2.51E+00   3.16E+00   3.98E+00
     5.01E+00   6.30E+00   7.94E+00   1.00E+01   1.15E+01   25.
c
c  for gammas
e22  0.01   0.015   0.02   0.03   0.04   0.05   0.06   0.08   0.1
     0.15   0.2      0.3    0.4    0.5    0.6    0.8     1.   1.5
       2.    3.       4.     5.     6.     8.   10.0    12.    15.
c
c  ICRP 74 Dose Conversion coeffients
DE12  1.00E-09  1.00E-08  2.53E-08  1.00E-07  2.00E-07  5.00E-07
      1.00E-06  2.00E-06  5.00E-06  1.00E-05  2.00E-05  5.00E-05
      1.00E-04  2.00E-04  5.00E-04  1.00E-03  2.00E-03  5.00E-03
      1.00E-02  2.00E-02  3.00E-02  5.00E-02  7.00E-02  1.00E-01
      1.50E-01  2.00E-01  3.00E-01  5.00E-01  7.00E-01  9.00E-01
      1.00E+00  1.20E+00  2.00E+00  3.00E+00  4.00E+00  5.00E+00
      6.00E+00  7.00E+00  8.00E+00  9.00E+00  1.00E+01  1.20E+01
      1.40E+01  1.50E+01  1.60E+01  1.80E+01  2.00E+01  3.00E+01
      5.00E+01  7.50E+01  1.00E+02  1.25E+02  1.50E+02  1.75E+02
      2.01E+02
c
DF12  6.6  9   10.6  12.9  13.5  13.6  13.3  12.9   12   11.3  10.6
      9.9  9.4  8.9   8.3   7.9   7.7     8  10.5  16.6  23.7  41.1
       60   88  132   170   233   322   375   400   416   425   420
      412  408  405   400   405   409   420   440   480   520   540
      555  570  600   515   400   330   285   260   245   250   260
c
c  ICRP 74 Dose Conversion coeffients
DE25  1.00E-09  1.00E-08  2.53E-08  1.00E-07  2.00E-07  5.00E-07
      1.00E-06  2.00E-06  5.00E-06  1.00E-05  2.00E-05  5.00E-05
      1.00E-04  2.00E-04  5.00E-04  1.00E-03  2.00E-03  5.00E-03
      1.00E-02  2.00E-02  3.00E-02  5.00E-02  7.00E-02  1.00E-01
      1.50E-01  2.00E-01  3.00E-01  5.00E-01  7.00E-01  9.00E-01
      1.00E+00  1.20E+00  2.00E+00  3.00E+00  4.00E+00  5.00E+00
      6.00E+00  7.00E+00  8.00E+00  9.00E+00  1.00E+01  1.20E+01
      1.40E+01  1.50E+01  1.60E+01  1.80E+01  2.00E+01  3.00E+01
      5.00E+01  7.50E+01  1.00E+02  1.25E+02  1.50E+02  1.75E+02
      2.01E+02
c
DF25  6.6  9   10.6  12.9  13.5  13.6  13.3  12.9   12   11.3  10.6
      9.9  9.4  8.9   8.3   7.9   7.7     8  10.5  16.6  23.7  41.1
       60   88  132   170   233   322   375   400   416   425   420
      412  408  405   400   405   409   420   440   480   520   540
      555  570  600   515   400   330   285   260   245   250   260
c
c ICRP 74 DCCs for photons (pSv-cm2)
de32  0.01   0.015   0.02   0.03   0.04   0.05   0.06   0.08   0.1
     0.15   0.2      0.3    0.4    0.5    0.6    0.8     1.   1.5
       2.    3.       4.     5.     6.     8.   10.0
df32   0.061   0.83   1.05   0.81   0.64   0.55   0.51   0.53  0.61
       0.89    1.2    1.8    2.38   2.93   3.44   4.38    5.2   6.9
        8.6   11.1   13.4    15.5   17.6   21.6   25.6
c
mode n p
CUT:N  1J  1.e-10
CUT:P  1J   0.01
nps 1E7
```

B.12 AmBe in Tantalum MCNP Input

```
AmBe in 12 cm r Ta sphere
c Cell Cards
1 1 -1.214 (-2 -3 4):(-2 -5) imp:n=1 imp:p=1 $AmBe Source Region
2 0 -2 -4 5 #((72 -73 -63 66 -78 -77 5):&
(72 -73 67 -64 78 74 -76):(72 -73 67 -64 78 -71 -74):&
(72 -73 68 -65 77 -75):(72 -73 68 -65 75 -71)) imp:n=1 imp:p=1 $void spring area
3 2 -7.94 (-1 2):(3 -1)      imp:n=1 imp:p=1 $SS304 Shell
c leaf spring - center:left:far left:right:far right
60 2 -7.94 (72 -73 -63 66 -78 -77 5):(72 -73 67 -64 78 74 -76):&
(72 -73 67 -64 78 -71 -74):(72 -73 68 -65 77 -75):&
(72 -73 68 -65 75 -71) imp:n=1 imp:p=1
c ** Ta Sphere **
304 304 -1.24e-3 (307 -322 #((316 -312 314 -313):(312 -311 310 -313):&
(-317 318 -360 361 313 -312 315):&
(-317 318 -312 315 -320):&
(-317 318 -312 315 -319):(-501 502 503 -504 505 -506):&
((-501 531 513 515 -503 -525):(-501 531 503 515 -523 -505))&
:((-501 531 524 -514 515 -505):(-501 531 504 -514 515 -525))&
:((-501 531 513 -516 -503 526):(-501 531 503 -516 -523 506))&
:((-501 531 524 -514 -516 506):(-501 531 504 -514 -516 526))&
:((-531 543 545 -503 -525):(-531 503 545 -523 -505))&
:((-531 524 -544 545 -505):(-531 504 -544 545 -525))&
:((-531 543 -546 -503 526):(-531 503 -546 -523 506))&
:((-531 524 -544 -546 506):(-531 504 -544 -546 526))&
:((501 -553 551 -552))&
))&
:(-308 #(310 -313 -311 312) &
#(314 -313 -312 315)):-309 &
 imp:n=1   imp:p=1 $air from Ta surface to tally sphere
305 304 -1.24e-3 322 -306   imp:n=1 imp:p=1 $air from sphere to edge of universe
306 303 -16.69  -307 301 308 309 imp:n=1 imp:p=1 $Ta Sphere
307 0      306                  imp:n=0 imp:p=0 $Void space outside universe
308 305 -2.7 310 -313 -311 312 imp:n=1 imp:p=1 $aluminum ring 1 (in groove)
309 305 -2.7 (314 -313 -312 315):(-317 318 -360 361 313 -312 315):&
(-317 318 -312 315 -320):&
(-317 318 -312 315 -319)  imp:n=1 imp:p=1 $aluminum ring 2
310 305 -2.7 314 -313 -315 316 imp:n=1 imp:p=1 $aluminum ring 3
c * Al table top*
501 305 -2.7 -501 502 503 -504 505 -506 imp:n=1 imp:p=1 $Al table top
511 305 -2.7 (-501 531 513 515 -503 -525):(-501 531 503 515 -523 -505) &
imp:n=1 imp:p=1 $bl leg
512 305 -2.7 (-501 531 524 -514 515 -505):(-501 531 504 -514 515 -525) &
imp:n=1 imp:p=1 $br leg
513 305 -2.7 (-501 531 513 -516 -503 526):(-501 531 503 -516 -523 506) &
imp:n=1 imp:p=1 $tl leg
514 305 -2.7 (-501 531 524 -514 -516 506):(-501 531 504 -514 -516 526) &
imp:n=1 imp:p=1 $tr leg
541 305 -2.7 (-531 -322 543 545 -503 -525):(-531 -322 503 545 -523 -505) &
imp:n=1 imp:p=1 $bl thick leg
542 305 -2.7 (-531 -322 524 -544 545 -505):(-531 -322 504 -544 545 -525) &
imp:n=1 imp:p=1 $br thick leg
543 305 -2.7 (-531 -322 543 -546 -503 526):(-531 -322 503 -546 -523 506) &
imp:n=1 imp:p=1 $tl thick leg
544 305 -2.7 (-531 -322 524 -544 -546 506):(-531 -322 504 -544 -546 526) &
imp:n=1 imp:p=1 $tr thick leg
551 305 -2.7 501 -553 551 -552 imp:n=1 imp:p=1 $Al stabilizer ring
c **

c Surface Cards
1  SO 3.048   $Outer surface of source sphere
2  SO 2.7305  $Inner Radius of SS304 Layer
3  PZ 2.3876  $Upper Bound on AmBe Material
4  PZ 0.3175  $Upper Bound on Void Space
5  PZ -0.3175 $Lower Bound on Void Space
63 C/Y 0 -.83185 1.149349  $leaf spring middle circle outer
64 C/Y -1.12299 .0381 0.35559 $leaf spring left circle outer
```

```
65 C/Y 1.12299 .0381 0.35559 $leaf spring right circle outer
66 C/Y 0 -.83185 1.07315  $leaf spring middle circle inner
67 C/Y -1.12299 .0381 0.2794 $leaf spring left circle inner
68 C/Y 1.12299 .0381 0.2794 $leaf spring right circle inner
71 PZ -.15875 $end spring l/r
72 PY -1.27 $edge of width of spring
73 PY 1.27 $edge of width of spring
74 PX -1.12299 $used to treat inner half of small curve different for cutoffs
75 PX 1.12299 $used to treat inner half of small curve different for cutoffs
76 PZ 0.01 $used to fix what 75 does in allowing top of circles
77 p 1 0 -1 .9525 $diagonal to fit two curves of spring at tangent
78 p -1 0 -1 .9525 $diagonal to fit two curves of spring at tangent
c **Ta Sphere **
301  SO 3.048   $Outer surface of source sphere
306  SO 500     $Edge of the Universe
307  SO 12   $radius of Ta spherical shell
308  tz 0 0 .75 12 .45 .45 $top groove
309  tz 0 0 -.75 12 .45 .45 $bottom groove
322  SO 100     $100cm Sphere around source
310  cz 11.7  $Al ring inner radius in groove
313  cz 14.1  $Al ring outer radius (all)
311  pz .9 $top of Al ring in groove
312  pz .6 $bottom of Al Ring in groove / top of ring 2
314  cz 12.1  $Al ring inner radius (ring 2/3)
315  pz .3 $bottom of ring 2 / top of ring 3
316  pz 0  $bottom of ring 3
317  py 1.9 $top of lift arms
318  py -1.9 $bot of lift arms
319  C/Z -32.7 0 1.9 $l round edge of lift arm
320  C/Z 32.7 0 1.9 $r round edge of lift arm
360  px 32.7 $cutoff of straight part of lift arm
361  px -32.7 $cutoff of straight part of lift arm
c *Al table top*
501  pz -12.0 $top of Al table top
502  pz -12.6 $bot of Al table top
503  px -25.325 $left of Al table top
504  px 25.325 $right of Al table top
505  py -25.325 $front of Al table top
506  py 25.325 $back of Al table top
513  px -25.475 $left of Al table leg
514  px 25.475 $right of Al table leg
515  py -25.475 $front of Al table leg
516  py 25.475 $back of Al table leg
523  px -20.575 $cutoff of Al table top
524  px 20.575 $cutoff of Al table top
525  py -20.575 $cutoff of Al table top
526  py 20.575 $cutoff of Al table top
531  pz -28.6 $bot of thin legs/top of thick legs
543  px -26.075 $left of Al table thick leg
544  px 26.075 $right of Al table thick leg
545  py -26.075 $front of Al table thick leg
546  py 26.075 $back of Al table thick leg
551  cz 6.25 $inner radius of Al stabilizer
552  cz 8.75 $outer radius of Al stabilizer
553  pz -11.35 $top of Al stablizer
c **
c
c  The next set of planes will be used to segment surface 22 to do the angular
c  dependent tally.  They do not have to be used in the cell descriptions.
c
324 PZ 98.7688340595138
325 PZ 95.1056516295154
326 PZ 89.1006524188368
327 PZ 80.9016994374947
328 PZ 70.7106781186548
329 PZ 58.7785252292473
330 PZ 45.3990499739547
331 PZ 30.9016994374947
332 PZ 15.6434465040231
```

```
333 PZ 0
334 PZ -15.6434465040231
335 PZ -30.9016994374947
336 PZ -45.3990499739547
337 PZ -58.7785252292473
338 PZ -70.7106781186547
339 PZ -80.9016994374947
340 PZ -89.1006524188368
341 PZ -95.1056516295154
342 PZ -98.7688340595138
c **

c Material Cards
c
c
m1 95241.66c -.2 4009.62c -.8 $AmBe
c SS304
m2 6000 -.0008 14000 -.01 15031 -.00045 24000 -.19 &
   25055.61c -.02 26000 -.68375 28000 -.095
c ** Ta Sphere **
m303 73181  1.0 $Ta
m305 13027 1.0 $Al
c **
m304 7014 -.7558 8016 -.2314 18000 -.0128 $air
c **
c
c Source
sdef par=1 erg=d1  RAD=D2  CEL=1
c
SI1   4.14e-7  0.11  0.166  0.224  0.302  0.369   0.45   0.55         &
      0.672  0.821   1.003  1.108  1.225  1.353  1.496  1.653   1.827 &
      2.019  2.123   2.231  2.346  2.466  2.592  2.725  2.865   3.012 &
      3.166  3.329   3.499  3.679  3.867  4.066  4.274  4.493   4.724 &
      4.966  5.221   5.488  5.627  5.770  5.916  6.065  6.219   6.376 &
      6.538  6.703   6.873  7.047  7.225  7.408  7.596  7.788   7.985 &
      8.187  8.395   8.607  8.825  9.048  9.277  9.512  9.753   10.0  &
     10.253 10.513  10.779 11.052 11.331
c
sp1  0 .014036  .006889  .007264  .009769  .008391  .010163  .012457  &
       .015032  .016573  .017775  .00844   .00773   .006091  .006321  &
       .006287  .006968  .011401  .00702   .00804   .0099    .012154  &
       .013445  .015515  .018104  .021269  .023188  .0267    .0324    &
       .0337    .029836  .031177  .034159  .036369  .038848  .037056  &
       .038803  .037562  .017426  .0172    .01537   .013832  .013948  &
       .013378  .013805  .014282  .014806  .014082  .011839  .012698  &
       .014484  .01617   .01612   .014402  .013867  .012271  .014014  &
       .006684  .004591  .005624  .007721  .008642  .007526  .006221  &
       .00401   .001699  .00033
sb1 0 1 65R
c
SI2  0.0   2.7305
SP2  -21 2
c
c Tallies
F2:N  322
FC2  Neutron Flux
FS2 -334 -332 T $plus/minus 15.6cm cutoffs
c Current Tally of whole sphere
F1:N  322
FC1 number of neutrons per spherical surface segments at 100 cm
c Segmented Tally across z plans of the sphere
FS1  -342 -341 -340 -339 -338 -337 -336 -335 -334 -333 -332 -331 &
-330 -329 -328 -327 -326 -325 -324
c
F12:N 322
FC12  Icrp 74 ambient dose equivalent on spherical surface at 100 cm
c Segmented Tally across z plans of the sphere
FS12  -342 -341 -340 -339 -338 -337 -336 -335 -334 -333 -332 -331 &
-330 -329 -328 -327 -326 -325 -324
```

```
c
c  gamma fluence tally at 100 cm
F22:P  322
FC22  Gamma Ray Fluence induced by neutrons at 100 cm
FS22 -334 -332 T $plus/minus 15.6cm cutoffs
c
F32:P   322
FC32  Gamma Ray Dose rate at 100 cm
FS32 -334 -332 T $plus/minus 15.6cm cutoffs
c
F5:N -100.0001 0 0 .1
FC5 Point Neutron Detector at 100cm
c
F25:N -100.0001 0 0 .1
FC25 ICRP 74 ambient dose equivalent on Point Neutron Detector at 100cm
c Energy groups used to bin fluence
e1   1.00E-09   2.15E-09   4.64E-09   1.00E-08   2.15E-08   4.64E-08
     1.00E-07   2.15E-07   4.64E-07   1.00E-06   2.15E-06   4.64E-06
     1.00E-05   2.15E-05   4.64E-05   1.00E-04   2.15E-04   4.64E-04
     1.00E-03   2.15E-03   4.64E-03   1.00E-02   1.25E-02   1.58E-02
     1.99E-02   2.51E-02   3.16E-02   3.98E-02   5.01E-02   6.30E-02
     7.94E-02   1.00E-01   1.25E-01   1.58E-01   1.99E-01   2.51E-01
     3.16E-01   3.98E-01   5.01E-01   6.30E-01   7.94E-01   1.00E+00
     1.25E+00   1.58E+00   1.99E+00   2.51E+00   3.16E+00   3.98E+00
     5.01E+00   6.30E+00   7.94E+00   1.00E+01   1.15E+01   25.
c
e2   1.00E-09   2.15E-09   4.64E-09   1.00E-08   2.15E-08   4.64E-08
     1.00E-07   2.15E-07   4.64E-07   1.00E-06   2.15E-06   4.64E-06
     1.00E-05   2.15E-05   4.64E-05   1.00E-04   2.15E-04   4.64E-04
     1.00E-03   2.15E-03   4.64E-03   1.00E-02   1.25E-02   1.58E-02
     1.99E-02   2.51E-02   3.16E-02   3.98E-02   5.01E-02   6.30E-02
     7.94E-02   1.00E-01   1.25E-01   1.58E-01   1.99E-01   2.51E-01
     3.16E-01   3.98E-01   5.01E-01   6.30E-01   7.94E-01   1.00E+00
     1.25E+00   1.58E+00   1.99E+00   2.51E+00   3.16E+00   3.98E+00
     5.01E+00   6.30E+00   7.94E+00   1.00E+01   1.15E+01   25.
c
e5   1.00E-09   2.15E-09   4.64E-09   1.00E-08   2.15E-08   4.64E-08
     1.00E-07   2.15E-07   4.64E-07   1.00E-06   2.15E-06   4.64E-06
     1.00E-05   2.15E-05   4.64E-05   1.00E-04   2.15E-04   4.64E-04
     1.00E-03   2.15E-03   4.64E-03   1.00E-02   1.25E-02   1.58E-02
     1.99E-02   2.51E-02   3.16E-02   3.98E-02   5.01E-02   6.30E-02
     7.94E-02   1.00E-01   1.25E-01   1.58E-01   1.99E-01   2.51E-01
     3.16E-01   3.98E-01   5.01E-01   6.30E-01   7.94E-01   1.00E+00
     1.25E+00   1.58E+00   1.99E+00   2.51E+00   3.16E+00   3.98E+00
     5.01E+00   6.30E+00   7.94E+00   1.00E+01   1.15E+01   25.
c
e12   1.00E-09   2.15E-09   4.64E-09   1.00E-08   2.15E-08   4.64E-08
     1.00E-07   2.15E-07   4.64E-07   1.00E-06   2.15E-06   4.64E-06
     1.00E-05   2.15E-05   4.64E-05   1.00E-04   2.15E-04   4.64E-04
     1.00E-03   2.15E-03   4.64E-03   1.00E-02   1.25E-02   1.58E-02
     1.99E-02   2.51E-02   3.16E-02   3.98E-02   5.01E-02   6.30E-02
     7.94E-02   1.00E-01   1.25E-01   1.58E-01   1.99E-01   2.51E-01
     3.16E-01   3.98E-01   5.01E-01   6.30E-01   7.94E-01   1.00E+00
     1.25E+00   1.58E+00   1.99E+00   2.51E+00   3.16E+00   3.98E+00
     5.01E+00   6.30E+00   7.94E+00   1.00E+01   1.15E+01   25.
c
e25   1.00E-09   2.15E-09   4.64E-09   1.00E-08   2.15E-08   4.64E-08
     1.00E-07   2.15E-07   4.64E-07   1.00E-06   2.15E-06   4.64E-06
     1.00E-05   2.15E-05   4.64E-05   1.00E-04   2.15E-04   4.64E-04
     1.00E-03   2.15E-03   4.64E-03   1.00E-02   1.25E-02   1.58E-02
     1.99E-02   2.51E-02   3.16E-02   3.98E-02   5.01E-02   6.30E-02
     7.94E-02   1.00E-01   1.25E-01   1.58E-01   1.99E-01   2.51E-01
     3.16E-01   3.98E-01   5.01E-01   6.30E-01   7.94E-01   1.00E+00
     1.25E+00   1.58E+00   1.99E+00   2.51E+00   3.16E+00   3.98E+00
     5.01E+00   6.30E+00   7.94E+00   1.00E+01   1.15E+01   25.
c
c  for gammas
e22  0.01   0.015   0.02   0.03   0.04   0.05   0.06   0.08   0.1
     0.15   0.2      0.3    0.4    0.5    0.6    0.8     1.   1.5
```

```
       2.    3.       4.     5.     6.     8.   10.0    12.    15.
c
c  ICRP 74 Dose Conversion coeffients
DE12  1.00E-09  1.00E-08  2.53E-08  1.00E-07  2.00E-07  5.00E-07
      1.00E-06  2.00E-06  5.00E-06  1.00E-05  2.00E-05  5.00E-05
      1.00E-04  2.00E-04  5.00E-04  1.00E-03  2.00E-03  5.00E-03
      1.00E-02  2.00E-02  3.00E-02  5.00E-02  7.00E-02  1.00E-01
      1.50E-01  2.00E-01  3.00E-01  5.00E-01  7.00E-01  9.00E-01
      1.00E+00  1.20E+00  2.00E+00  3.00E+00  4.00E+00  5.00E+00
      6.00E+00  7.00E+00  8.00E+00  9.00E+00  1.00E+01  1.20E+01
      1.40E+01  1.50E+01  1.60E+01  1.80E+01  2.00E+01  3.00E+01
      5.00E+01  7.50E+01  1.00E+02  1.25E+02  1.50E+02  1.75E+02
      2.01E+02
c
DF12  6.6  9   10.6  12.9  13.5  13.6  13.3  12.9   12   11.3  10.6
      9.9  9.4  8.9   8.3   7.9   7.7     8  10.5  16.6  23.7  41.1
       60   88  132   170   233   322   375   400   416   425   420
      412  408  405   400   405   409   420   440   480   520   540
      555  570  600   515   400   330   285   260   245   250   260
c
c  ICRP 74 Dose Conversion coeffients
DE25  1.00E-09  1.00E-08  2.53E-08  1.00E-07  2.00E-07  5.00E-07
      1.00E-06  2.00E-06  5.00E-06  1.00E-05  2.00E-05  5.00E-05
      1.00E-04  2.00E-04  5.00E-04  1.00E-03  2.00E-03  5.00E-03
      1.00E-02  2.00E-02  3.00E-02  5.00E-02  7.00E-02  1.00E-01
      1.50E-01  2.00E-01  3.00E-01  5.00E-01  7.00E-01  9.00E-01
      1.00E+00  1.20E+00  2.00E+00  3.00E+00  4.00E+00  5.00E+00
      6.00E+00  7.00E+00  8.00E+00  9.00E+00  1.00E+01  1.20E+01
      1.40E+01  1.50E+01  1.60E+01  1.80E+01  2.00E+01  3.00E+01
      5.00E+01  7.50E+01  1.00E+02  1.25E+02  1.50E+02  1.75E+02
      2.01E+02
c
DF25  6.6  9   10.6  12.9  13.5  13.6  13.3  12.9   12   11.3  10.6
      9.9  9.4  8.9   8.3   7.9   7.7     8  10.5  16.6  23.7  41.1
       60   88  132   170   233   322   375   400   416   425   420
      412  408  405   400   405   409   420   440   480   520   540
      555  570  600   515   400   330   285   260   245   250   260
c
c ICRP 74 DCCs for photons (pSv-cm2)
de32  0.01   0.015   0.02   0.03   0.04   0.05   0.06   0.08   0.1
     0.15   0.2      0.3    0.4    0.5    0.6    0.8     1.   1.5
       2.    3.       4.     5.     6.     8.   10.0
df32   0.061   0.83   1.05   0.81   0.64   0.55   0.51   0.53  0.61
       0.89    1.2    1.8    2.38   2.93   3.44   4.38    5.2   6.9
        8.6   11.1   13.4    15.5   17.6   21.6   25.6
c
mode n p
CUT:N  1J  1.e-10
CUT:P  1J   0.01
nps 1E7
```

APPENDIX C: COMPARISON OF ^{252}Cf SOURCE SPECTRA WITH AND WITHOUT STYROFOAM SPHERE

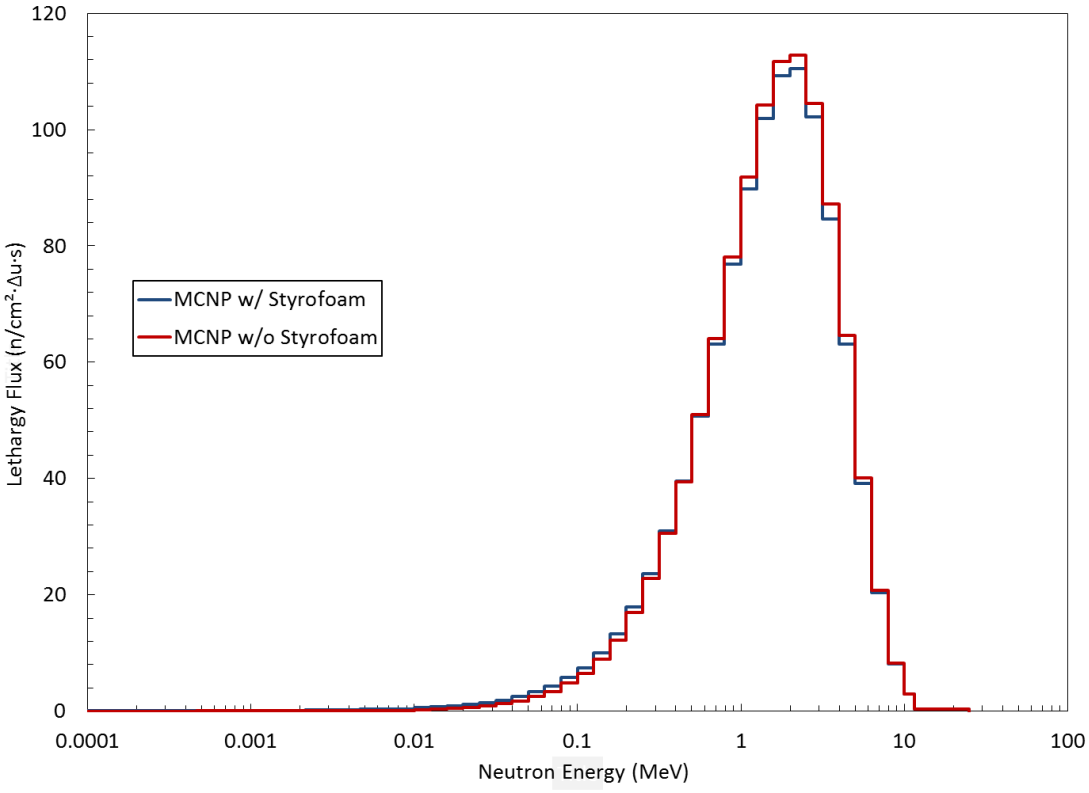

Figure C.1. Comparison of ^{252}Cf Source Spectra from MCNP with and without Styrofoam Sphere

APPENDIX D: ISO 8529 NEUTRON FLUENCE SPECTRA FOR SOURCES

Table D.1. Values of neutron fluence at 1 meter per logarithmic energy interval for a ^{252}Cf spontaneous fission source (derived from Table A.1 of reference [22])

Energy Bin top (MeV)	neutrons/cm^2/s/lethargy
4.14E-07	
1.00E-02	1.07E-02
5.00E-02	6.68E-01
1.00E-01	3.02E+00
2.00E-01	8.11E+00
2.50E-01	1.47E+01
3.00E-01	1.92E+01
4.00E-01	2.61E+01
5.00E-01	3.56E+01
6.00E-01	4.48E+01
7.00E-01	5.38E+01
8.00E-01	6.21E+01
1.00E+00	7.33E+01
1.20E+00	8.60E+01
1.40E+00	9.62E+01
1.50E+00	1.02E+02
1.60E+00	1.05E+02
1.80E+00	1.09E+02
2.00E+00	1.12E+02
2.20E+00	1.13E+02
2.30E+00	1.12E+02
2.40E+00	1.12E+02
2.60E+00	1.10E+02
2.80E+00	1.08E+02
3.00E+00	1.04E+02
3.40E+00	9.77E+01
3.70E+00	8.92E+01
4.20E+00	7.92E+01
4.60E+00	6.77E+01
5.00E+00	5.82E+01
5.50E+00	4.85E+01
6.00E+00	3.92E+01
6.50E+00	3.12E+01
7.00E+00	2.46E+01
7.50E+00	1.93E+01
8.00E+00	1.50E+01
8.50E+00	1.16E+01

Table D.1. Continued

9.00E+00	8.89E+00
9.50E+00	6.80E+00
1.00E+01	5.19E+00
1.10E+01	3.46E+00
1.20E+01	1.96E+00
1.30E+01	1.10E+00
1.40E+01	6.09E-01
1.60E+01	2.58E-01
1.80E+01	7.80E-02

Table D.2. Values of neutron fluence at1 meter per logarithmic energy interval for an AmBe (α, n) source (derived from Table A.1 of reference [22])

Energy Bin top (MeV)	neutrons/cm^2/s/lethargy
4.14E-07	0
1.10E-01	1.15E-03
3.30E-01	3.04E-02
5.40E-01	6.35E-02
7.50E-01	8.56E-02
9.70E-01	9.72E-02
1.18E+00	1.09E-01
1.40E+00	1.16E-01
1.61E+00	1.25E-01
1.82E+00	1.57E-01
2.04E+00	1.95E-01
2.25E+00	2.19E-01
2.47E+00	2.41E-01
2.68E+00	2.79E-01
2.90E+00	3.74E-01
3.11E+00	5.09E-01
3.32E+00	5.64E-01
3.54E+00	5.39E-01
3.75E+00	5.32E-01
3.97E+00	5.26E-01
4.18E+00	5.22E-01
4.39E+00	5.84E-01
4.61E+00	6.50E-01
4.82E+00	6.90E-01
5.04E+00	7.47E-01

Table D.2. Continued

5.25E+00	7.45E-01
5.47E+00	6.67E-01
5.68E+00	6.19E-01
5.89E+00	5.67E-01
6.11E+00	4.95E-01
6.32E+00	5.23E-01
6.54E+00	5.96E-01
6.75E+00	5.79E-01
6.96E+00	5.32E-01
7.18E+00	5.39E-01
7.39E+00	5.83E-01
7.61E+00	6.42E-01
7.82E+00	6.75E-01
8.03E+00	6.37E-01
8.25E+00	5.31E-01
8.46E+00	3.85E-01
8.68E+00	2.54E-01
8.89E+00	1.78E-01
9.11E+00	1.50E-01
9.32E+00	1.67E-01
9.53E+00	2.27E-01
9.75E+00	2.74E-01
9.96E+00	2.59E-01
1.02E+01	2.14E-01
1.04E+01	1.81E-01
1.06E+01	1.39E-01
1.08E+01	7.37E-02
1.10E+01	1.89E-02
1.11E+01	0.00E+00

APPENDIX E: SAMPLE BUMS OUTPUT WITH REMARKS

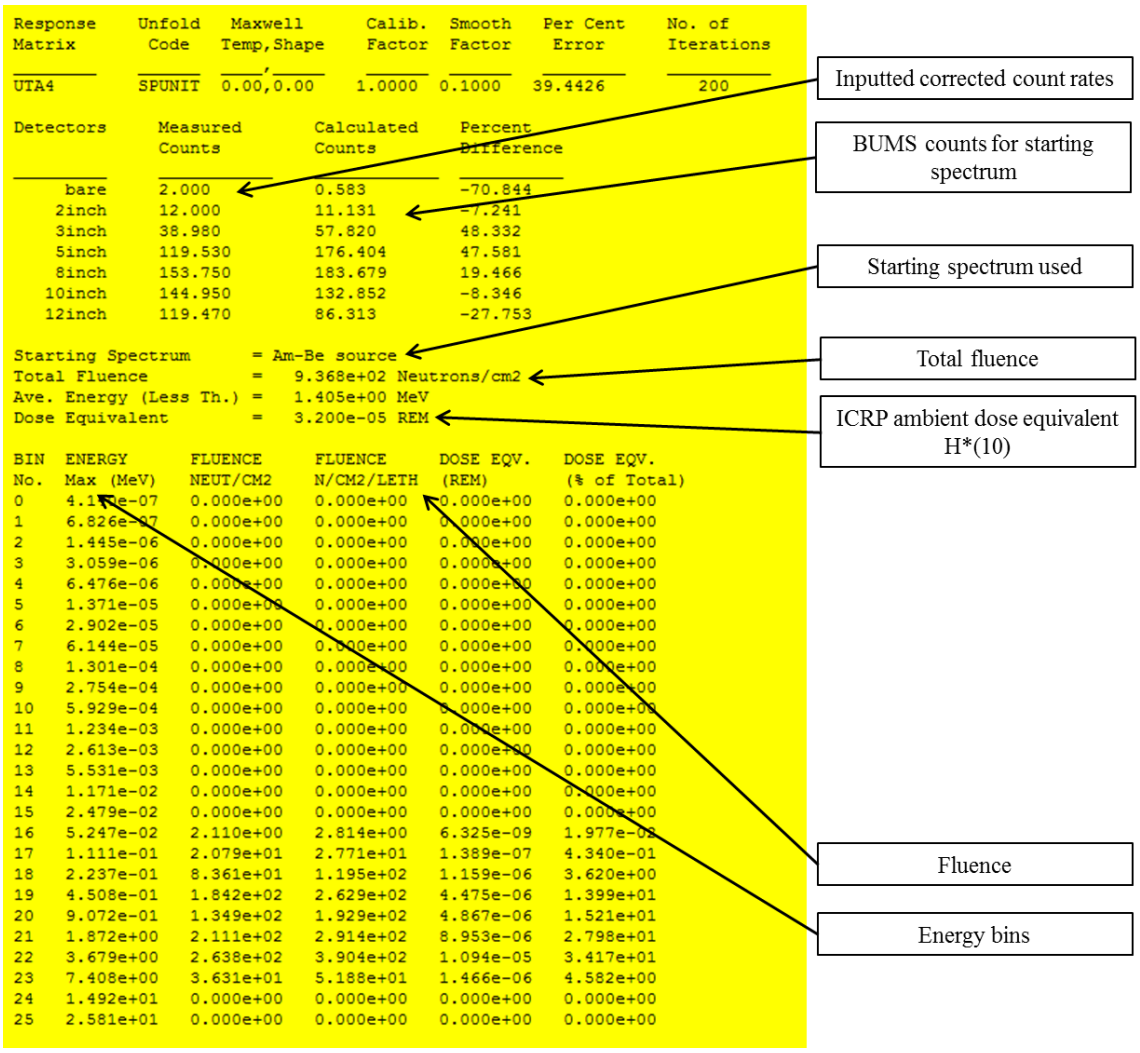

Figure E.1. Sample BUMS output with remarks

APPENDIX F: SAMPLE OUTPUT TALLIES

F.1 Sample F2 (Neutron Fluence) Tally

```
{Excerpt from AmBe Bare MCNP output file}
surface  322
 segment:         334     -332
      energy
    1.0000E-09   0.00000E+00 0.0000
    2.1500E-09   0.00000E+00 0.0000
    4.6400E-09   0.00000E+00 0.0000
    1.0000E-08   0.00000E+00 0.0000
    2.1500E-08   0.00000E+00 0.0000
    4.6400E-08   0.00000E+00 0.0000
    1.0000E-07   0.00000E+00 0.0000
    2.1500E-07   0.00000E+00 0.0000
    4.6400E-07   0.00000E+00 0.0000
    1.0000E-06   0.00000E+00 0.0000
    2.1500E-06   0.00000E+00 0.0000
    4.6400E-06   0.00000E+00 0.0000
    1.0000E-05   0.00000E+00 0.0000
    2.1500E-05   0.00000E+00 0.0000
    4.6400E-05   0.00000E+00 0.0000
    1.0000E-04   0.00000E+00 0.0000
    2.1500E-04   1.01344E-11 0.7071
    4.6400E-04   6.95978E-11 0.2616
    1.0000E-03   1.48432E-10 0.1795
    2.1500E-03   5.23023E-10 0.0996
    4.6400E-03   1.56122E-09 0.0564
    1.0000E-02   5.42431E-09 0.0305
    1.2500E-02   3.32450E-09 0.0391
    1.5800E-02   4.79223E-09 0.0327
    1.9900E-02   6.78534E-09 0.0274
    2.5100E-02   1.02209E-08 0.0225
    3.1600E-02   1.55049E-08 0.0184
    3.9800E-02   2.61075E-08 0.0144
    5.0100E-02   2.72009E-08 0.0138
    6.3000E-02   4.48539E-08 0.0124
    7.9400E-02   5.88812E-08 0.0094
    1.0000E-01   7.90740E-08 0.0082
    1.2500E-01   1.04913E-07 0.0073
    1.5800E-01   1.49662E-07 0.0061
    1.9900E-01   2.00605E-07 0.0051
    2.5100E-01   2.75011E-07 0.0044
    3.1600E-01   3.54101E-07 0.0039
    3.9800E-01   4.58426E-07 0.0034
    5.0100E-01   5.70311E-07 0.0030
    6.3000E-01   7.87818E-07 0.0026
    7.9400E-01   8.93573E-07 0.0024
    1.0000E+00   9.15157E-07 0.0024
    1.2500E+00   9.55212E-07 0.0023
    1.5800E+00   9.69974E-07 0.0023
    1.9900E+00   8.65569E-07 0.0024
    2.5100E+00   7.21112E-07 0.0027
    3.1600E+00   5.33208E-07 0.0031
    3.9800E+00   3.66648E-07 0.0037
    5.0100E+00   2.24636E-07 0.0048
    6.3000E+00   1.30754E-07 0.0062
    7.9400E+00   6.73557E-08 0.0087
    1.0000E+01   2.67923E-08 0.0138
    1.1500E+01   5.85584E-09 0.0295
    2.5000E+01   3.35901E-09 0.0389
      total      9.86454E-06 0.0007
```

F.2 Sample F12 (ICRP 74 ambient dose equivalent H*(10)) Tally

```
{Excerpt from AmBe Bare MCNP output file}
surface  322
 segment:         342      341      340      339      338      337      336      335
334      333     -332
      energy
    1.0000E-09   0.00000E+00 0.0000
    2.1500E-09   0.00000E+00 0.0000
    4.6400E-09   0.00000E+00 0.0000
    1.0000E-08   0.00000E+00 0.0000
    2.1500E-08   0.00000E+00 0.0000
    4.6400E-08   0.00000E+00 0.0000
    1.0000E-07   0.00000E+00 0.0000
    2.1500E-07   0.00000E+00 0.0000
    4.6400E-07   0.00000E+00 0.0000
    1.0000E-06   0.00000E+00 0.0000
    2.1500E-06   0.00000E+00 0.0000
    4.6400E-06   0.00000E+00 0.0000
    1.0000E-05   0.00000E+00 0.0000
    2.1500E-05   0.00000E+00 0.0000
    4.6400E-05   0.00000E+00 0.0000
    1.0000E-04   0.00000E+00 0.0000
    2.1500E-04   9.30255E-11 1.0000
    4.6400E-04   6.90222E-10 0.3393
    1.0000E-03   1.01137E-09 0.2721
    2.1500E-03   3.82564E-09 0.1411
    4.6400E-03   1.23367E-08 0.0796
    1.0000E-02   5.46453E-08 0.0419
    1.2500E-02   4.11049E-08 0.0533
    1.5800E-02   6.49023E-08 0.0457
    1.9900E-02   1.11627E-07 0.0378
    2.5100E-02   2.00413E-07 0.0307
    3.1600E-02   3.72710E-07 0.0253
    3.9800E-02   7.91349E-07 0.0195
    5.0100E-02   1.06610E-06 0.0189
    6.3000E-02   2.22850E-06 0.0161
    7.9400E-02   3.73288E-06 0.0130
    1.0000E-01   6.50958E-06 0.0112
    1.2500E-01   1.08471E-05 0.0097
    1.5800E-01   1.96937E-05 0.0087
    1.9900E-01   3.30258E-05 0.0070
    2.5100E-01   5.43329E-05 0.0059
    3.1600E-01   8.48796E-05 0.0052
    3.9800E-01   1.27665E-04 0.0046
    5.0100E-01   1.86661E-04 0.0041
    6.3000E-01   2.88312E-04 0.0035
    7.9400E-01   3.64384E-04 0.0033
    1.0000E+00   4.04666E-04 0.0032
    1.2500E+00   4.48745E-04 0.0031
    1.5800E+00   4.66696E-04 0.0031
    1.9900E+00   4.23384E-04 0.0032
    2.5100E+00   3.59927E-04 0.0034
    3.1600E+00   2.72190E-04 0.0040
    3.9800E+00   1.94292E-04 0.0046
    5.0100E+00   1.23790E-04 0.0058
    6.3000E+00   7.38058E-05 0.0074
    7.9400E+00   3.83732E-05 0.0104
    1.0000E+01   1.60047E-05 0.0163
    1.1500E+01   3.82864E-06 0.0347
    2.5000E+01   2.40510E-06 0.0460
      total      4.01310E-03 0.0009
```

F.3 Sample F15 (Ring detector in –y direction) Tally

```
{Excerpt from AmBe Bare MCNP output file}
1tally  15        nps =    10000000
+                                  Ring detector for neutron fluence in -y direction
```

tally type 5 particle flux at a ring detector. units 1/cm**2
tally for neutrons

detector symmetric about y-axis located at y = 1.00000E+02 with radius = 1.00000E+01

energy		
1.0000E-09	0.00000E+00	0.0000
2.1500E-09	0.00000E+00	0.0000
4.6400E-09	0.00000E+00	0.0000
1.0000E-08	0.00000E+00	0.0000
2.1500E-08	0.00000E+00	0.0000
4.6400E-08	0.00000E+00	0.0000
1.0000E-07	0.00000E+00	0.0000
2.1500E-07	0.00000E+00	0.0000
4.6400E-07	0.00000E+00	0.0000
1.0000E-06	0.00000E+00	0.0000
2.1500E-06	0.00000E+00	0.0000
4.6400E-06	0.00000E+00	0.0000
1.0000E-05	0.00000E+00	0.0000
2.1500E-05	0.00000E+00	0.0000
4.6400E-05	0.00000E+00	0.0000
1.0000E-04	7.10914E-13	0.7225
2.1500E-04	3.97869E-12	0.4260
4.6400E-04	4.14473E-11	0.2274
1.0000E-03	1.31728E-10	0.1366
2.1500E-03	4.75055E-10	0.0813
4.6400E-03	1.48768E-09	0.0397
1.0000E-02	4.97489E-09	0.0230
1.2500E-02	3.15864E-09	0.0265
1.5800E-02	4.54548E-09	0.0212
1.9900E-02	6.13783E-09	0.0182
2.5100E-02	9.58347E-09	0.0225
3.1600E-02	1.44402E-08	0.0142
3.9800E-02	2.36147E-08	0.0158
5.0100E-02	2.46321E-08	0.0091
6.3000E-02	3.95658E-08	0.0073
7.9400E-02	5.35129E-08	0.0065
1.0000E-01	7.33969E-08	0.0066
1.2500E-01	9.58984E-08	0.0047
1.5800E-01	1.36996E-07	0.0049
1.9900E-01	1.83555E-07	0.0039
2.5100E-01	2.52613E-07	0.0051
3.1600E-01	3.26184E-07	0.0026
3.9800E-01	4.21161E-07	0.0023
5.0100E-01	5.28008E-07	0.0021
6.3000E-01	7.29622E-07	0.0017
7.9400E-01	8.28498E-07	0.0016
1.0000E+00	8.56942E-07	0.0015
1.2500E+00	8.93166E-07	0.0015
1.5800E+00	9.09764E-07	0.0015
1.9900E+00	8.25676E-07	0.0018
2.5100E+00	6.90751E-07	0.0021
3.1600E+00	5.22164E-07	0.0034
3.9800E+00	3.61099E-07	0.0036
5.0100E+00	2.26690E-07	0.0048
6.3000E+00	1.31837E-07	0.0060
7.9400E+00	6.91209E-08	0.0082
1.0000E+01	2.69534E-08	0.0130
1.1500E+01	6.07587E-09	0.0294
2.5000E+01	3.38860E-09	0.0403
total	9.28587E-06	0.0005

APPENDIX G: MODERATED SPECTRA PLOTTED AGAINST BARE SOURCE SPECTRA

Appendix notes:

1. The graphs in this appendix show the relative fluence rates for the different source/moderator combinations.
2. In the first graph for each source, all the used source/moderator combinations are plotted together, each normalized so that their area under the curve equaled 1. The idea is to show the shape of each spectra against each other, allowing the reader to see in which energy ranges each source/moderator combination leaks neutrons.
3. The subsequent graphs for each source show each source/moderator combination versus the bare source. This allows the reader to see the energy shift from the original spectrum more clearly.

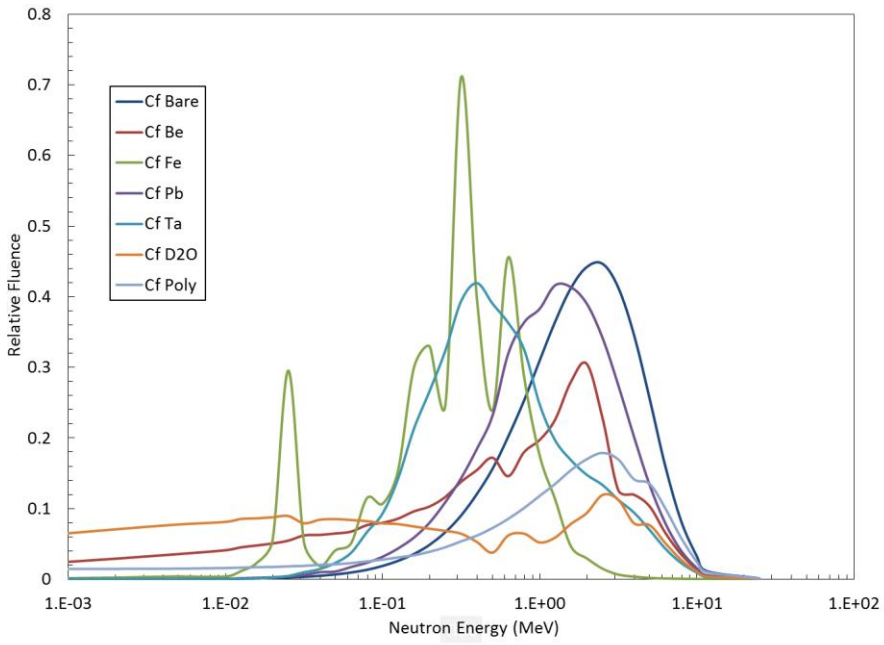

Figure G.1. All ^{252}Cf Spectra, normalized by total flux

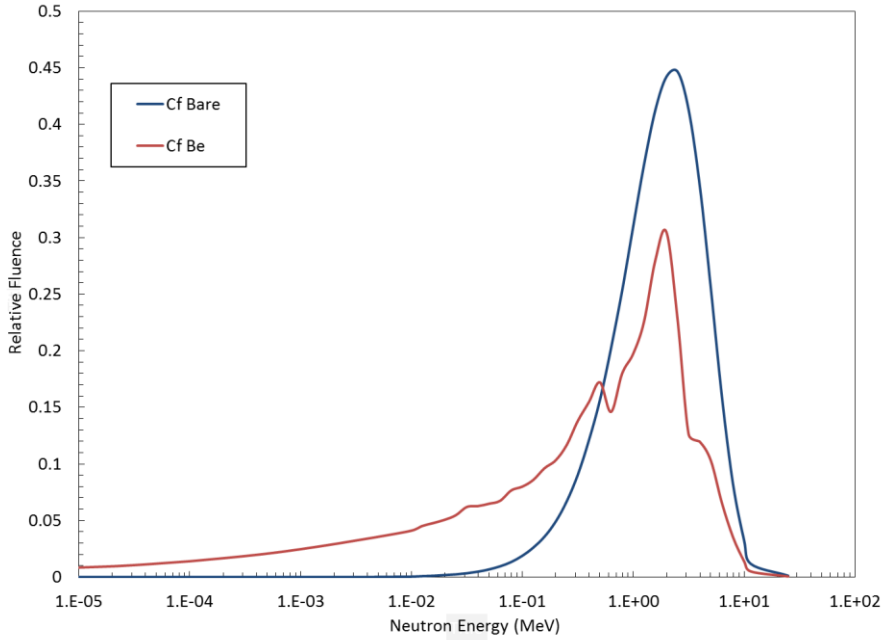

Figure G.1.1. ^{252}Cf in Beryllium and bare source Spectra, normalized by total flux

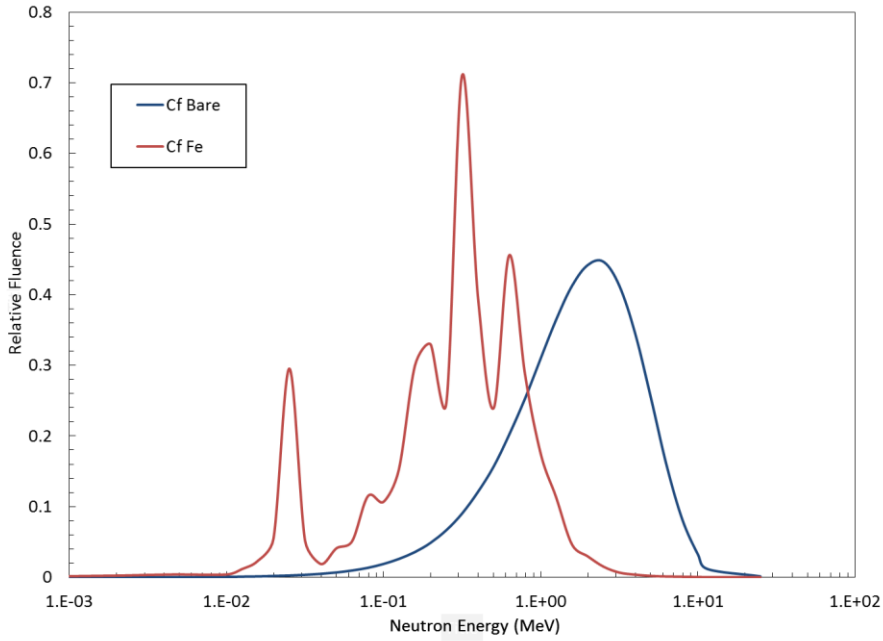

Figure G.1.2. ^{252}Cf in Iron and bare source Spectra, normalized by total flux

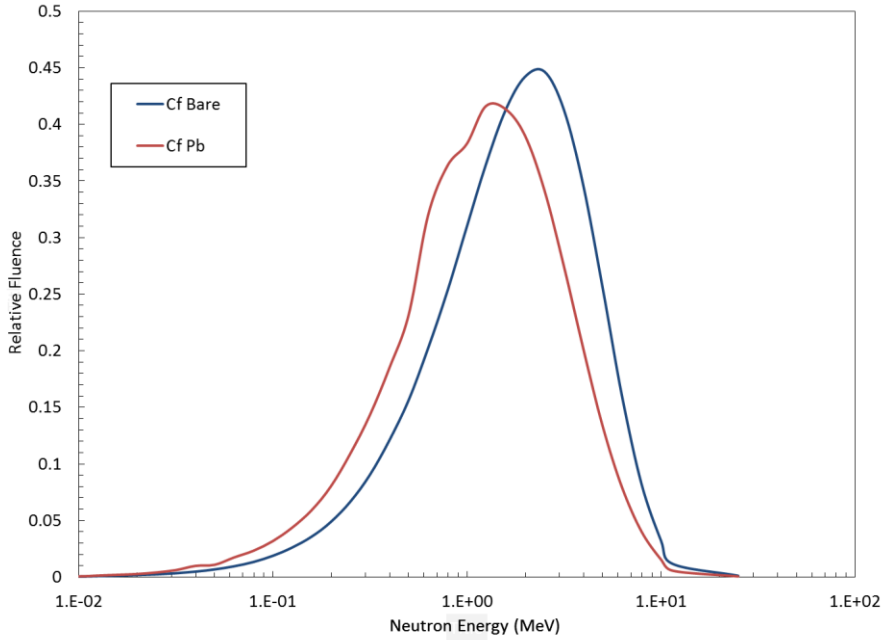

Figure G.1.3. ^{252}Cf in Lead and bare source Spectra, normalized by total flux

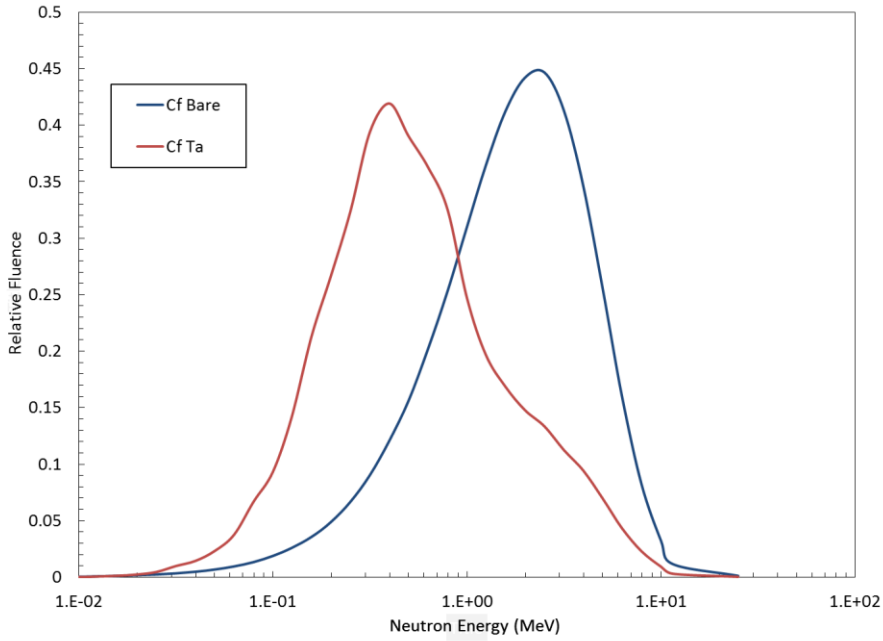

Figure G.1.4. ^{252}Cf in Tantalum and bare source Spectra, normalized by total flux

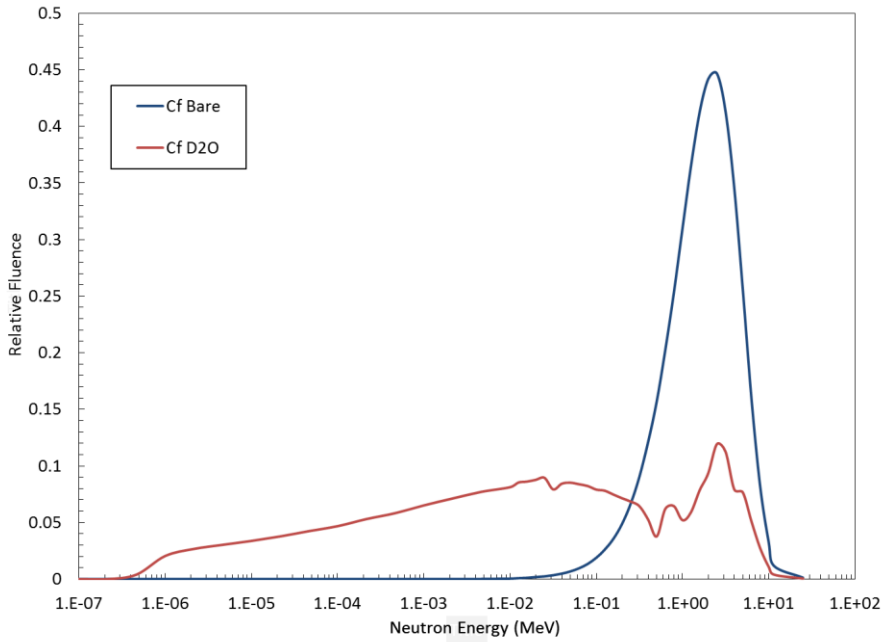

Figure G.1.5. ^{252}Cf in Heavy Water and bare source Spectra, normalized by total flux

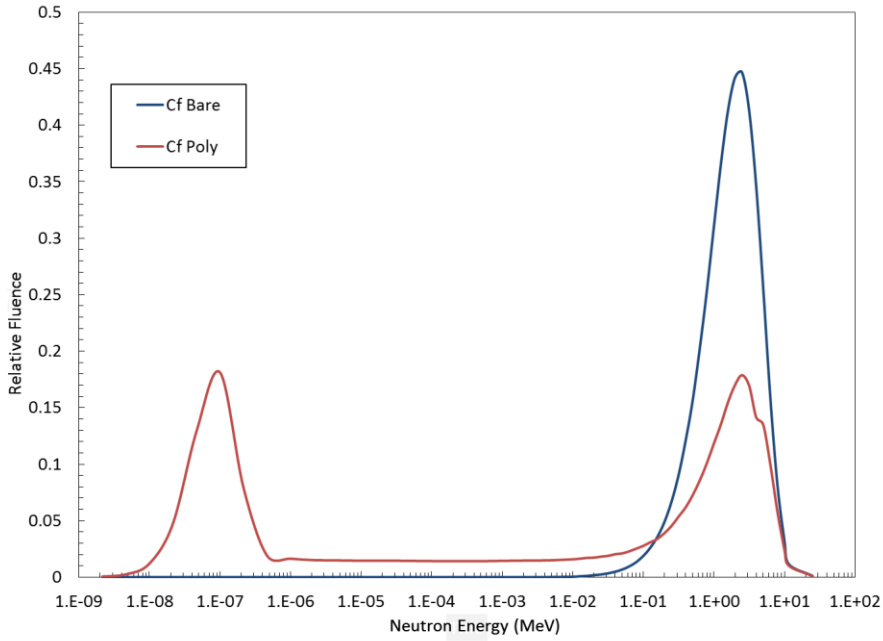

Figure G.1.6. ^{252}Cf in Polyethylene and bare source Spectra, normalized by total flux

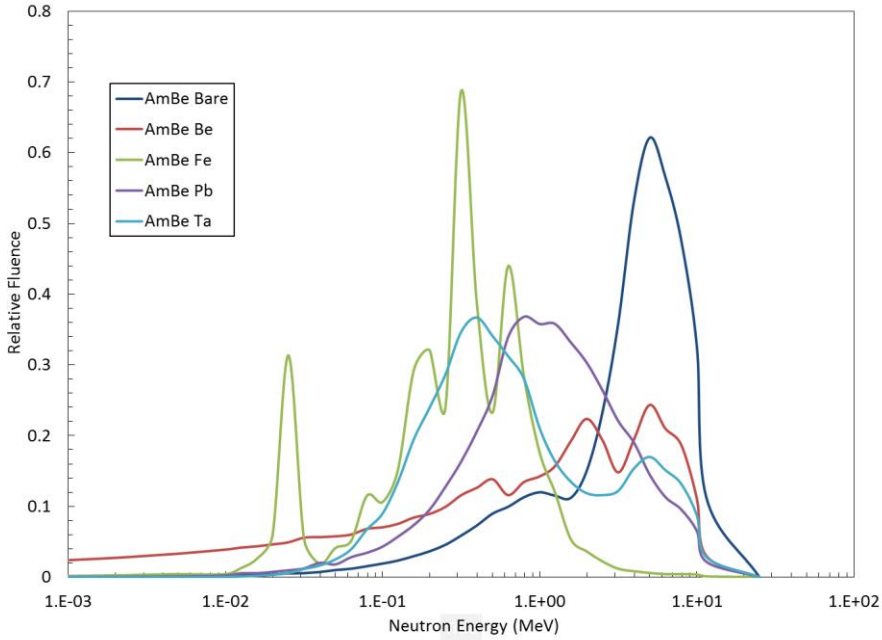

Figure G.2. All AmBe Spectra, normalized by total flux

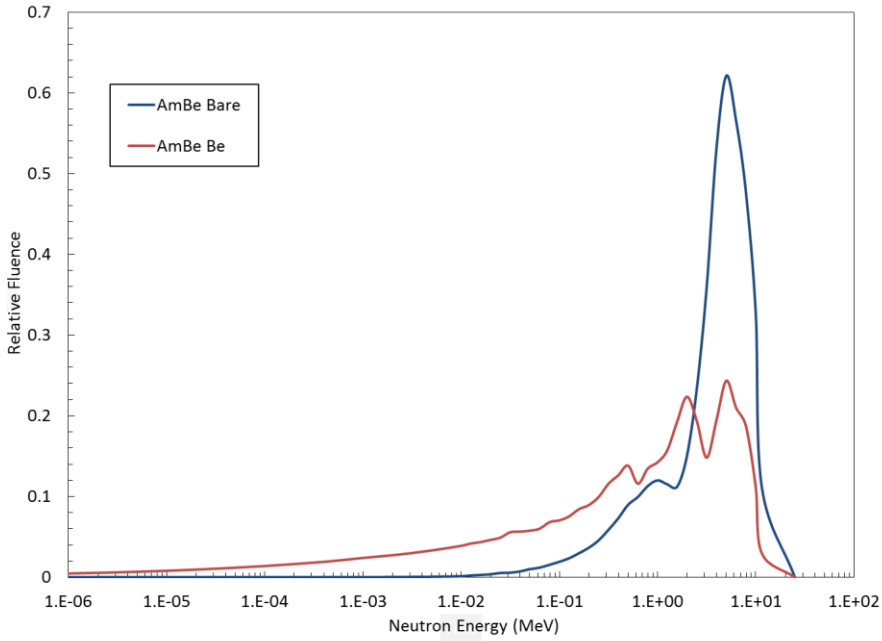

Figure G.2.1. AmBe in Beryllium and bare source Spectra, normalized by total flux

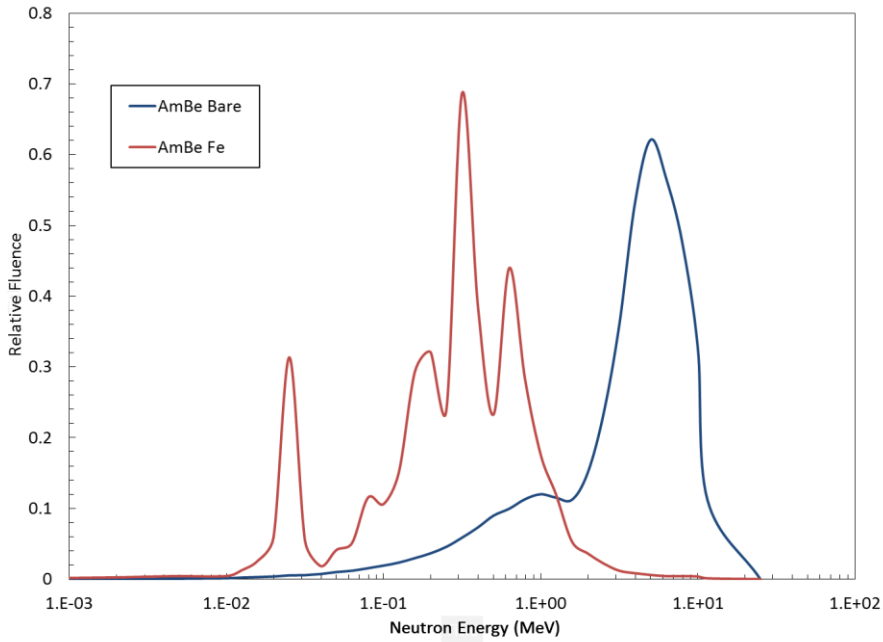

Figure G.2.2. AmBe in Iron and bare source Spectra, normalized by total flux

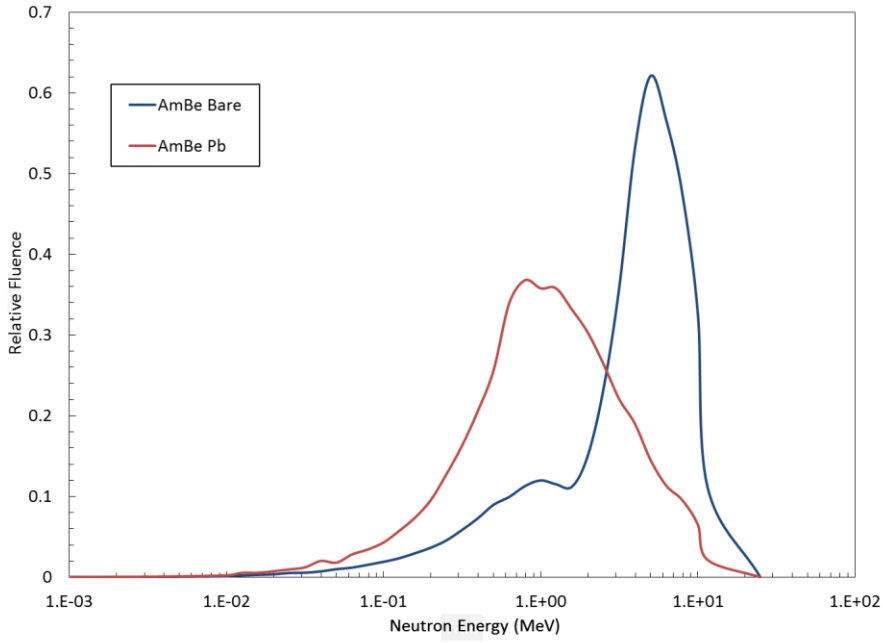

Figure G.2.3. AmBe in Lead and bare source Spectra, normalized by total flux

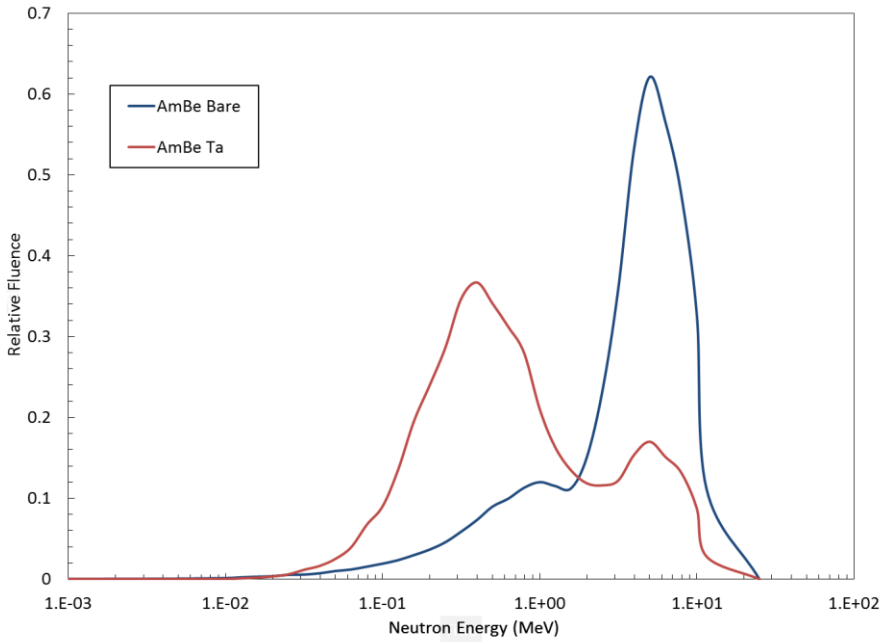

Figure G.2.4. AmBe in Tantalum and bare source Spectra, normalized by total flux

REFERENCES

1. "Atomic Energy Act of 1954, as Amended." Public Law no. 83-703, referenced from NUREG-0980, Nuclear Regulatory Commission (2011).

2. Kapur, S. P. "Deterring Nuclear Terrorists" in *Complex Deterrence: Strategy in the Global Age,* Chicago, Illinois: The University of Chicago Press, (2009).

3. Haga, Y. K., Kumazawa, S., and Niimura, N. *Gamma-ray Sensitivity and Shielding of a Neutron Imaging Plate.* Journal of Applied Crystallography **32**, 878-882 (1999).

4. Knoll, G. F. *Radiation Detection and Measurements.* 3rd Edition. Hoboken, New Jersey: John Wiley & Sons, Inc., 2000.

5. Kouzes, R. T. "The ^{3}He Supply Problem." http://www.pnl.gov/main/publications/external/technical_reports/PNNL-18388.pdf (accessed 12 April 2011).

6. Bogart, D., Shook, D. F., and Fieno, D. *Transport Analysis of Measured Neutron Leakage Spectra from Spheres as Tests of Evaluated High-Energy Cross Sections.* Nuclear Science and Engineering **53**, 285-303 (1974).

7. Eisenhauer, C. M., Hunt, J. B., and Schwartz, R. B. *Calibration Techniques for Neutron Personal Dosimetry.* Radiation Protection Dosimetry **10**(1-4), 43-57 (1985).

8. Bramblett, R. L., Ewing, R. I., and Bonner, T. W. *A New Type of Neutron Spectrometer*. Nuclear Instruments and Methods **9**, 1-12 (1960).

9. Ludlum Measurements, Inc. "Model 42-5 Manual." http://www.ludlums.com/images/stories/product_manuals/m42-5mar89.pdf (accessed 13 April 2011).

10. Hertel, N. E. and Davidson, J. W. *The Response of Bonner Spheres to Neutrons from Thermal Energies to 17.3 MeV.* Nuclear Instruments and Methods in Physics Research Section A, **238**(2-3), 509-516 (1985).

11. Thomas, D. J. and Alevra, A. V. *Bonner Sphere Spectrometers – a Critical Review.* Nuclear Instruments and Methods in Physics Research A **476**, 12-20 (2002).

12. Sweezy, J. E. *A Multisphere Neutron Spectrometer Measurement of the Georgia Tech Research Reactor Bio-Medical Facility.* MS Thesis, Atlanta, Georgia: Georgia Institute of Technology (1996).

13. Martin, R. C., Knauer, J. B., and Balo, P. A. *Production, Distribution, and Applications of Californium-252 Neutron Sources.* Oak Ridge, Tennessee: Oak Ridge National Laboratory (1999).

14. Williams, R. G. III, Gesh, C. J., and Pagh, R. T. "Compendium of Material Composition Data for Radiation Transport Modeling." Richland, Washington: Pacific Northwest National Laboratory (2006).

15. National Aeronautics and Space Administration. "Instruction Manual for Americium-Beryllium Neutron Source." Cleveland, Ohio: Lewis Research Center (1966).

16. Office of Radiological Safety, Georgia Institute of Technology. "Radiation Safety Policy Manual." Atlanta, Georgia: Georgia Institute of Technology (2009).

17. Axford, T. H., Hines, K. C. and Pollard, J. P. *Neutron Slowing-Down Spectra in Beryllium and Beryllium Oxide.* Journal of Nuclear Energy Parts A/B **18**, 131-139 (1964).

18. Gulf General Atomic, Incorporated. *Measurement of Neutron Penetration Standards, Volume I.* (1969).

19. Schwartz, R. B. and Eisenhauer, C. M. *The Design and Construction of a D_2O-Moderated ^{252}Cf Source for Calibrating Neutron Personnel Dosimeters Used at Nuclear Power Reactors.* Washington, DC: National Bureau of Standards (1980).

20. Schwartz, R. B., Eisenhauer, C. M. and Grundl, J. A. *Experimental Verification of the Neutron Spectrum from the D_2O-Moderated ^{252}Cf Source.* Washington, DC: National Bureau of Standards (1983).

21. Hunt, J.B. *The Calibration of Neutron Sensitive Spherical Devices.* Radiation Protection Dosimetry **8**(4), 239-251 (1984).

22. Sweezy, J. E., Hertel, N. E., Veinot, K. G., and Karam, R. A. *Performance of Multisphere Spectrometry Systems.* Radiation Protection Dosimetry **78**(4), 263-272 (1998).

23. Veinot, K. G. and Bogard, J. S. *Anisotropy Factors for a ^{252}Cf Source.* Nuclear Technology **168**(2), 364-368 (2009).

24. Axton, E. J. *The Effective Centre of a Moderating Sphere When Used as an Instrument for Fast Neutron Flux Measurements.* Journal of Nuclear Engineering **26**, 581-583 (1972).

25. Burgett, E. A. *A Broad Spectrum Neutron Spectrometer Utilizing a High Energy Bonner Sphere Extension.* MS Thesis, Atlanta, Georgia: Georgia Institute of Technology (2008).

26. Sweezy, J. E., Hertel, N. E., and Veinot, K. G. *BUMS – Bonner sphere Unfolding Made Simple: an HTML Based Multisphere Neutron Spectrometer Unfolding Package.* Nuclear Instruments and Methods in Physics Research A **476**, 263-269 (2002).

27. X-5 Monte Carlo Team. "MCNP - A General Monte Carlo N-Particle Transport Code Version 5, Volume I: Overview and Theory." Los Alamos, New Mexico: Los Alamos National Laboratory (2004).

28. Scwarz, A. L., Schwarz, R. A. and Carter, L. L. "MCNP/MCNPX Visual Editor Computer Code Manual." Los Alamos, New Mexico: Los Alamos National Laboratory (2008).

29. International Commission on Radiological Protection. "ICRP Publication 74: Conversion Coefficients for Use in Radiological Protection against External Radiation." Annals of the ICRP (1996).

30. International Organization for Standardization. *Neutron Reference Radiations for Calibrating Neutron-Measuring Devices Used for Radiation Protection Purposes and for Determining their Response as a Function of Neutron Energy.* ISO 8529, Figure A.2-A.3, 14 (1989).